Final Report • November 1995

CHARACTERIZATION OF HYDROGEN INGRESS IN HIGH-STRENGTH ALLOYS

Bruce G. Pound, Group Leader
Corrosion Science and Technology
Materials Research Center

SRI Project PYU-2969

Prepared for:

Office of Naval Research, Code 3312
800 N. Quincy Street
Arlington, VA 22217-5000

Attn: Dr. A. J. Sedriks, Program Manager

Contract No. N00014-91-C-0263

Approved:

R. Thomas Podoll
Laboratory Director
Materials and Chemical Engineering Laboratory

David M. Golden
Senior Vice President
Sciences and Technology Group

REPORT DOCUMENTATION PAGE

Form Approved
OMB No. 0704-0188

1. AGENCY USE ONLY *(Leave blank)*	2. REPORT DATE	3. REPORT TYPE AND DATES COVERED
	Nov 95	Final 15 Sept 93-14 Sept 95

4. TITLE AND SUBTITLE
Characterization of Hydrogen Ingress in High-Strength Alloys

5. FUNDING NUMBERS
N00014-91-C-0263

6. AUTHOR(S)
Bruce G. Pound

7. PERFORMING ORGANIZATION NAME(S) AND ADDRESS(ES)
SRI International
333 Ravenswood Ave.
Menlo Park, CA 94025

8. PERFORMING ORGANIZATION REPORT NUMBER
PYU-2969

9. SPONSORING/MONITORING AGENCY NAME(S) AND ADDRESS(ES)
Office of Naval Research, Code 3312
800 N. Quincy St.
Arlington, VA 22217-5000

10. SPONSORING/MONITORING AGENCY REPORT NUMBER

11. SUPPLEMENTARY NOTES

12a. DISTRIBUTION/AVAILABILITY STATEMENT
Approved for public release - distribution unlimited

12b. DISTRIBUTION CODE

13. ABSTRACT *(Maximum 200 words)*

The ingress of hydrogen (H) in various high-strength alloys was investigated with a view to characterizing their susceptibility to hydrogen embrittlement (HE). A potentiostatic pulse technique was applied to three Fe-base alloys (AerMet 100, H11, and A-286), two Cu-containing alloys (Be-Cu and alloy K-500), a superferritic stainless steel (Sea-Cure), and three Beta-Ti alloys (Ti-15V-3Cr-3Al-3Sn, Beta-21S, and Beta-C) in 1 mol/L acetic acid-1 mol/L sodium acetate. The data were analyzed using a diffusion/trapping model to obtain the irreversible trapping constant (k) and H entry flux for each alloy. The order of the k values for AerMet 100, H11, and two high-strength steels previously studied (4340 and 18Ni) inversely parallels their threshold stress intensities for stress corrosion cracking. Likewise, the k values for the other alloys can be correlated with their observed resistances to HE according to the following groups: (i) alloy A-286, 18Ni steel, H11, Be-Cu, and also alloy 718 from earlier work; (ii) annealed/aged and direct aged alloy K-500; and (iii) Ti alloys. The trapping characteristics of Sea-Cure could not be determined. However, the propensity of the S44660 alloy to undergo HE at cathodic protection potentials can be attributed to changes in the oxide that lead to a less restricted entry of H.

14. SUBJECT TERMS	15. NUMBER OF PAGES
Iron-Base Alloys, Copper Alloys, Beta-Titanium Alloys, Stainless Steel, Potentiostatic Pulse, Hydrogen Trapping, Trapping Model, Hydrogen Ingress	106
	16. PRICE CODE

17. SECURITY CLASSIFICATION OF REPORT	18. SECURITY CLASSIFICATION OF THIS PAGE	19. SECURITY CLASSIFICATION OF ABSTRACT	20. LIMITATION OF ABSTRACT
UNCLASSIFIED	UNCLASSIFIED	UNCLASSIFIED	UL

CLASSIFIED BY:

DECLASSIFY ON:

CONTENTS

PREFACE

This final report describes work performed under Office of Naval Research (ONR) Contract No. N00014-91-C-0263 in a continuation of our program to investigate hydrogen ingress into various high-strength alloys, particularly in terms of irreversible trapping, with a view to characterizing the susceptibility of the alloys to hydrogen embrittlement (HE). A technique referred to as hydrogen ingress analysis by potentiostatic pulsing (HIAPP) was used to obtain anodic current transients for the alloys in 1 mol L^{-1} acetic acid/1 mol L^{-1} sodium acetate, and the transients were analyzed using a diffusion/trapping model under interface control conditions to evaluate the trapping constant and hydrogen entry flux in each case.

The report is presented as an Executive Summary followed by six papers that will be published in journals or in conference proceedings:

1. "Hydrogen Trapping in High-Strength Iron-Base Alloys," submitted to *Acta Metallurgica et Materialia.*
2. "The Effect of Aging on Hydrogen Trapping in Copper-Containing Alloys," submitted to *Corrosion.*
3. "The Ingress of Hydrogen into a Superferritic Stainless Steel," to be submitted.
4. "Hydrogen Trapping in Aged β-Titanium Alloys," submitted to *Acta Metallurgica et Materialia.*
5. "The Resistance of High-Strength Alloys to Hydrogen Embrittlement," in *Proceedings of the Tri-Service Conference on Corrosion* (Wright-Patterson Air Force Base, Dayton, OH, 1994), in press.
6. "The Role of Traps in Determining the Resistance to Hydrogen Embrittlement," in *Proceedings of the 5th International Conference on Hydrogen Effects on Material Behavior*, N. R. Moody and A. W. Thompson, Eds. (The Minerals, Metals & Materials Society, Warrendale, PA, 1994), in press.

The first paper covers two high-strength steels (AerMet 100 and AISI Type H11) and a stainless steel (A-286). The next two concern Cu-containing alloys (Be-Cu and two heats of alloy K-500) and a superferritic stainless steel (Sea-Cure) in its standard, hydrogen-resistant, and intermediate grades, while the fourth paper deals with three β-Ti alloys (unaged and aged Ti-15V-3Cr-3Al-3Sn and Beta-21S, and partially aged Beta-C). The final two papers review the progress made in characterizing hydrogen trapping in high-strength alloys studied during our program with ONR; some of the work reported there was supported by our earlier ONR contract, No. N00014-86-C-0233.

The principal investigator would like to acknowledge Mr. J. Eckenrod of Crucible Research for supplying samples of the three grades of Sea-Cure; Dr. M. Natishan, formerly at the David Taylor Research Center, Department of the Navy and now at the University of Maryland, for providing samples of the two heats of alloy K-500; and Professors R. Gangloff and J. Scully of the University of Virginia for providing samples of Ti-15-3 and Beta-21S Ti.

EXECUTIVE SUMMARY

High performance alloys are often required to possess a combination of properties such as strength, toughness, and corrosion resistance. However, their resistance to hydrogen embrittlement (HE) remains a concern in many situations. Microstructural defects in these and other alloys provide potential trapping sites for hydrogen and so can play a crucial role in determining an alloy's intrinsic susceptibility to HE. However, whether embrittlement will actually occur is also affected by other factors, including the amount of hydrogen entering the alloy. Consequently, alloys need to be characterized in terms of both trapping capability and the rate of hydrogen entry to assess their likelihood of embrittlement.

This report describes work performed during a continuation of our program with the Office of Naval Research (ONR) to investigate hydrogen ingress in various alloys, particularly in terms of irreversible trapping, with a view to characterizing the susceptibility of the alloys to HE. A technique referred to as hydrogen ingress analysis by potentiostatic pulsing (HIAPP) was used to obtain anodic current transients for the alloys in 1 mol L^{-1} acetic acid/1 mol L^{-1} sodium acetate containing 15 ppm As_2O_3. The transients were analyzed using a diffusion/trapping model under interface control conditions to evaluate the apparent trapping constant (k_a) and hydrogen entry flux in each case. Where possible, k_a was then used to determine the irreversible trapping constant (k) and the density of irreversible traps.

The first part of this work focused on investigating the trapping behavior of three high-strength iron-base alloys (AerMet 100, H11 steel, and alloy A-286). Overaged/annealed and aged specimens of AerMet 100 exhibited a marked difference in trapping. In contrast to the overaged alloy, the aged alloy displayed a significant level of irreversible trapping. The order of the k values for AerMet 100, H11, and two high-strength steels previously studied (4340 and 18Ni) inversely parallels their threshold stress intensities for stress corrosion cracking (K_{ISCC}); that is, the lower the value of k, the higher the value of K_{ISCC}.

The value of k for alloy A-286 is lower than that for AerMet 100 and intermediate between those for two Ni-base alloys examined previously (718 and 925). Thus, alloy A-286 is intrinsically less susceptible to HE than the three steels and alloy 718 but more so than alloy 925. The k values of alloys 718, A-286, 18Ni steel, and H11 are consistent with test data for their relative resistance to HE. The results for AerMet 100, H11, and alloy A-286 extend the previously reported correlation between k and HE resistance.

The second part of the study involved three Cu-containing alloys: Be-Cu and two annealed and aged (AA) heats of alloy K-500. The values of k were compared with those for previously studied alloys, including direct aged (DA) alloy K-500. These values showed that unaged (unannealed cold-drawn) and DA Be-Cu are intrinsically more susceptible to HE than unaged and DA alloy K-500, respectively. The intrinsic susceptibility for aged Be-Cu and two other alloys—718 and A-286—can be correlated with their observed resistance to HE. The trapping behavior of alloy K-500 is markedly affected by the type of heat treatment. The values of k for the two AA alloys are similar but are more than twice as large as that for the DA alloy. The intrinsic susceptibilities, as defined by k, for AA and DA alloy K-500 match their observed resistances to HE. Hence, H trapping is a principal—possibly predominant—factor determining the HE resistance of alloy K-500. The primary irreversible traps in alloy K-500 are believed to involve grain boundary S in the DA alloy and graphitic C in the AA alloy. Higher levels of grain boundary C in alloy K-500 provide little additional trapping capability. The intrinsic susceptibility of AA alloy K-500 with different levels of grain boundary C is consistent with the resistance to HE observed under high cathodic polarization.

The next part of the work addressed a superferritic stainless steel—Sea-Cure (UNS S44660)—in its standard grade, its hydrogen-resistant grade, and an intermediate grade. The three grades of UNS S44660 proved difficult to investigate in terms of trapping. In all cases, the hydrogen entry flux was still low up to a charging potential of -0.6 V (SCE) when the surface oxide began to change markedly in its electrochemical behavior. As a result of the low flux, negligible hydrogen entered the alloys, and so their trapping characteristics could not be determined. On the other hand, it was clear that the surface oxides were effective barriers to hydrogen entry and therefore that these superferritics should be resistant to HE in mildly acidic or near-neutral solutions, at least at potentials less cathodic than -0.6 V (SCE). The propensity of superferritics to undergo HE in seawater when they are cathodically polarized to potentials in the range -0.9 to -1.4 V (SCE) may result from changes in the oxide leading to less restricted entry of hydrogen into the alloy. An effective way of rendering the UNS S44660 alloy more resistant to HE is to reduce the intrinsic susceptibility by controlling the number and type of carbide particles, as has apparently been done for the hydrogen-resistant grade.

The fourth part of the work was concerned with three β-titanium alloys (unaged and aged Ti-15V-3Cr-3Al-3Sn and Beta-21S, and partially aged Beta-C). The results were compared with those for other β-Ti alloys studied previously (Ti-10-2-3, fully aged Beta-C, and Ti-13-11-3). Aging caused a negligible change in k_a for Ti-15-3, whereas a marked increase was observed for Beta-21S and the other β-Ti alloys. Among the aged alloys, Ti-13-11-3 had the highest value of k_a and Ti-15-3 had the lowest value. The intrinsic suceptibilities of Beta-C and Beta-21S to HE, as

represented by the trapping constants, were comparable to one another and significantly higher than that of Ti-15-3. The susceptibilities were consistent with the relative resistances to HE observed for these alloys.

HYDROGEN TRAPPING IN HIGH-STRENGTH IRON-BASE ALLOYS*

Abstract—The ingress of hydrogen into three high-strength iron-base alloys—AerMet 100, H11 steel, and alloy A-286—was studied using a potentiostatic pulse technique. Values of the irreversible trapping constant (k) and the hydrogen entry flux were determined for these alloys in 1 mol L^{-1} acetic acid/1 mol L^{-1} sodium acetate. The order of the k values for AerMet 100, H11, and two high-strength steels (4340 and 18Ni) previously studied inversely parallels their threshold stress intensities for stress corrosion cracking. The value of k for alloy A-286 is lower than that for AerMet 100 and intermediate between those for two Ni-base alloys (718 and 925) examined previously. The k values of alloys 718, A-286, 18Ni steel, and H11 are consistent with test data for their relative resistance to hydrogen embrittlement (HE). The results for AerMet 100, H11, and alloy A-286 extend the previously reported correlation between k and HE resistance.

INTRODUCTION

Various steels are used for aircraft components such as landing gear and arresting hooks because of their high-strength characteristics. However, these steels must meet stringent requirements with respect not only to strength but also to fracture toughness and resistance to environmentally assisted cracking. One of the alloys developed for aerospace applications is a martensitic steel—AerMet 100—that is strengthened by precipitation of M_2C carbides (M = Mo and Cr, with Fe also being identified in one study) [1,2]. This steel is reported to possess a balanced combination of the required properties, including a higher resistance to hydrogen-assisted cracking in 3.5% NaCl than 18Ni maraging steel, 300M, and AISI Types 4340 and H11 steel [3-5]. However, precipitation-hardened martensitic iron-base alloys as a group tend to be rather prone to hydrogen embrittlement (HE) [6-8]. Austenitic iron-base alloys such as A-286, in which the strength is imparted by precipitation of the γ' phase composed of $Ni_3(Al,Ti)$, have also been found to undergo HE [9-11]. Thus, the possibility of HE remains a major concern in the use of high-strength iron-base alloys, irrespective of the type of matrix and strengthening precipitates.

The resistance of an alloy to HE is strongly affected by the interaction of hydrogen (H) with microstructural defects that act as H traps [12]. The type of defect plays a crucial role in determining an alloy's intrinsic susceptibility to HE, with large irreversible (high binding energy)

* Submitted to *Acta Metallurgica et Materialia.*

traps typically imparting a high susceptibility [13,14]. Hence, characterization of alloys in terms of irreversible trapping can allow their intrinsic HE susceptibility to be assessed and provide a basis for examining the effect of traps on the observed resistance to HE.

The entry and trapping of H in a wide range of high-strength alloys have been investigated in previous work using an electrochemical technique referred to as hydrogen ingress analysis by potentiostatic pulsing (HIAPP) [15-18]. The rates of H entry and rate constants (k) for irreversible trapping were determined, and it appeared that, for most of these alloys, there was a correlation between the intrinsic susceptibility, as represented by k, and the actual resistance to HE observed in mechanical tests.

In the present work, HIAPP was used to obtain the rates of H entry and irreversible trapping constants for AerMet 100 in the overaged and aged conditions, for hardened AISI Type H11 steel (UNS T20811), and for aged alloy A-286 (UNS S66286). AerMet 100 and H11 extended the range of high-strength steels (4340 and 18Ni) examined previously [15,16], while alloy A-286 provided a comparison with two precipitation-hardened nickel-base superalloys (718 and 925) that had already been studied [16]. The research was aimed in part at characterizing the intrinsic susceptibility of each alloy to HE in terms of its irreversible trapping constant. The intrinsic susceptibilities for AerMet 100, H11, and alloy A-286 were then compared with those for the previous two steels and Ni-base alloys, respectively, and with results for the actual resistance to HE observed in tests by other workers. A further goal, where possible, was to identify the principal irreversible traps in each alloy.

EXPERIMENTAL PROCEDURE

The composition of each alloy is given in Table 1. The alloys were supplied in the form of rods with a diameter of 1.36 cm for AerMet 100, 1.30 cm for H11, and 1.27 cm for alloy A-286. The AerMet 100 was received in an overaged/annealed (677°C/16 h) condition. It was subsequently solution treated at 885°C for 1 h, air cooled to 66°C over 1-2 h, then further cooled to -73°C for 1 h, and finally aged at 482°C for 5 h to give a yield strength of about 1834 MPa. Pulse tests were performed on both the overaged (annealed) and aged alloy.

The microstructure of AerMet 100 was not examined in this study, since it has been investigated in detail by other workers [1,2]. The alloy was shown to have an Fe-Ni lath martensite structure. Aging at temperatures above 454°C causes precipitation of coherent M_2C carbides within the martensite, as noted above. Novotny [2] found that the M_2C carbides produced by a 482°C/5 h age are well-dispersed, very fine rod-shaped precipitates with an average length of 9.1 nm. Similar observations were made by Ayer and Machmeier [1], who reported the

carbides as having a length of ~8 nm and a diameter of ~3 nm. Ayer and Machmeier found that the M_2C carbides contained Cr, Mo, and Fe and that there was no Fe_3C, at least at the grain boundaries, in a 482°C-aged sample. In contrast, Novotny reported that only Mo and Cr constituted the metallic components in the M_2C carbides and that rod-shaped Fe_3C precipitates (40 nm long × 5 nm wide) were present. In addition to the carbides, a small amount of austenite is formed when the alloy is aged at ≥468°C. This reverted austenite is present as a thin film (~3 nm) at the martensite lath boundaries.

The H11 steel was obtained in an annealed condition with a hardness of HRC 20. The steel was heat treated in accordance with the procedure recommended by the producer: 1010°C for 0.5 h, Ar (instead of air) cool, followed by three treatments at 538°C for 2.5 h with an Ar cool between each treatment. The resulting yield strength of the hardened alloy was 1661 MPa. Only the hardened alloy was tested in the present work. The steel was examined under the scanning electron microscope and found to be free of sulfide inclusions, at least at the micrometer-sized level.

The alloy A-286 was used as-received in the solution-annealed (900°C/2h) and aged (720°C/16 h) condition. The yield strength of the aged alloy was 848 MPa. In addition to the γ' phase precipitated during aging, alloy A-286 also exhibited Ti-rich particles that appeared to be carbides. The characteristic dimension of the particles was determined to be 3 μm and the particle concentration was 6.6×10^{13} m^{-3}.

Details of the electrochemical cell and instrumentation have been given previously [15]. The test electrodes of each alloy consisted of a 1.27-cm length of rod press-fitted into a polytetrafluoroethylene sheath so that only the planar end surface was exposed to the electrolyte. The surface was polished before each experiment with SiC paper followed by 0.05-μm alumina powder. The electrolyte contained 1 mol L^{-1} acetic acid and 1 mol L^{-1} sodium acetate (pH 4.8) with 15 ppm As_2O_3 and was deaerated continuously with argon before and throughout data acquisition. The potentials were measured with respect to a saturated calomel electrode (SCE). All tests were performed at 22 ± 1°C.

The test electrode was cathodically charged with hydrogen at a constant potential E_c for a time t_c, after which the potential was stepped in the positive direction to a value 10 mV negative of the open-circuit potential E_{oc}. Anodic current transients were obtained over a range of charging times, typically from 5 to 60 s, at different overpotentials ($\eta = E_c - E_{oc}$). The open-circuit potential of the test electrode was measured immediately before each charging time and was also used to monitor the stability of the alloy surface.

RESULTS

The current transients were analyzed using a diffusion/trapping model based on a constant entry flux at the surface [15,19]. According to the model, the total anodic charge (C m^{-2}) is given by

$$q'(\infty) = FJt_c\{1 - e^{-R}/(\pi R)^{1/2} - [1 - 1/(2R)]\mathrm{erf}(R^{1/2})\} \quad (1)$$

where F is the Faraday constant, J is the ingress flux in mol m^{-2} s^{-1}, and $R = k_a t_c$. The charge $q'(\infty)$ is equated to the charge (q_a) passed during the experimental anodic transients. The adsorbed charge is almost invariably negligible, so q_a can be associated entirely with absorbed H. k_a is an apparent trapping constant measured for irreversible traps in the presence of reversible traps. It is related to the irreversible trapping constant by kD_a/D_L where D_a is the apparent diffusivity and D_L is the lattice diffusivity of H. The use of k as an index of the intrinsic susceptibility has been discussed elsewhere [18].

For aged AerMet 100, H11, and alloy A-286, equation (1) could be fitted to the experimental data for q_a to obtain values of k_a and J, where J was independent of charging time at each potential. In the case of overaged AerMet 100, q_a increased linearly with t_c (Fig. 1), indicating that $k_a = 0$ and therefore that irreversible trapping was negligible. In contrast, the aged alloy exhibited moderately high values of k_a, which were indicative of pronounced irreversible trapping. Values of k_a and J for two tests with aged AerMet 100 are given in Table 2. In both tests, k_a was independent of charging potential, which is to be expected, since the trapping characteristics should be unaffected by electrochemical conditions unless the traps become filled to a significant extent. The overall mean value of k_a was 0.069 ± 0.004 s^{-1}. The flux in general did not change significantly with overpotential.

The H11 steel usually exhibited a few blue/black tarnish spots at the end of each test. The presence of these spots is not desirable, since the surface conditions for H entry may be affected in those areas during the test. A further issue was that values of k_a could be obtained only over a narrow potential range that was limited by the rate of H entry at lower overpotentials and by bubble formation at high overpotentials. Despite these two issues, the values of k_a were surprisingly consistent between tests, as shown in Table 3. The mean value of k_a was 0.080 ± 0.004 s^{-1}.

Alloy A-286, like the other two hardened alloys, displayed irreversible trapping, and data for k_a and J obtained from three tests with alloy A-286 are given in Table 4. In all three tests, k_a was independent of overpotential, the mean value of k_a for the three tests being 0.073 ± 0.005 s^{-1}.

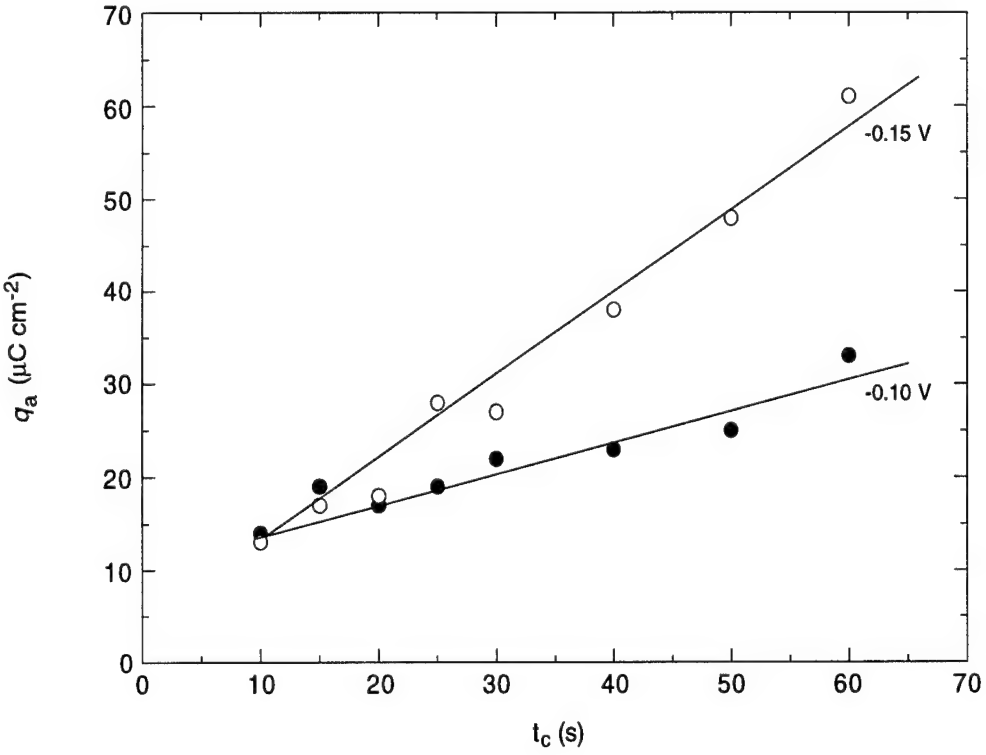

Figure 1. Dependence of anodic charge on charging time for overaged AerMet 100 at two charging potentials.

The flux, however, in contrast to that for aged AerMet 100, showed a marked increase with potential. The dependence of J on E_c was shown to be logarithmic (Fig. 2), which is characteristic of Nernstian-type behavior and implies that the surface coverage of adsorbed H responded rapidly to changes in potential.

DISCUSSION

Irreversible trapping constants

Evaluation of k from k_a requires that the effect of reversible trapping be taken into account. The minor alloying elements, either in their atomic form or as intermetallics that are precipitated during aging, are assumed to be largely responsible for reversible trapping in AerMet 100, H11, and alloy A-286, though for different reasons. In the case of body-centered cubic (bcc) Fe, elements such as Cr are known to have a marked effect on the diffusivity of H [20]. For example, the addition of 5 at.% Cr to Fe decreases the diffusivity by over two orders of magnitude at 27°C. Significant effects could therefore be expected with minor elements that act as reversible traps in alloys with a martensitic lattice, such as AerMet 100. Moreover, based on the case of Cr, these effects are likely to dominate those from microstructural defects such as dislocations.

For face-centered cubic (fcc) alloys, defects such as vacancies or edge dislocations are unlikely to contribute significantly to reversible trapping, since the binding energy of hydrogen to defects such as vacancies or edge dislocations in an fcc lattice is somewhat (a factor of 4) smaller than the activation energy for diffusion [21]. Thus, reversible trapping in alloy A-286, which has an austenitic lattice, should be influenced more by composition than by microstructural defects.

The effect of reversible trapping is determined using the values of D_L and D_a, corresponding to the diffusivity for the "pure" alloy and for the actual alloy, respectively. Although Co is a prominent alloying element in AerMet 100, it is regarded as an anti-trap in Fe [12] and has been shown to have little effect on the diffusivity [22]. Thus, the pure alloys were assumed to be Fe-11Ni-3Cr for AerMet 100, Fe-5Cr for H11, and Fe-24Ni-14Cr for alloy A-286.

AerMet 100. The diffusivity was not available for Fe-11Ni-3Cr, so a value was estimated for D_L from data for Fe-3Cr [20]. The effect of Ni on the diffusivity for Fe is much smaller than that of Cr; for example, 5Ni decreases the diffusivity by a factor of only 1.3, compared with ~140 for 5Cr [20,23]. Hence, it was assumed that the effect of 11Ni on the diffusivity could be neglected. The presence of two phases (α and γ) in Fe-Ni alloys containing between 10 and 33% Ni [24,25] was ignored for the purposes of estimating data for a martensitic steel. Thus, D_L was taken simply as the diffusivity for Fe-3Cr: $(7.5 \pm 0.5) \times 10^{-11}$ m^2 s^{-1}.

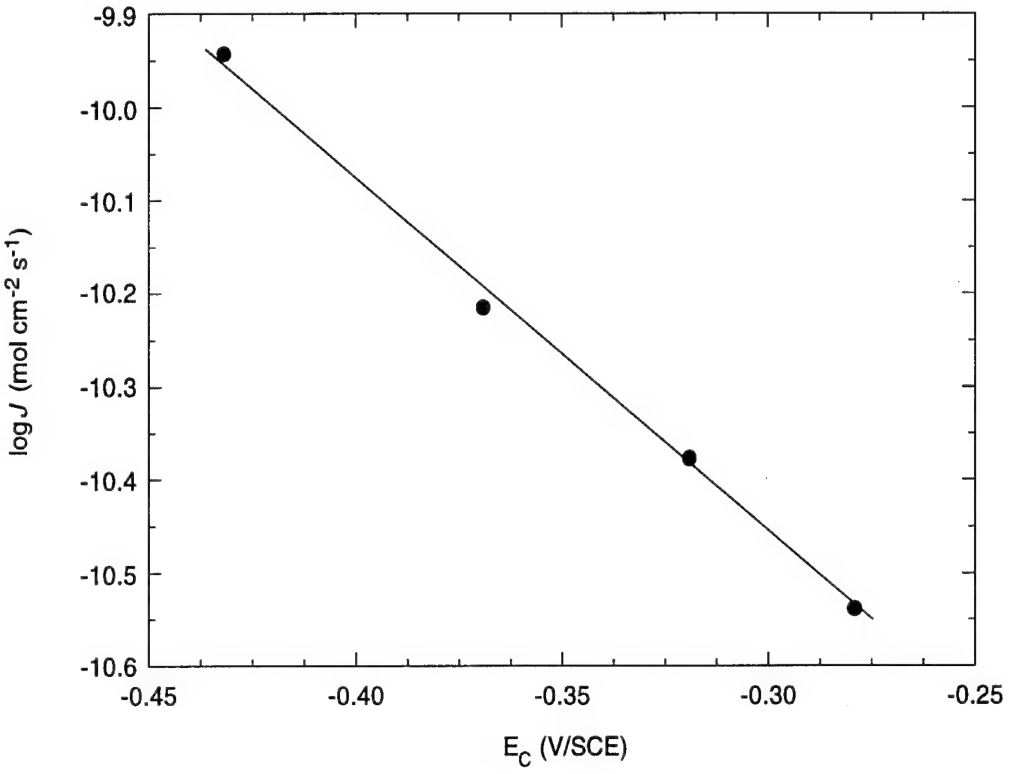

Figure 2. Dependence of entry flux on charging potential for alloy A-286.

Diffusivity data were also not available for AerMet 100. However, the diffusivity for another high-strength steel—D6AC with a yield strength of 1550 MPa—has been studied [26] and, although this steel contains only 1.08Cr, was considered to provide the most appropriate value of D_a. The diffusivity obtained from electrochemical permeation measurements for D6AC is $(7.8 \pm 0.5) \times 10^{-12}$ m^2 s^{-1}. By using this value for D_a and the value given above for D_L, k was calculated to be 0.66 ± 0.12 s^{-1} for aged AerMet 100. In the case of the overaged alloy, k_a was approximately zero, which implies that $k = 0$.

H11 Steel. The diffusivity for Fe-5Cr is $(1.3 \pm 0.1) \times 10^{-11}$ m^2 s^{-1} [20]. The diffusivity for H11 has been determined from permeation measurements and is $(3.0 \pm 0.2) \times 10^{-13}$ m^2 s^{-1} [26]. Hence, the value of k was found to be 3.5 ± 0.7 s^{-1} for H11.

Alloy A-286. Diffusivity data were not available for either Fe-24Ni-14Cr or alloy A-286. However, data have been obtained for other austentic stainless steels (301, 304, and 310) at temperatures from 100° to 350°C [27]. Diffusivities for these alloys at 25°C were estimated by extrapolation and are given in Table 5. The values shown indicate that the differences in diffusivity between the three alloys are relatively small, which is consistent with other work indicating that H transport in austenitic stainless steels is essentially independent of the austenite composition [28]. Accordingly, the minor elements were assumed to have a negligible effect on the diffusivity and so the ratio of D_L to D_a was taken to be ~1. Thus, k was approximately equal to k_a, with a value of 0.073 ± 0.031 s^{-1}.

Comparison of trapping parameters

The trapping constants for AerMet 100 and H11 are compared with those for other steels in Table 6. AerMet 100 has a lower k value than 4340, H11, and 18 Ni maraging steel and therefore has the lowest intrinsic susceptibility to HE of the four steels. The order of the k values for these four steels inversely parallels typical values of their threshold stress intensities for stress corrosion cracking (K_{ISCC}) in 3.5% NaCl [3,4] (Fig. 3); that is, a lower value of k corresponds to a higher value of K_{ISCC}. This trend is underscored by the similarity in k values matching the similarity in K_{ISCC} values for the two most susceptible steels—4340 and H11. The k values indicate that the intrinsic susceptibility may actually be a little lower for H11. The order of this difference is consistent with test results showing that, for these two steels in distilled water, the failure times at various applied stress intensities were longer for H11 [29].

The parallel between k and K_{ISCC} supports the general view that hydrogen plays the predominant role in stress corrosion cracking of martensitic steels [30]. Thus, for these four steels, the observed resistance to HE, as represented by K_{ISCC}, can be correlated with the intrinsic

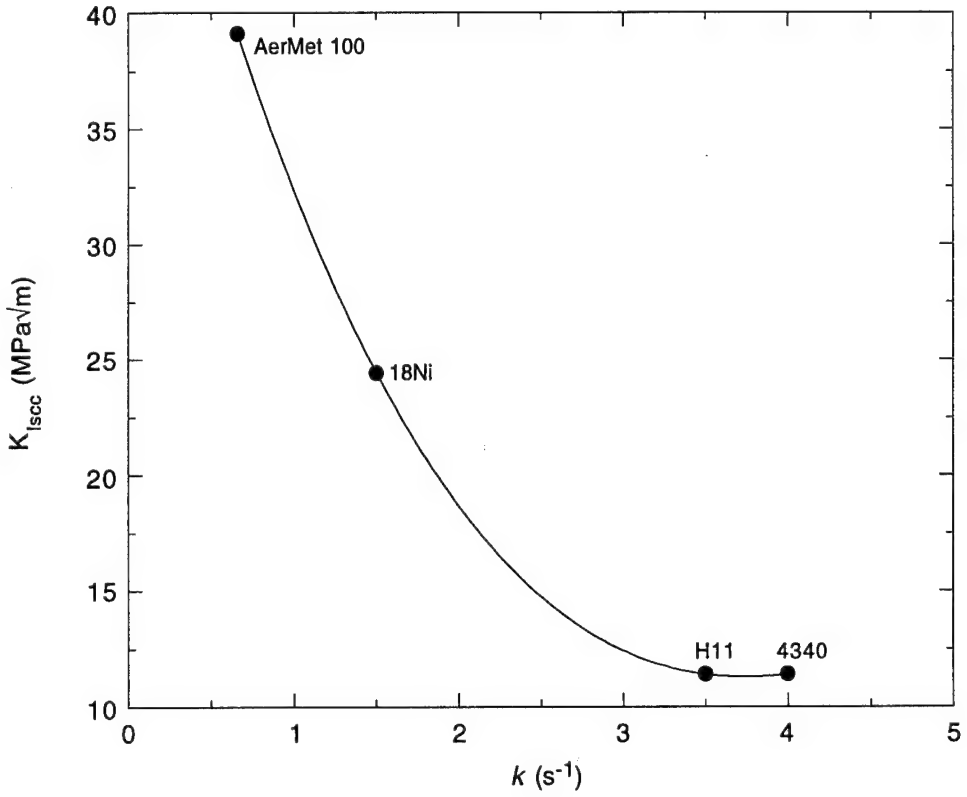

Figure 3. Variation of K_{ISCC} with k for high-strength steels.

susceptibility, as represented by k. In other words, the intrinsic susceptibility is a primary—possibly the predominant—factor determining the observed resistance of these high-strength steels to HE.

Table 6 also shows a comparison between the trapping constants for alloy A-286 and those for two other precipitation-hardened alloys (718 and 925). Alloy A-286 is intermediate in its k value between alloys 718 and 925. Hence, it is intrinsically less susceptible than alloy 718 but more so than alloy 925. Measurements of the reduction in notch tensile strength and ductility in gas-phase charging tests have shown that alloy 718 undergoes extreme HE whereas alloy A-286 exhibits negligible embrittlement [31]. Corresponding measurements have also been made in cathodic charging tests on alloys 718 and A-286 aged to strengths that, relative to each other, were similar to those used in the present work. As in the gas-phase tests, it was found that alloy 718 undergoes a greater decrease in notch tensile strength and ductility than alloy A-286 [32]. Thus, irrespective of the type of charging, the intrinsic susceptibility seems to parallel the relative resistance to HE for alloys 718 and A-286. The cathodic charging tests suggested that the stronger the alloy, the greater the decrease in strength and ductility with increasing H concentration. However, the observed resistance to HE is generally considered more directly an effect of microstructure than of strength [30.33]. In the case of alloys 718 and A-286, the trapping constants parallel the mechanical properties, so it is quite possible that the microstructure through its traps could be the key factor for these alloys too.

The irreversible trapping constants for AerMet 100, H11, and alloy A-286 are compared with the values for other alloys in Table 7. The value of k for alloy A-286 is lower than those for AerMet 100 and several Ni-base alloys, so alloy A-286 has a lower intrinsic susceptibility than the four steels and these Ni-base alloys. It has been found that alloy 718, like alloy A-286, is more resistant to HE than 18Ni (1723 MPa) maraging steel in a gaseous hydrogen environment [31]. Moreover, electrolytic charging tests on these alloys together with H11 have shown that the degree of embrittlement decreases in the order H11, 18Ni steel, 718, and, by implication, A-286 (as discussed above) [34]. Hence, the values of k for the three precipitation-hardened alloys (718, alloy A-286, and 18Ni steel) as well as H11 are consistent with their relative resistances to HE observed in tests. The results for AerMet 100, H11, and alloy A-286 therefore appear to extend the previously reported correlation between k and HE resistance to include these alloys.

A lack of appropriate mechanical test data in the literature makes it difficult to determine whether the position of alloy A-286 is justified with respect to that of alloy C-276 and the other precipitation-hardened alloy, 925; alloy 716 was found to be an exception to the correlation because its HE resistance appears to be determined by the H entry flux [35]. The difficulty in

evaluating the relative position of A-286 is compounded by some uncertainty in the values of k, particularly for C-276. Nevertheless, on the basis of these values, it would be predicted that the resistance to HE observed in tests would be higher for alloy A-286 than for alloy C-276 but lower than for alloy 925.

Identification of irreversible traps

The density of particles or defects (N_i) providing irreversible traps can be obtained from k_a according to equation (2) [16,36]:

$$N_i = k_a a/(4\pi d^2 D_a) \qquad (2)$$

where a is the diameter of the metal atom and d is the trap radius. The value of a for an alloy is taken as the mean of the atomic diameters weighted in accordance with the atomic fraction of each element. The trap radius is estimated from the dimensions of heterogeneities that are potential irreversible traps, and trap densities are then calculated for the different values of d. In this way, the principal irreversible trap can be identified by comparing the values of N_i with the actual concentrations of specific heterogeneities [18].

AerMet 100. As noted above, aging causes precipitation of M_2C carbides and formation of a thin film of austenite at the lath boundaries. Since irreversible trapping was negligible in the overaged/annealed alloy but pronounced in the aged alloy, it seems reasonable to assume that either the carbides or the austenite could provide the principal irreversible traps in the aged alloy. In our previous studies [15-18], carbide and carbonitride precipitates were shown to be the principal irreversible traps in various engineering alloys. However, the carbides in these cases were large (>1 μm) particles, which appeared to have the predominant influence on the value of k because of their density and size. Small (<<1 μm) particles can often be beneficial in terms of HE, but the contribution of such particles to k appears to be overwhelmed by that of larger particles in these alloys, since k correlates with the observed resistance to HE [18].

The M_2C carbides in AerMet 100 are nanometer-sized particles, and since k (and k_a) is proportional to d^2, such particles, even if numerous, tend to make a relatively small contribution to k. Moreover, as discussed previously [18], small particles are not expected to increase the intrinsic susceptibility (as determined by the irreversible traps). Also, trapping becomes more reversible as the coherency of the particle increases [37], so the coherent M_2C carbides in AerMet 100 may not even be irreversible traps.

In view of these factors, k for aged AerMet 100 is more likely to reflect an irreversible trapping capability of the lath boundary austenite. Since the laths are present as blocks within the

packets of martensite making up each grain [4], cracking might be expected to initiate within grains, if the austenite provided equally detrimental H traps at all the lath boundaries. (A similar argument applies to the M_2C carbides.) However, Lee [38] has shown that stress corrosion cracking in AerMet 100 proceeds intergranularly, which implies either that lath boundary austenite may not provide the principal irreversible traps or that only austenite in the vicinity of grain boundaries may make the main contribution to trapping.

Lee observed that the crack propagated along nearly parallel alternating bands which result from microsegregation of alloying elements in the original ingot. A greater portion of the crack appeared to align with bands that were a little lower in Cr, Ni, and Mo, and Lee therefore attributed the preferential crack growth to the lower concentration of these elements. However, the differences in the elemental concentrations between the bands were relatively small. For example, the concentration of Cr was 3.17 wt% in one band and 2.86 wt% in the other, both concentrations lying below the level (≤5 wt%) at which rapid attack can occur at grain boundaries in Ni-Cr-Fe alloys [39]. Grain boundaries with 8 wt% Cr were more resistant to attack, and with 12 wt% Cr they became immune. Thus, differences in resistance to intergranular cracking tend to be associated with more pronounced differences in grain boundary chemistry, and so it is questionable whether compositional differences between the bands can alone account for the crack path in AerMet 100.

It is difficult to conceive of heterogeneities other than the reverted austenite that might account for the change in irreversible trapping when AerMet 100 is aged (carbides are discounted for the reasons discussed above). The lack of other candidates leaves open the possibility that lath boundary austenite in the proximity of grain boundaries might be linked to the intergranular cracking. Provided that the lath boundary austenite acts as an irreversible trap, the unresolved question then is why this austenite could have the predominant influence on the irreversible trapping and so lead to intergranular cracking in AerMet 100.

H11 steel. Irreversible trapping in H11, as in other quenched and tempered steels, might be expected to occur at particle-matrix interfaces associated with sulfide inclusions and carbide precipitates, and at high angle grain boundaries [37]. However, as noted above, the steel is essentially free of sulfide inclusions, and it does not contain Ti, which is a prominent irreversible trap as a carbide. On the other hand, H11 does contain the carbide-formers Cr and Mo, and specimens heated to 1010°C, air-quenched, and double-tempered at 510°C exhibit a small amount of very fine carbide [40]. As discussed above, the effect of small irreversible traps in engineering alloys is usually dominated by that of large traps. Hence, the principal contribution to irreversible trapping in H11 is speculated to come from grain boundaries rather than any carbides.

Alloy A-286. The presence of the $Ni_3(Al,Ti)$ γ' phase precipitated during aging appears to be critical to the H-induced losses in ductility [41,42]. In particular, the misfit between the γ' particles and the austenitic matrix affects the strain at which the γ' particles lose coherency and begin to accumulate H at the particle/matrix interface. Thus, the γ' particles may provide irreversible traps in alloy A-286, although intermetallic precipitates in alloys such as maraging steels tend to be reversible traps [16,43].

Although the γ' phase has been implicated in the HE of alloy A-286, a value of N_i was calculated on the basis of the Ti-rich particles observed in this alloy, since Ti carbide and carbonitride particles have often been identified as the principal irreversible traps in other alloys [18]. By using $D_a = (3.5 \pm 0.5) \times 10^{-16}$ m^2 s^{-1}, $d = 1.5 \times 10^{-6}$ m, and $a = 250 \times 10^{-12}$ m in equation (2), N_i was found to be $(1.8 \pm 0.4) \times 10^{15}$ m^{-3}, whereas the actual concentration of Ti-rich particles was 6.6×10^{13} m^{-3}. The factor of 27 difference in the two values indicates that these particles are not the principal traps. This finding is consistent with the results of other work [42], in which it was found that the TiC phase could not be correlated with the overall H-induced ductility loss of alloy A-286.

Since the Ti-rich particles are discounted as the *principal* irreversible traps, the γ' precipitates are assumed to fill this role in alloy A-286. However, for this alloy and for H11 and AerMet 100, the roles of the γ' phase, lath boundary austenite, and grain boundaries, respectively, as the principal irreversible traps are speculative and have not been verified.

SUMMARY

- AerMet 100 exhibited a marked difference in irreversible trapping between overaged/annealed and aged specimens. In contrast to the overaged alloy, the aged alloy displayed a significant level of irreversible trapping, which appeared more likely to be associated with lath boundary austenite than with M_2C carbides.
- AerMet 100 has a lower value of k than two other high-strength steels, 4340 and 18Ni maraging steel. In contrast, H11 has a value of k similar to that of 4340 steel. Hence, AerMet 100 has the lowest intrinsic susceptibility to HE of the four steels, whereas H11 and 4340 steel are the most susceptible. For these four steels, the observed resistance to HE, as represented by K_{ISCC}, can be correlated with the intrinsic susceptibility, as represented by k.
- The value of k for alloy A-286 is lower than that for AerMet 100 and intermediate between those for the two Ni-base alloys, 718 and 925. Thus, alloy A-286 is intrinsically less

susceptible to HE than the four steels and alloy 718 but more so than alloy 925. The intrinsic susceptibilities (defined by k) of alloys 718, A-286, 18Ni, and H11 are consistent with their observed resistances to HE. The results for AerMet 100, H11, and alloy A-286 therefore appear to extend the previously reported correlation between k and HE resistance to include these alloys.

- The principal irreversible traps were assumed to be associated with the $Ni_3(Al,Ti)$ γ' phase in alloy A-286, grain boundaries in H11, and possibly the lath boundary austenite in aged AerMet 100. However, the role of these heterogeneities as the principal irreversible traps has not been verified.

ACKNOWLEDGEMENTS

Financial support of this work by the U.S. Office of Naval Research under Contract N00014-91-C-0263 is gratefully acknowledged.

REFERENCES

1. R. Ayer and P. M. Machmeier, *Metall. Trans.* **24A**, 1943 (1993).

2. P. M. Novotny, in *Proc. Gilbert R. Speich Symposium: Fundamentals of Aging and Tempering in Bainitic and Martensitic Steel Products*, p. 215. Iron and Steel Society, Warrendale, PA (1992).

3. T. J. McCaffrey, *Advanced Maters. Processes* **9**, 47 (1992).

4. P. M. Novotny and J. M. Dahl, in *Proc. 32nd Conf. on Mechanical Working and Steel Processing*, Vol. XXVIII, p. 275. Iron and Steel Society, Warrendale, PA (1991).

5. C. E. Neu, E. U. Lee, E. W. Lee, J. B. Boodey, J. Kozol, J. W. Morris, and J. Waldman, in *Proc. of the 40th Sagamore Army Materials Research Conference: Metallic Materials for Lightweight Applications*, p. 389 (1993).

6. A. W. Thompson, *Metall. Trans.* **4**, 2819 (1973).

7. A. W. Thompson, in *Fracture 1977: Proc. Fourth Int. Conf. on Fracture* (edited by D.M.R. Taplin), Vol. 2, p. 237. University of Waterloo Press, Waterloo, Ontario, Canada (1977).

8. D. P. Dautovich and S. Floreen, in *Proc. Conf. on Stress Corrosion Cracking and Hydrogen Embrittlement of Iron-Base Alloys* (edited by R. W. Staehle, J. Hochman, R. D. McCright, and J. E. Slater), p. 798. National Association of Corrosion Engineers, Houston, TX (1977).

9. J. Papp, R. F. Hehemann, and A. R. Troiano, in *Hydrogen in Metals* (edited by I. M. Bernstein and A. W. Thompson), p. 657. American Society for Metals, Metals Park, OH (1974).

10. J. LeGrand, M. Caput, C. Couderc, R. Broudeur, and J.-P. Fidelle, *Mem. Sci. Rev. Met.* **68**, 861 (1971).

11. A. W. Thompson, in *Hydrogen in Metals* (edited by I. M. Bernstein and A. W. Thompson), p. 91. American Society for Metals, Metals Park, OH (1974).

12. I. M. Bernstein and G. M. Pressouyre, in *Hydrogen Degradation of Ferrous Alloys* (edited by R. A. Oriani, J. P. Hirth, and M. Smialowski), p. 641. Noyes Publications, Park Ridge, NJ (1985).

13. G. M. Pressouyre and I. M. Bernstein, *Metall. Trans.* **9A**, 1571 (1978).

14. G. M. Pressouyre and I. M. Bernstein, *Acta Metall.* **27**, 89 (1979).

15. B. G. Pound, *Corrosion* **45**, 18 (1989).

16 B. G. Pound, *Acta Metall.* **38**, 2373 (1990).

17. B. G. Pound, *Acta Metall.* **39**, 2099 (1991).

18. B. G. Pound, in *Proc. Fifth Int. Conf. on Hydrogen Effects on Material Behavior* (edited by N. R. Moody and A. W. Thompson), in press. The Minerals, Metals & Materials Society, Warrendale, PA (1995).

19. R. McKibbin, D. A. Harrington, B. G. Pound, R. M. Sharp, and G. A. Wright, *Acta Metall.* **35**, 253 (1987).

20. J. O'M. Bockris, M. A. Genshaw, and M. Fullenwider, *Electrochim. Acta* **15**, 47 (1970).

21. W. D. Wilson and S. C. Keeton, in *Advanced Techniques for Characterizing Hydrogen in Metals* (edited by N. F. Fiore and B. J. Berkowitz), p. 3. The Metallurgical Society of AIME, Warrendale, PA (1981).

22. K. W. Lange and H. J. Koning, in *Proc. Second Int. Conf. on Hydrogen in Metals* (edited by P. Azou), paper 1A5 (1973).

23. W. Beck, J. O'M. Bockris, M. A. Genshaw, and P. K. Subramanyan, *Metall. Trans.* **2**, 883 (1971).

24. D. Hanson and J. R. Freeman, *J. Iron Steel Inst.* **154**, 301 (1923).

25. R. E. Ogilvie, *Trans. TMS-AIME* **223**, 2083 (1965).

26. C. S. Kortovich and E. A. Steigerwald, *Eng. Fract. Mech.* **4**, 637 (1972).

27. T.-P. Perng and C. J. Altstetter, *Acta Metall.* **34**, 1771 (1986).

28. M. R. Louthan, Jr., and R. G. Derrick, *Corrosion Sci.* **15**, 565 (1975).

29. W. D. Benjamin and E. A. Steigerwald, *Metall. Trans.* **2**, 606 (1971).

30. A. W. Thompson and I. M. Bernstein, in *Advances in Corrosion Science and Technology* (edited by R. W. Staehle and M. Fontana), p. 53. Plenum Press, New York (1979).

31. R. J. Walter, R. P. Jewett, and W. T. Chandler, *Mater. Sci. Eng.* **5**, 98 (1969/70).

32. P. D. Hicks and C. J. Alstetter, in *Proc. Fourth Int. Conf. on Hydrogen Effects on Material Behavior* (edited by N. R. Moody and A. W. Thompson), p. 613. The Minerals, Metals & Materials Society, Warrendale, PA (1990).

33. I. M. Bernstein and A. W. Thompson, *Int. Met. Rev.* **21**, 269 (1976).

34. T. P. Groeneveld, E. E. Fletcher, and A. R. Elsea, *A Study of Hydrogen Embrittlement of Various Alloys*, Summary Report, Contract No. NAS8-20029. National Aeronautics and Space Administration, Marshall Space Flight Center, Huntsville, AL (1966).

35. B. G. Pound, *Scripta Metall.* **29**, 1433 (1993).

36. B. G. Pound, R. M. Sharp, and G. A. Wright, *Acta Metall.* **35**, 263 (1987).

37. G. M. Pressouyre, *Metall. Trans.* **10A**, 1571 (1979).

38. E. U. Lee, *Metall. Mater. Trans.* **26A**, 1313 (1995).

39. G. S. Was and V. B. Rajan. *Metall. Trans.* **18A**, 1313 (1987).

40. *Metals Handbook*, 9th Ed., Vol. 9, p. 271. ASM International, Materials Park, OH (1985).

41. A. W. Thompson, in *Hydrogen in Metals* (edited by I. M. Bernstein and A. W. Thompson), p. 91. American Society for Metals, Metals Park, OH (1974).

42. A. W. Thompson and J. A. Brooks, *Metall. Trans.* **6A**, 1431 (1975).

43. V. I. Sarrak, G. A. Filippov, and G. G. Kush, *Phys. Met. Metall.* **55**, 94 (1983).

Table 1. Alloy composition (wt%)

Element	AerMet 100	H11	A-286
Al	0.005		0.13
B			0.0046
C	0.24	0.41	0.024
Co	13.47		0.08
Cr	3.00	4.88	14.02
Cu		0.03	0.10
Fe	71.00	Bal	57.08
Mn	0.01	0.30	0.28
Mo	1.19	1.32	1.37
N	<0.0010		
Nb+Ta			5.30
Ni	11.07	0.04	24.38
O	<0.0010		
P	0.002	0.011	0.019
S	<0.0005	0.003	0.001
Si	<0.01	0.88	0.22
Ti	0.009		2.09
V		0.45	0.20

Table 2. Values of k_a and J for aged AerMet 100

Test	η (V)	E_c (V/SCE)	k_a (s^{-1})	J (nmol cm^{-2} s^{-1})	Mean k_a
1	-0.10	-0.561	0.059	0.058	
	-0.15	-0.613	0.079	0.054	
	-0.20	-0.670	0.066	0.046	0.069 ± 0.006
	-0.25	-0.727	0.070	0.046	
2	-0.20	-0.666	0.068	0.059	0.069 ± 0.001
	-0.25	-0.722	0.069	0.061	

Table 3. Values of k_a and J for hardened H11 steel

Test	η (V)	E_c (V/SCE)	k_a (s^{-1})	J (nmol cm^{-2} s^{-1})
1	-0.150	-0.753	0.082	0.061
	-0.175	-0.777	0.084	0.070
2	-0.200	-0.804	0.083	0.089
3	-0.200	-0.796	0.080	0.080
4	-0.200	-0.795	0.070	0.042

Table 4. Values of k_a and J for aged alloy A-286

Test	η (V)	E_c (V/SCE)	k_a (s^{-1})	J (nmol cm^{-2} s^{-1})	Mean k_a
1	-0.15	-0.279	0.075	0.029	
	-0.20	-0.319	0.070	0.042	0.077 ± 0.005
	-0.25	-0.369	0.075	0.061	
	-0.30	-0.432	0.086	0.114	
2	-0.15	-0.268	0.072	0.023	
	-0.20	-0.313	0.080	0.037	0.071 ± 0.006
	-0.30	-0.428	0.062	0.087	
3	-0.15	-0.258	0.074	0.026	
	-0.20	-0.296	0.064	0.041	0.071 ± 0.004
	-0.25	-0.346	0.074	0.059	

Table 5. Diffusivities for austenitic stainless steels

Alloy	Ni	Cr	D_a (m^2 s^{-1})
301	7	17	3.09×10^{-16}
304	9	18	3.49×10^{-16}
310	20	25	3.67×10^{-16}

Table 6. Trapping parameters

Alloy	Yield Strength (MPa)	k_a (s^{-1})	D_L/D_a	k (s^{-1})
Steels				
4340	1792	0.008 ± 0.001	500	4.0 ± 0.5
H11	1661	0.080 ± 0.004	43.3 ± 6.2	3.5 ± 0.7
18Ni	1954	0.005 ± 0.002	300 ± 90	1.50 ± 1.05
AerMet 100	1834	0.069 ± 0.004	9.6 ± 1.3	0.66 ± 0.12
Precipitation-hardened alloys				
718	1238	0.031 ± 0.002	4.0 ± 0.5	0.124 ± 0.024
A-286	848	0.073 ± 0.005	1.0 ± 0.4	0.073 ± 0.031
925	758	0.006 ± 0.003	5.6 ± 0.6	0.034 ± 0.004

Table 7. Irreversible trapping constants for a range of alloys

Alloy	Test Condition	k (s^{-1})
4340	Hardened (HRC 53)	4.0 ± 0.5
H11	Hardened (HRC 51)	3.5 ± 0.7
18Ni (300)	Aged	1.50 ± 1.05
AerMet 100	Overaged/annealed, aged	0.66 ± 0.12
716	Annealed, aged, 4% cold work	0.20 ± 0.06
718	Solution treated	0.124 ± 0.024
C-276	Hot rolled, 27% cold work	0.090 ± 0.030
A-286	Annealed, aged	0.073 ± 0.031
K-500	Cold drawn, aged	0.042 ± 0.006
Ti grade 2 (high H)	Annealed	0.040 ± 0.008
925	Annealed, aged	0.034 ± 0.004
Ti grade 2 (low H)	Annealed	0.028 ± 0.002
35N	Cold drawn, aged	0.026 ± 0.002
625	Annealed, 17% cold work	0.014 ± 0.010

The Effect of Aging on Hydrogen Trapping in Copper-Containing Alloys*

ABSTRACT

Hydrogen (H) trapping was investigated for three Cu-containing alloys (Be-Cu [UNS C17200] and two annealed and aged (AA) heats of Alloy K-500 [UNS N05500]) to examine differences in their susceptibility to hydrogen embrittlement (HE). A potentiostatic pulse technique was used to determine irreversible trapping constants (k) and H entry fluxes for the alloys at various charging potentials in 1 mol L^{-1} acetic acid (CH_3COOH)/1 mol L^{-1} sodium acetate (CH_3COONa). The values of k were compared with those for alloys, including direct aged (DA) Alloy K-500, studied in earlier work. These values showed that unaged (unannealed cold-drawn) and DA Be-Cu are intrinsically more susceptible to HE than unaged and DA Alloy K-500, respectively. The intrinsic susceptibility for aged Be-Cu and two other alloys—718 [UNS N07718] and A-286 [UNS S66286]—can be correlated with their observed resistance to HE. The trapping behavior of Alloy K-500 is markedly affected by the type of heat treatment. The values of k for the two AA alloys are similar but are more than twice as large as that for the DA alloy. The intrinsic susceptibilities, as defined by k, for AA and DA Alloy K-500 match their observed resistances to HE. Hence, H trapping is a principal—possibly predominant—factor determining the HE resistance of Alloy K-500. The primary irreversible traps in Alloy K-500 are believed to involve grain boundary S in the DA alloy and graphitic C in the AA alloy. Higher levels of grain boundary C in Alloy K-500 provide little additional trapping capability. The intrinsic susceptibility of AA Alloy K-500 with different levels of grain boundary C is consistent with the resistance to HE observed under high cathodic polarization.

INTRODUCTION

Various copper-containing alloys can be precipitation-hardened to high yield strengths. Be-Cu alloys, for example, are strengthened by precipitation of (Cu,Co)Be in a matrix of α-Cu,[1] while in Ni-Cu alloys such as K-500 (UNS N05500), the strength is imparted by precipitation of γ′ particles composed of $Ni_3(Al,Ti)$.[2] The ability of these alloys to be aged allows them to be used in a wide range of applications but makes them more vulnerable to hydrogen embrittlement (HE), as observed for Alloy K-500.[3]

---

* Submitted to *Corrosion*.

HE in Ni[4-6] and Ni-Co alloys[7] is known to be assisted by S segregated at grain boundaries. In Ni-base alloys, the presence of sulfide-formers such as Ti can often limit the grain boundary segregation of S,[8] but it is TiN and TiC particles that are usually present in Alloy K-500.[9-11] The HE resistance of two Ni-base alloys—UNS R30035, which contained 0.8% Ti, and C-276 [UNS N10276]—was found to correlate with aging treatment, which in turn could be correlated with the concentration of grain boundary S and P.[12,13] The level of grain boundary impurities in Cu-containing alloys may likewise be associated with differences in the resistance to HE, such that the type of heat treatment used for these alloys could have a marked effect on their propensity to embrittlement.

Microstructural defects in alloys provide potential trapping sites for hydrogen (H) and so can be crucial in determining an alloy's resistance to HE.[14] The local concentration of H trapped at a defect must reach some critical level (C_k) for cracks to be initiated.[14,15] Large irreversible (high binding energy) traps typically impart a high intrinsic susceptibility to an alloy because they have a relatively high probability of being located in a crack-sensitive region and therefore are associated with low values of C_k.[14] However, small irreversible traps may also be detrimental—that is, have a low C_k—if they lie in a vulnerable region such as a grain boundary. For example, in the case of Alloy C-276, it has been suggested that an increased level of grain boundary P could reduce the critical concentration of H required for fracture.[12] Thus, the intrinsic susceptibility of an alloy to HE depends highly on the type of microstructural defect and could be increased considerably by segregation of impurities to grain boundaries.

The entry and trapping of H in a wide range of high-strength alloys were investigated in previous work, using an electrochemical technique referred to as hydrogen ingress analysis by potentiostatic pulsing (HIAPP).[16] The rates of H entry and rate constants (k) for irreversible trapping were determined, and for almost all of these alloys, there was a correlation between the intrinsic susceptibility, as represented by k, and the actual resistance to HE observed in mechanical tests. The alloys used in the previous work included a 77Cu-15Ni alloy and direct aged (DA) Alloy K-500 (65Ni-30Cu).[17] From an analysis of these alloys' trapping characteristics, it was concluded that the S and P segregated at grain boundaries were probably the principal irreversible traps.

In the present work, HIAPP was used to determine the rates of H entry and trapping constants for three Cu-containing alloys: unaged and aged Be-Cu (UNS C17200) and two annealed and aged (AA) heats of Alloy K-500. The research was aimed at characterizing the intrinsic susceptibility of each alloy to HE in terms of its irreversible trapping constant. The values of k for these alloys were compared with those for the 77Cu-15Ni alloy and DA Alloy K-500 studied previously to relate k to the relative resistance of each alloy to HE.

EXPERIMENTAL PROCEDURE

The Be-Cu alloy contained 1.8/2.0 Be and was supplied as rod with a diameter of 6.35 mm. This alloy was received in an unaged condition with a Rockwell B hardness of 93-95 (Rockwell C hardness [HRC] of 17-18), which corresponded to a yield strength of 585-613 MPa. A section of alloy was aged at 315°C for 2 h in Ar to give an HRC of 36. The yield strength corresponding to this hardness was ~860 MPa. Aged Be-Cu, as noted above, contains (Cu,Co)Be precipitates in the Cu matrix, these precipitates being small, mainly spheroidal, and uniformly dispersed.[1]

Table 1 gives the composition of each heat of Alloy K-500 and, for comparison, the composition of the 77Cu-15Ni alloy. The two heats of Alloy K-500 were supplied as sections of bar that had been solution-annealed and aged at 607°C for 16 h to give a yield strength in the range 689-724 MPa. The two heats are denoted as AA-1 and AA-2. Cylindrical specimens with a diameter of 1.27 cm were machined from the sections of bar. In contrast to the present specimens, the DA Alloy K-500 studied previously was supplied as cold-drawn (CD), 1.27-cm-diameter rod that was aged to give a yield strength of about 1096 MPa. The direct aging treatment followed the procedure recommended by the alloy producer for CD rods (≤3.8 cm in diameter): Heat at 600°C for 8 h and then cool to 480°C at a rate of 11°/h.[2]

The grain boundary chemistry of the AA alloys was investigated by Natishan and coworkers, using high resolution scanning Auger electron spectroscopy.[10,18] It was found that, although the alloys had a similar bulk composition, the AA-2 alloy exhibited a moderate amount (~20%) of graphitic C at the grain boundaries, whereas the AA-1 alloy contained only a small amount (1%-3%) of grain boundary C.

Details of the electrochemical cell and instrumentation were given previously.[19] The test electrodes of each alloy consisted of a 1.27-cm length of rod (as-supplied or machined) press-fitted into a polytetrafluoroethylene sheath so that only the planar end surface was exposed to the electrolyte. The surface was polished before each experiment with SiC paper and then 0.05-μm alumina powder. The electrolyte contained 1 mol L^{-1} acetic acid (CH_3COOH) and 1 mol L^{-1} sodium acetate (CH_3COONa) with 15 ppm As_2O_3 and was deaerated continuously with Ar before and throughout data acquisition. The potentials were measured with respect to a saturated calomel electrode (SCE). All tests were performed at 22 ± 1°C.

The test electrode was cathodically charged with H at a constant potential E_c for a time t_c, after which the potential was stepped in the positive direction to a value 10 mV negative of the open-circuit potential E_{oc}. Anodic current transients were obtained over a range of charging times, typically from 5 to 60 s, at different overpotentials ($\eta = E_c - E_{oc}$). The open-circuit potential of the

test electrode was measured immediately before each charging time and was also used to monitor the stability of the alloy surface.

RESULTS

The current transients were analyzed using a diffusion/trapping model that was based on a constant entry flux of H at the surface.[19,20] According to the model, the total anodic charge (C m^{-2}) is given by

$$q'(\infty) = FJt_c\{1 - e^{-R}/(\pi R)^{1/2} - [1 - 1/(2R)]\mathrm{erf}(R^{1/2})\} \quad (1)$$

where F is the Faraday constant, J is the ingress flux in mol m^{-2} s^{-1}, and $R = k_a t_c$. The charge $q'(\infty)$ is equated to the charge (q_a) passed during the experimental anodic transients. q_a can be associated entirely with absorbed H, since the adsorbed charge is almost invariably negligible. k_a is an apparent trapping constant measured for irreversible traps in the presence of reversible traps. It is related to the irreversible trapping constant by kD_a/D_L, where D_a is the apparent diffusivity and D_L is the lattice diffusivity of H.

For the constant flux model to be applicable, it must be possible to determine a trapping constant for which J is independent of charging time. Equation (1) could in fact be fitted to the experimental data for q_a to obtain values of k_a and J that satisfy this requirement at each potential.

Values of k_a and J for tests on Be-Cu are given in Table 2. k_a was found to be independent of charging potential, as is required for the model to be valid, because the trapping characteristics should be unaffected by electrochemical conditions at the metal surface unless the traps become filled to a significant extent. The overall mean values of k_a were 0.045 ± 0.006 s^{-1} for the unaged alloy and 0.042 ± 0.009 s^{-1} for the aged alloy. Aging therefore did not have a significant effect on k_a.

The flux for both unaged and aged Be-Cu was constant over the range of charging times for each overpotential and, as expected, increased with overpotential because of the dependence of J on the surface coverage of adsorbed H. Log J was found to vary linearly with η (Figure 1), indicating that the surface coverage responded rapidly to changes in potential.

Values of k_a and J for two tests on each heat of Alloy K-500 are given in Table 3. k_a appears to be independent of charging potential in both cases and has a mean value of 0.060 ± 0.006 s^{-1} for AA-1 and 0.063 ± 0.003 s^{-1} for AA-2. The flux for each heat typically showed only a slight dependence on overpotential.

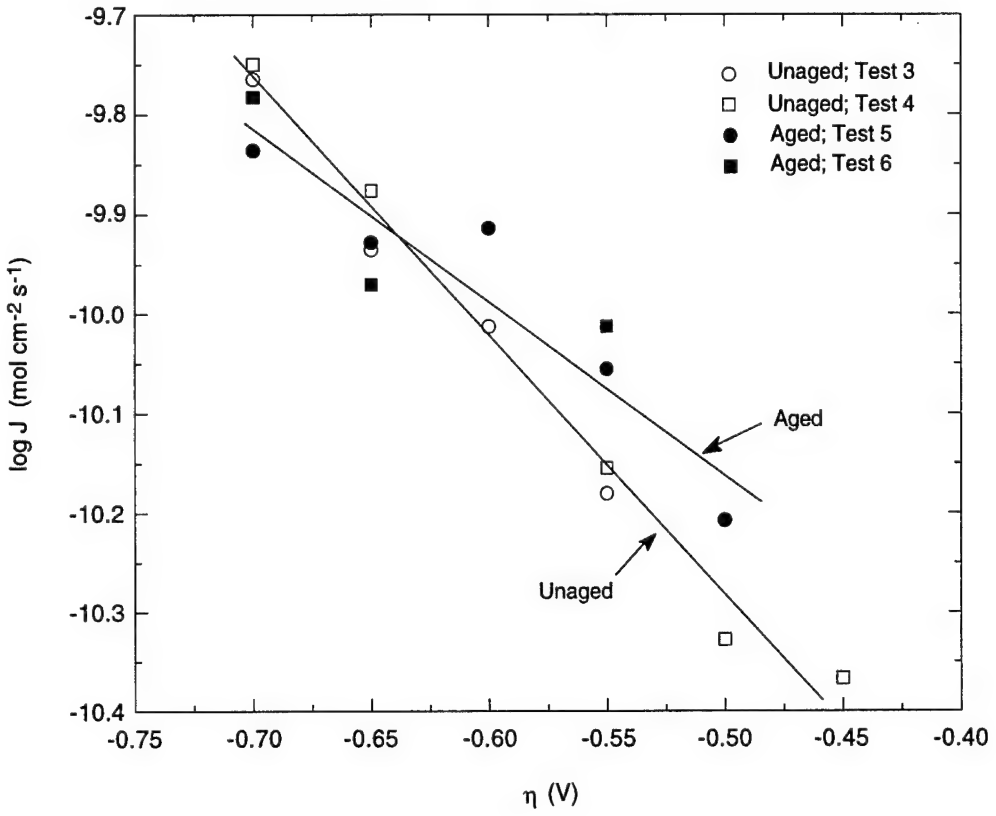

Figure 1. Dependence of entry flux on overpotential for Be-Cu in two identical tests.

DISCUSSION

Irreversible Trapping Constants

The irreversible trapping constants (k) were derived from k_a by using diffusivity data for the "pure" alloy to obtain the lattice diffusivity (D_L) and for the actual alloy to obtain the apparent diffusivity (D_a), so that the effect of reversible traps could be taken into account. The "pure" alloy (or metal in some cases) was considered to be Cu for Be-Cu and Cu-65Ni for Alloy K-500, so the minor alloying elements, either in their atomic form or as intermetallics precipitated during aging, were assumed to be largely responsible for reversible trapping in the actual alloys. For face-centered cubic alloys, defects such as vacancies or edge dislocations are unlikely to contribute significantly to reversible trapping, since the binding energy of H to such defects is a factor of 4 smaller than the activation energy for diffusion.[21]

Alloy K-500 — The lattice diffusivity was determined by interpolation of data for a range of binary Cu-Ni alloys and was found to be $(3.0 \pm 0.1) \times 10^{-14}$ m^2 s^{-1} for 35 wt% Cu-65% Ni at 25°C.[22] The level of Cu differs slightly between the 35Cu-65Ni alloy and Alloy K-500 (30Cu), but the error in using the diffusivity of the 35Cu alloy for D_L was considered negligible. The diffusivity for AA Alloy K-500 (assumed to be at ambient temperature) is 1.90×10^{-14} m^2 s^{-1}, which is slightly higher than the value of 1.48×10^{-14} m^2 s^{-1} for the DA alloy.[3] By using these data for D_L and D_a, k was found to be 0.095 ± 0.013 s^{-1} for the AA-1 alloy and 0.099 ± 0.008 s^{-1} for the AA-2 alloy.

Be-Cu — The diffusivity of H in α-Cu over the temperature range 47°-657°C is given by [22]

$$D = 9.0 \times 10^{-7} \exp [-43.5 \text{ (kJ/mol)}/RT] \text{ m}^2 \text{ s}^{-1} \quad (2)$$

Extrapolation to 25°C gave a value of 2.1×10^{-14} m^2 s^{-1}. In transition metals, defects that introduce an electron vacancy will attract H.[23] On this basis, Be is unlikely to attract H in Cu and therefore unlikely to significantly affect the diffusivity. Hence, D_a for unaged Be-Cu was assumed to be similar in value to D_L; therefore, in this case, $k \sim k_a$.

No data were available for the diffusivity in the aged alloy. However, in the case of Alloy K-500, the intermetallic particles appear to have little effect on D_a compared with that of the minor alloying elements in solid solution: D_a for the aged alloy was only about a factor of 2 smaller than D_L. Since most solutes introducing an electron vacancy provide reversible traps that could largely account for this factor, the intermetallics must be presumed to add little to the effect of the minor elements. Hence, it was assumed that the intermetallic particles in Be-Cu have only a small effect on D_a and that the value of D_L/D_a for DA Alloy K-500 represented the upper limit of this ratio for DA Be-Cu. k was therefore estimated to be $\leq 0.084 \pm 0.021$ s^{-1}.

Susceptibility to HE

Table 4 lists the irreversible trapping constants for the range of Cu-containing alloys. They are also presented graphically in Figure 2 to highlight differences between them. The unaged Be-Cu alloy has a higher k than that for unaged Alloy K-500 (unannealed CD) and thus is intrinsically more susceptible to HE. DA Be-Cu similarly has a higher intrinsic susceptibility than DA Alloy K-500.

The trapping behavior of Alloy K-500 was markedly affected by the type of heat treatment. The values of k were similar for the two AA specimens (yield strength of 689-724 MPa) but were more than twice as large as that for the DA specimen (yield strength of 1096 MPa). The k value for the aged 77Cu-15Ni alloy (yield strength of 793 MPa) previously studied is similar to that of DA Alloy K-500.[17]

Table 5 compares the value of k for aged Be-Cu with the values previously determined[24,25] for aged alloys 718 [UNS N07718] and A-286 [UNS S66286]. Also shown is the reduction of notched strength, which was determined for these three alloys from room temperature tensile tests in 69 MPa hydrogen.[26] The order of k values parallels the reduction of strength (Figure 3), so the intrinsic susceptibility, as represented by k, is consistent with the resistance to HE for these alloys.

Tests on Alloy K-500 showed that the decrease in elongation was the same (71%) for DA and AA specimens cathodically precharged for 16 days.[3] (The loss in ductility can be defined in terms of the percent decrease in elongation, analogously to the reduction of area [RA] used by other workers.[27,28]) However, the ultimate tensile strength shows a difference in behavior between the DA and AA alloys for the same precharging period. In the case of the AA alloy, the strength decreased by 35% over the 16 days, whereas the strength of the DA alloy actually increased slightly. Similarly, work by Hicks and Altstetter on aged alloys 718 and A-286 showed that, although the effect of H on notched tensile strength (NTS) is less marked than the effect on the RA, the difference in behavior between the two alloys was more pronounced for the NTS; the ratio of the decreases for the two alloys was 2.3 for the NTS compared with 1.5 for the RA.[29]

The tensile strength results indicate that AA Alloy K-500 is less resistant to HE than the DA alloy. Thus, the intrinsic susceptibilities (defined by k) for the two types of aged Alloy K-500 match their observed resistances to HE, implying that H trapping is a principal factor determining the HE resistance of Alloy K-500.

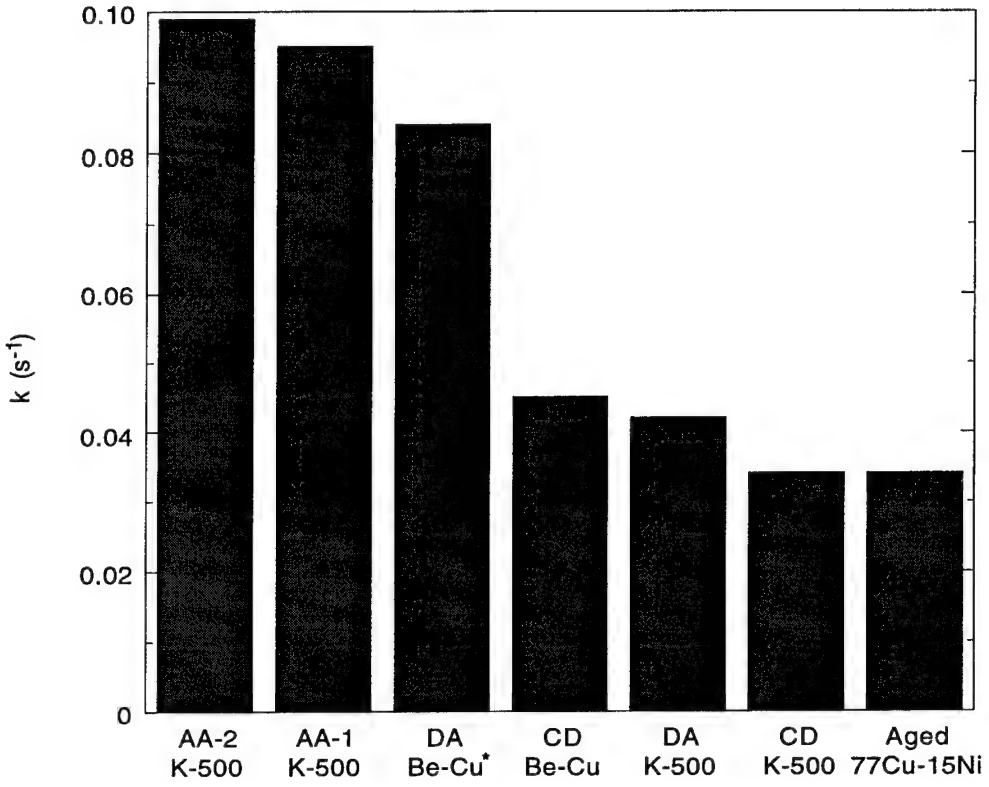

Figure 2. Variation in k for Be-Cu, the 77Cu-15Ni alloy, and Alloy K-500 in annealed and aged (AA), direct-aged (DA), and cold-drawn (CD) unannealed/unaged conditions.

*k shown is upper limit.

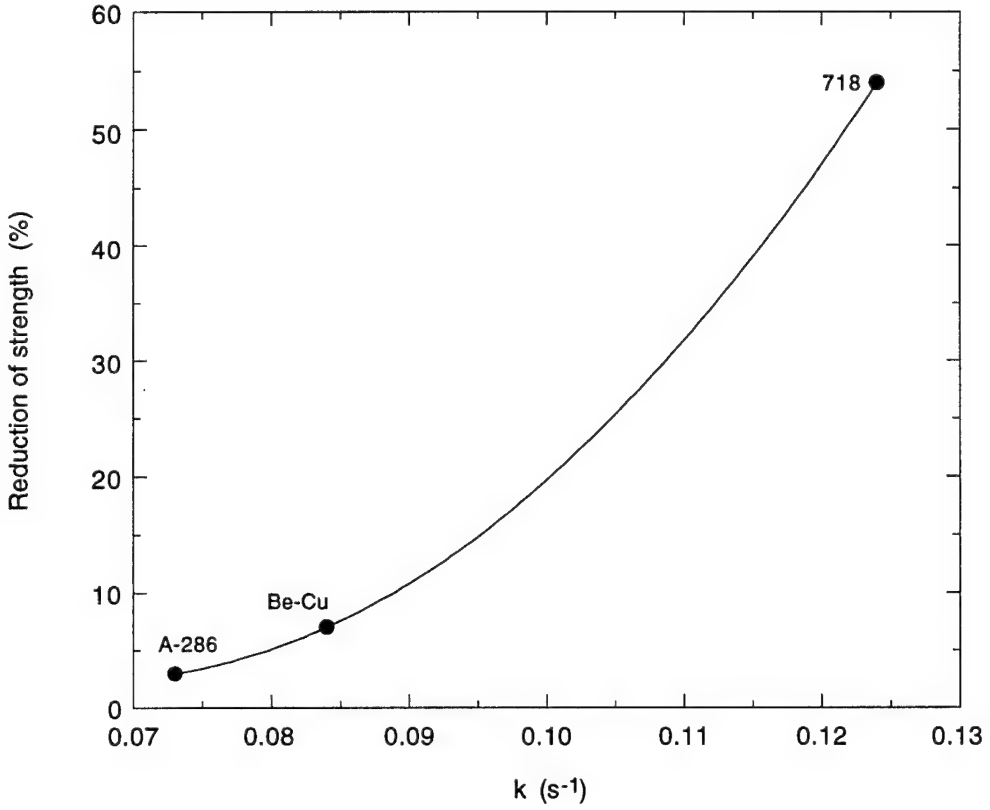

Figure 3. Variation of reduction of notched strength with k for Be-Cu* and alloys 718 and A-286.

*k shown is upper limit.

Identification of Irreversible Traps

The density of particles or defects (N_i) providing irreversible traps is related to k_a by Equation (3):

$$N_i = k_a a/(4\pi d^2 D_a) \quad (3)$$

where a is the diameter of the metal atom and d is the trap radius.[24,30] The value of a for an alloy is taken as the mean of the atomic diameters weighted in accordance with the atomic fraction of each element. The trap radius is estimated from the dimensions of heterogeneities that are potential irreversible traps, and trap densities are then calculated for the different values of d. In this way, the dominant irreversible trap can be identified by comparing the values of N_i with the actual concentrations of specific heterogeneities.

Be-Cu — The unaged alloy was examined under the scanning electron microscope and found to be free of any particles. Some microvoids were present and could account for part of the irreversible trapping. However, the principal irreversible traps appeared to be associated with some other heterogeneity, possibly grain boundaries.

Aged Be-Cu, as noted above, contains small, uniformly dispersed (Cu,Co)Be precipitates. Since k (and k_a) is proportional to d^2, small particles, even if numerous, tend to make a relatively small contribution to k. Moreover, small particles, as discussed previously,[16] are not expected to increase the intrinsic susceptibility (as determined by the irreversible traps). Also, trapping becomes more reversible as the coherency of a particle increases,[37] and it is possible that (Cu,Co)Be precipitates are not even irreversible traps. Thus, the principal irreversible traps in aged Be-Cu were more likely to have been the same as those in the unaged alloy.

Alloy K-500 — In the previous work on DA Alloy K-500, the irreversible traps predominantly encountered by H in Alloy K-500 were assumed to be provided by S segregated at grain boundaries.[17] This assumption was based on two factors: First, the intergranular HE of Ni and Ni-Co alloys, as noted above, is assisted by S segregated at grain boundaries and H also probably segregates to the grain boundaries as in Ni.[6] Second, in the case of alloys C-276 and UNS R30035, the calculated trap densities were in close agreement with the amount of grain boundary S and P distributed per unit volume of the alloy, whereas there were large differences between N_i and the bulk S-P content of these alloys.[16]

The absence of data for S segregation in Alloy K-500 meant that the identity of the principal irreversible traps could not be verified by comparing N_i with the grain boundary concentration in this case. However, it was apparent that the principal traps were not associated with matrix S, since N_i was about 3 orders of magnitude less than the S content of the alloy (1.6×10^{24} atoms

m^{-3}). Ti nitride/carbide particles present in Alloy K-500 were likewise ruled out as the principal traps because of a 2-orders-of-magnitude difference between the corresponding value of N_i and the particle concentration. Further support was provided by results for the 77Cu-15Ni alloy, which was found to have a higher trap density than the Alloy K-500 (65Ni-30Cu).[17] Even allowing for some difference in the degree of segregation between the two alloys, the higher trap density was consistent with a higher level of grain boundary segregants, based on the higher S-P content (0.015 wt%) of the 77Cu-15Ni alloy; in the case of Ni, the intergranular S concentration increases with the total S content,[31] and it seems reasonable to expect similar behavior for Ni-Cu alloys.

Aging increases the amount of grain boundary S in Ni.[31,32] However, the presence of Cu in Ni is thought to reduce the volume diffusion of S.[31] Such an effect would explain the small increase in k for Alloy K-500 with direct aging, thus supporting the assertion that grain boundary S is the principal irreversible trap in DA Alloy K-500. Additional evidence for the importance of segregated S was obtained by Bruemmer and coworkers, who examined the influence of S, P, and Sb on the intergranular HE of Ni and found that S was the critical segregant because of its large enrichment at the grain boundaries.[5] C and O were also observed on the fracture surfaces but were within the levels expected from adsorption in an ultra-high vacuum environment, as used for the elemental (Auger electron spectroscopic) analysis.

Recent work by Natishan and coworkers, however, has suggested that intergranular cracking of *annealed and aged* Alloy K-500 may be due to grain boundary C.[10,18,33] The two AA heats used by these workers were the same as those in the present study. An energy dispersive spectroscopic analysis did not detect known embrittling elements such as P and S on the fracture surfaces, but high-resolution scanning Auger electron spectroscopy showed graphitic C to be located on the intergranular facets and within grain boundaries.[10]

The AA and DA specimens show only minor differences between their compositions (Table 1), but microstructural differences clearly exist between the specimens, as indicated by their different values of k. The AA specimens have a lower yield strength but higher values of k, so the HE susceptibility of Alloy K-500 does not depend directly on strength. Instead, the differences in trapping and hence susceptibility must be related to the differences in thermomechanical processing that are presumably responsible for differences in the species at grain boundaries.

The main differences in heat treatment between the DA and AA specimens are the annealing step and the aging time (16 h for AA compared with 8 h for DA). In the case of Ni 200 (≤0.15 C), prolonged exposure between 425° and 650°C can cause graphite precipitation,[34] which has been found to occur at grain boundaries in Ni 200 aged for 24 h at 450° to 650°C.[32] Thus, aging time may be a key difference between the DA and AA Alloy K-500 with respect to graphite

precipitation. However, annealing may play the crucial role, since the AA specimens differed in heat treatment only with respect to annealing time yet exhibited levels of grain boundary C from 1%-3% (AA-1) up to >20% (AA-2). The implication is that annealing renders the alloy more prone to graphite precipitation during aging.

It is unclear why S was not detected at the grain boundaries in AA Alloy K-500. Although diffusion of S may be affected by the presence of Cu, S does segregate to grain boundaries in AA Ni 200 containing ≤0.25 Cu. However, Loier and Boos pointed out that the grain boundary S concentration in Ni (and presumably Ni alloys) can be influenced by up to seven factors: purity of the Ni (or alloy), total S content, heat treatment temperature and cooling rate, heat treatment time, treatment atmosphere, and grain boundary structure.[31] Although the effects of these factors on S segregation in Ni have been studied,[31] they have not been determined for Alloy K-500.

Lee and Latanision found that the effect of S segregation on intergranular HE of Ni was most prominent when the grain boundaries were free of graphite precipitates.[32] Accordingly, in the case of Alloy K-500, it is postulated that S governs HE of the DA alloy but C predominates in the AA alloy. If the respective critical segregants are S and C, k might be expected to be higher for the AA alloy, since the total content of C is over 2 orders of magnitude greater than that of S. This rationale is in fact consistent with the actual results showing that k is higher for the AA-1 and AA-2 alloys than for the DA alloy.

Role of Trapping

Alloy K-500 containing 1%-3% grain boundary C undergoes a sizable decrease in NTS (24% at -1.0 V and 48% at -1.5 V; the reference electrode was not specified) under cathodic polarization in seawater.[18,33] Thus, even a little grain boundary C, as in the AA-1 specimen, can render Alloy K-500 very susceptible to HE. Specimens containing little grain boundary C also exhibit a relatively high intrinsic susceptibility (represented by k), which matches the susceptibility observed in mechanical tests. The implication is that the C precipitates, through a combination of their size and number density, provide a trapping capability that is high enough in crack-sensitive (grain boundary) regions to cause a loss of mechanical properties.

The parallel between the intrinsic susceptibility (k) and the resistance to HE (based on tensile strength) for DA and AA Alloy K-500 suggests that the AA-1 and AA-2 specimens, on the basis of their k values, should have a similar resistance to HE. However, Natishan and Poor found that AA specimens containing more than 15% grain boundary C exhibited little effect (4%) of H on the NTS at -1.0 V, though a larger effect (38%) was observed at -1.5 V.[18,33] Hence, it would initially appear that the trapping constants do not match the HE resistance of the AA alloys. The apparent lack of consistency is explained by the fact that the grain boundary C itself can cause

brittle intergranular fracture in Alloy K-500.[10] Thus, the degradation of AA-2's mechanical properties at lower potentials will be dominated by embrittlement resulting from extensive amounts of grain boundary C.

Natishan and Poor concluded that the presence of significant amounts of grain boundary C causes intergranular fracture to such an extent that further fracture due to H is minimal until large amounts of H are generated at the crack tip.[18] The k values for the AA alloys should therefore be compared only with the decrease in NTS under high cathodic polarization. At -1.5 V, the decreases in NTS due to H alone are roughly comparable (48% versus 38%) for the AA-1 and AA-2 alloys, especially if allowance is made for the fact that the embrittling effect of C probably influences that of H. The comparison based on changes in NTS at highly cathodic potentials indicates that the trapping constants are in fact consistent with the observed resistance to embrittlement associated primarily with H.

If the relatively high k for AA Alloy K-500 is associated with grain boundary C, the difference in the amounts of grain boundary C between AA-1 and AA-2 would be expected to result in a difference in their k values. However, the value of k for AA-2 with a moderate amount of grain boundary C is only slightly higher than that for AA-1 with relatively little grain boundary C; in fact, the values are essentially the same within the limits of uncertainty. The similarity in the k values suggests that the grain boundary C in AA-2 offers little more trapping capability ($N_i d^2$) than is found in AA-1.

Natishan and coworkers found that some grain boundary graphite precipitates were discrete while others formed a continuous coating.[10] At high levels of grain boundary C, the presence of continuous precipitates as well as discrete precipitates may result in a higher average d but a lower effective N_i compared with the values at low C levels, such that $N_i d^2$ and therefore k increase only slightly with the amount of grain boundary C.

A modification of this hypothesis is that the discrete C governs the irreversible trapping behavior, with the continuous films making only a minor contribution. Lee and Latanision speculated that for Ni 200 the graphite particles precipitated at grain boundaries act as discrete traps for H.[32] If the discrete graphitic C precipitates in Alloy K-500 are the main contributers to irreversible trapping, the similarity in trapping constants implies that the amount of discrete C differs little between specimens with high and low grain boundary C. This lack of difference in discrete C is possible, since at high levels of grain boundary C a large part of the C precipitate occurred as continuous films.

Discrete precipitates of titanium and iron carbides were also found to be present within grains and at grain boundaries in AA Alloy K-500.[10] These precipitates are known to be

irreversible traps in steels[14] and might play a similar role in Alloy K-500. However, this possibility can probably be discounted, since the density of carbide precipitates tends to decrease as the amount of grain boundary C increases. A decrease in the density of precipitates should cause a decrease in k, which is contrary to the observed behavior.

SUMMARY

- Unaged Be-Cu has a higher k than unaged (unannealed CD) Alloy K-500 and therefore is intrinsically more susceptible to HE. DA Be-Cu similarly has a higher intrinsic susceptibility than DA Alloy K-500. The intrinsic susceptibility for aged Be-Cu and Alloys 718 and A-286 can be correlated with their observed resistance to HE.
- The trapping behavior of Alloy K-500 is markedly affected by the type of heat treatment. The values of k were similar for the two AA specimens but were more than twice as large as that for the DA specimen. The intrinsic susceptibilities, as defined by k, for AA and DA Alloy K-500 match their observed resistances to HE. Hence, H trapping is a principal—possibly predominant—factor determining the HE resistance of Alloy K-500.
- The primary irreversible traps in Alloy K-500 are believed to involve grain boundary S in the DA alloy and graphitic C in the AA alloy. The small increase in k for Alloy K-500 with direct aging is consistent with limited volume diffusion of S in the presence of Cu. In addition, the order of k values for the DA and AA alloys appears to be consistent with the bulk content of their critical segregants (S and C, respectively).
- A comparison of the trapping constants with HE resistance for the two AA alloys is complicated by embrittlement resulting from extensive amounts of grain boundary C. However, under high cathodic polarization, the trapping constants are consistent with the observed resistances to embrittlement associated primarily with H.
- Higher levels of grain boundary C in Alloy K-500 provide little additional trapping capability. The presence of continuous as well as discrete precipitates may result in a larger average trap size but a lower effective trap density compared with the values at low C levels. Another possibility is that the discrete C precipitates govern the irreversible trapping behavior.

ACKNOWLEDGMENTS

Financial support of this work by the U.S. Office of Naval Research under Contract N00014-91-C-0263 is gratefully acknowledged. The author is also grateful to Dr. M. Natishan,

formerly at the David Taylor Research Center, Department of the Navy, and now at the University of Maryland, for providing samples and information on the two heats of Alloy K-500.

REFERENCES

1 Metals Handbook, Vol. 2: Properties and Selection: Nonferrous Alloys and Pure Metals, 9th ed. (Materials Park, OH: ASM International, 1979), p. 303.

2. Monel Nickel-Copper Alloys, 4th ed. (Huntington, WV: Huntington Alloys, 1981).

3. J. A. Harris, R. C. Scarberry, C. D. Stephens, Corrosion 28, 2 (1972): p. 57.

4. R. M. Latanision, H. Opperhauser, Jr., Metall. Trans. 5, 2 (1974): p. 483.

5. S. M. Bruemmer, R. H. Jones, M. T. Thomas, D. R. Baer, Metall. Trans. 14A, 2 (1983): p. 223.

6. D. H. Lassila, H. K. Birnbaum, Acta Metall. 35, 7 (1987): p. 1815.

7. J. D. Frandsen, H. L. Marcus, A. S. Tetelman, in Effect of Hydrogen on Behavior of Materials, eds. A. W. Thompson, I. M. Bernstein (Warrendale, PA: The Metallurgical Society of AIME, 1976), p. 299.

8. W. C. Johnson, J. E. Doherty, B. H. Kear, A. F. Giamei, Scripta Metall. 8, 8 (1974): p. 971.

9. Metals Handbook, Vol. 9: Metallography and Microstructures, 9th ed. (Materials Park, OH: ASM International, 1985), p. 436.

10. M. E. Natishan, E. R. Sparks, M. L. Tims, in ISTFA '90: Proceedings of the International Symposium for Testing and Failure Analysis (Materials Park, OH: ASM International, 1990), p. 385.

11. G. K. Dey, P. Mukhopadhyay, Mats. Sci. Eng. 84, 1-2 (1986): p. 177.

12. B. J. Berkowitz, R. D. Kane, Corrosion 36, 1 (1980): p. 24.

13. R. D. Kane, B. J. Berkowitz, Corrosion 36, 1 (1980): p. 29.

14. I. M. Bernstein, G. M. Pressouyre, in Hydrogen Degradation of Ferrous Alloys, eds. R. A. Oriani, J. P. Hirth, M. Smialowski (Park Ridge, NJ: Noyes Publications, 1985), p. 641.

15. G. M. Pressouyre, I. M. Bernstein, Acta Metall. 27, 10 (1979): p. 89.

16. B. G. Pound, in Proceedings of the Fifth International Conference on Hydrogen Effects on Material Behavior, eds. N. R. Moody, A. W. Thompson (Warrendale, PA: The Minerals, Metals & Materials Society, 1994), in press.

17. B. G. Pound, Corrosion 50, 4 (1994): p. 301.

18. M. E. Natishan, W. C. Porr, Jr., "Issues Surrounding the Use of Nickel-Copper Alloy K-500 Fasteners in Seawater," CORROSION/94 (Houston, TX: NACE, 1994).

19. B. G. Pound, Corrosion 45, 1 (1989): p. 18.

20. R. McKibbin, D. A. Harrington, B. G. Pound, R. M. Sharp, G. A. Wright, Acta Metall. 35, 1 (1987): p. 253.

21. W. D. Wilson, S. C. Keeton, in Advanced Techniques for Characterizing Hydrogen in Metals, eds. N. F. Fiore, B. J. Berkowitz (Warrendale, PA: The Metallurgical Society of AIME, 1981), p. 3.

22. H. Hagi, Trans. Jpn. Inst. Metals, 27, 4 (1986): p. 233.

23. G. M. Pressouyre, Metall. Trans. 10A, 10 (1979): p. 1571.

24. B. G. Pound, Acta Metall. 38, 12 (1990): p. 2373.

25. B. G. Pound, "Hydrogen Trapping in High-Strength Iron-Base Alloys," submitted to Acta Metall. Mater.

26. R. J. Walter, R. P. Jewett, W. T. Chandler, Mater. Sci. Eng. 5, 2 (1969/70): p. 99.

27. A. W. Thompson, J. A. Brooks, Metall. Trans. 6A, 7 (1975): p. 1431.

28. A. W. Thompson, Metall. Trans. 7A, 2 (1976): p. 315.

29. P. D. Hicks, C. J. Alstetter, in Proceedings of the Fourth International Conference on Hydrogen Effects on Material Behavior, eds. N. R. Moody, A. W. Thompson (Warrendale, PA: The Minerals, Metals & Materials Society, 1990), p. 613.

30. B. G. Pound, R. M. Sharp, G. A. Wright, Acta Metall. 35, 1 (1987): p. 263.

31. C. Loier, J-Y. Boos, Metall. Trans. 12A, 7 (1981): p. 1223.

32. T.S.F. Lee, R. M. Latanision, Metall. Trans. 18A, 9 (1987): p. 1653.

33. M. E. Natishan, W. C. Porr, Jr., "The Effect of Grain Boundary Carbon on the Hydrogen Assisted Intergranular Failure of Nickel-Copper Alloy K-500 Fastener Material," ASTM STP 1236 on Structural Integrity of Fasteners, ed. P. Toor (Philadelphia, PA: ASTM, 1995).

34. Huntington Alloys Bulletin 10M2-79T-15 (Huntington, WV: Huntington Alloys Inc., 1979).

TABLE 1

Composition (wt%) of Cu-containing alloys

Element	K-500 DA	K-500 AA-1	K-500 AA-2	77Cu-15Ni
Al	2.92	2.95	2.95	1.61
C	0.16	<0.17	<0.14	0.010
Cr				0.40
Cu	29.99	29.53	29.8	76.8
Fe	0.64	<0.85	<0.74	0.96
Mg				0.02
Mn	0.72	<0.70	<0.58	4.36
Nb				0.69
Ni	64.96	65.29	65.1	15.00
P			<0.002	0.010
Pb				0.007
S	0.001	<0.001	<0.001	0.005
Si	0.15	<0.05	<0.15	0.05
Sn				<0.02
Ti	0.46	0.46	0.44	
Zn				0.02

TABLE 2

Values of k_a and J for Be-Cu

State	Test	η (V)	E_c (V/SCE)	k_a (s^{-1})	J (nmol cm^{-2} s^{-1})	Mean k_a
Unaged	1	-0.55	-0.696	0.035	0.066	
		-0.60	-0.746	0.048	0.097	
		-0.65	-0.780	0.049	0.116	0.047 ± 0.006
		-0.70	-0.836	0.054	0.172	
	2	-0.45	-0.620	0.045	0.043	
		-0.50	-0.659	0.038	0.047	
		-0.55	-0.694	0.035	0.070	0.044 ± 0.006
		-0.65	-0.778	0.051	0.133	
		-0.70	-0.841	0.052	0.178	
Aged	3	-0.50	-0.676	0.030	0.062	
		-0.55	-0.714	0.039	0.088	
		-0.60	-0.767	0.055	0.122	0.038 ± 0.007
		-0.65	-0.819	0.035	0.118	
		-0.70	-0.868	0.031	0.146	
	4	-0.55	-0.702	0.054	0.097	
		-0.65	-0.788	0.033	0.107	0.045 ± 0.008
		-0.70	-0.851	0.047	0.165	
	5	-0.50	-0.665	0.044	0.077	
		-0.55	-0.708	0.061	0.120	
		-0.65	-0.797	0.046	0.142	0.046 ± 0.007
		-0.70	-0.867	0.034	0.145	

TABLE 3

Values of k_a and J for Alloy K-500

Heat	Test	η (V)	E_c (V/SCE)	k_a (s^{-1})	J (nmol cm^{-2} s^{-1})	Mean k_a
AA-1	6	-0.25	-0.366	0.059	0.048	
		-0.30	-0.411	0.051	0.046	
		-0.35	-0.461	0.062	0.051	0.061 ± 0.006
		-0.40	-0.511	0.070	0.055	
	7	-0.25	-0.364	0.058	0.043	
		-0.30	-0.411	0.045	0.040	
		-0.35	-0.460	0.063	0.059	0.059 ± 0.006
		-0.40	-0.509	0.061	0.052	
		-0.45	-0.558	0.069	0.053	
AA-2	8	-0.25	-0.340	0.059	0.073	
		-0.30	-0.388	0.065	0.093	
		-0.35	-0.437	0.068	0.120	0.063 ± 0.004
		-0.40	-0.489	0.060	0.104	
	9	-0.30	-0.392	0.066	0.105	
		-0.35	-0.443	0.059	0.108	
		-0.40	-0.490	0.062	0.111	0.064 ± 0.003
		-0.45	-0.537	0.067	0.107	

TABLE 4

Trapping Constants for Cu-Containing Alloys

Alloy	State	Yield Strength (MPa)	k_a (s^{-1})	D_L/D_a	k (s^{-1})
K-500	AA-1	689-724	0.060 ± 0.006	1.6	0.095 ± 0.013
K-500	AA-2	689-724	0.063 ± 0.003	1.6	0.099 ± 0.008
Be-Cu	Aged	~860	0.042 ± 0.009	≤2.0	≤0.084 ± 0.021
Be-Cu	Unaged	585-613	0.045 ± 0.006	~1	0.045 ± 0.006
K-500	DA	1096	0.021 ± 0.003	2.0	0.042 ± 0.007
K-500	CD-Unaged	758	0.017 ± 0.003	2.0	0.034 ± 0.007
77Cu-15Ni	Aged	793	0.034 ± 0.004	~1	0.034 ± 0.015

TABLE 5

Comparison of Aged Be-Cu with Aged Alloys 718 and A-286

Alloy	k (s^{-1})	Reduction of strength (%)
718	0.124 ± 0.024	54
Be-Cu	<0.084 ± 0.021	7
A-286	0.073 ± 0.031	3

The Ingress of Hydrogen into a Superferritic Stainless Steel*

ABSTRACT

The ingress of hydrogen into a superferritic stainless steel — UNS S44660 in its standard grade, its hydrogen-resistant grade, and an intermediate grade — was studied using a technique referred to as hydrogen ingress analysis by potentiostatic pulsing (HIAPP). Anodic current transients were obtained for these alloys in 1 mol L^{-1} acetic acid/1 mol L^{-1} sodium acetate, but the three grades of UNS S44660 proved difficult to investigate in terms of trapping. In all cases, the hydrogen entry flux was still low up to a charging potential of -0.6 V (SCE) when the surface oxide began to change markedly in its electrochemical behavior. As a result of the low flux, negligible hydrogen entered the alloys, and so their trapping characteristics could not be determined. On the other hand, it was clear that the surface oxides were effective barriers to hydrogen entry and therefore that these superferritics should be resistant to hydrogen embrittlement (HE) in mildly acidic or near-neutral solutions, at least at potentials less cathodic than -0.6 V (SCE). The propensity of superferritics to undergo HE in seawater when they are cathodically polarized to potentials in the range -0.9 to -1.4 V (SCE) may result from changes in the oxide leading to a less restricted entry of hydrogen into the alloy. An effective way of rendering the UNS S44660 alloy more resistant to HE is to reduce the intrinsic susceptibility by controlling the number and type of carbide particles, as has apparently been done for the hydrogen-resistant grade.

INTRODUCTION

Superferritic stainless steels such as Sea-Cure† (UNS S44660) and 29-4C (UNS S44735) are used for tubes in power plant condensers that are seawater-cooled. In many cases, the waterboxes and tube sheets in the condensers must be cathodically protected. However, the superferritics exhibit hydrogen embrittlement (HE) when they are polarized to potentials in the range -0.9 to -1.4 V (SCE).[1] This problem led to the development of a grade of the UNS S44660 alloy that is reportedly resistant to HE at cathodic potentials up to -2.0 V (SCE).[2] The new grade, which is designated as Sea-Cure Hy-Resist†, was obtained by restricting the combined C and N content to a maximum of 0.02% and replacing Ti by Nb. These compositional changes are presumed to affect the alloy's intrinsic susceptibility to HE by modifying the number and type of carbide particles, which are known to be strong hydrogen traps.[3] Thus, the differences observed

---

* To be submitted.

† Trade names of Crucible Materials Corporation, Pittsburgh, PA.

in the HE resistance for the UNS S44660 alloy and its hydrogen-resistant grade should correspond to differences in their hydrogen trapping characteristics. In other words, the improvement in the HE resistance with the changes in stabilizing elements and impurity elements suggests that hydrogen trapping plays a crucial role in determining the resistance of these alloys to HE at highly cathodic potentials.

The entry and trapping of hydrogen in various alloys have been investigated in recent work using an electrochemical technique referred to as hydrogen ingress analysis by potentiostatic pulsing (HIAPP).[4] Values were determined for the rate of hydrogen entry and the rate constant for irreversible trapping (k). In addition, the trapping constants were analyzed to determine the density of particles or defects (N_i) providing irreversible traps. The objective of the present study was to determine the rate of H entry and trapping constants in the UNS S44660 alloy in its standard grade, its hydrogen-resistant grade, and an intermediate grade. The research was aimed at characterizing the intrinsic susceptibility in each case to HE in terms of the irreversible trapping constant and then relating the intrinsic susceptibility to the observed resistance to HE.

EXPERIMENTAL PROCEDURE

The thickness and composition of each grade of the stainless steel are given in Table 1. The stabilizing element is Ti in the standard grade and Nb in the hydrogen-resistant grade, whereas the intermediate grade contains both elements. The other significant difference is that the hydrogen-resistant grade has much less C and N than either of the other grades. A minor change was also made in that small amounts of Cu and Al were added to the intermediate and hydrogen-resistant grades.

Details of the electrochemical cell and instrumentation have been given previously.[5] The three grades of UNS S44660 were supplied as sheet. Test electrodes were fabricated by machining a disk (1.27 cm in diameter) from each sheet and press-fitting it into a polytetrafluoroethylene sheath so that only one surface was exposed. The electrode surface was polished before each experiment with SiC paper followed by 0.05-μm alumina powder. The electrolyte contained 1 mol L^{-1} acetic acid and 1 mol L^{-1} sodium acetate with 15 ppm As_2O_3 and was deaerated continuously with argon before and throughout data acquisition. The potentials were measured with respect to a saturated calomel electrode (SCE). All tests were performed at 22 ± 1°C.

The test electrode was charged with hydrogen at a constant potential E_c for times from 5 s to 60 s. Anodic current transients with a charge q_a were obtained for the different charging times at selected cathodic overpotentials ($\eta = E_c - E_{oc}$). The open-circuit potential (E_{oc}) of the test electrode was sampled immediately before each pulse and was also used to monitor the stability of the alloy surface.

TABLE 1
Composition (wt%) and Thickness of the UNS S44660 Alloy and Modified Grades

Element	Standard	Intermediate	H-Resistant
Al		0.058	0.09
C	0.018	0.027	0.006
Cr	27.00	27.18	26.90
Cu		0.11	0.06
Fe	66.45	65.66	66.53
Mn	0.26	0.38	0.36
Mo	3.40	3.26	3.51
Nb+Ta		0.37	0.26
N	0.025	0.025	0.006
Ni	1.99	1.96	1.92
P	0.021	0.029	0.025
S	0.001	0.001	0.001
Si	0.40	0.66	0.33
Ti	0.44	0.28	
Thickness (mm)	2.3	2.1	2.6

RESULTS

For most alloys, the charge (q_a) associated with the current transients can be analyzed using a diffusion/trapping model that has been derived for conditions imposed by the pulse technique.[6] The analysis yields values of the ingress flux (J) and an apparent trapping constant (k_a), which is used to determine the rate constant for irreversible trapping (k). However, all three grades of the UNS S44660 alloy showed little change in q_a with charging time at cathodic potentials up to about -0.6 V (SCE). Around this potential, E_{oc} showed a significant negative shift between each charging time. As a result, meaningful data could not be obtained because E_c was not maintained constant and because the shift indicated a change in the electrochemical behavior of the surface oxide.

It was evident that the hydrogen entry flux does not increase enough with overpotential to become significant before the oxide changes. Thus, q_a must correspond almost entirely to oxidation of the adsorbed layer of hydrogen. If the adsorbed hydrogen is assumed to respond very rapidly to a change in potential, the surface coverage might be expected to exhibit an exponential dependence on overpotential. For all three alloys, log q_a was found to vary linearly with η (Fig.

1), which suggests that Nernstian-type conditions do in fact exist at the surface of the alloys with respect to the discharge reaction.

DISCUSSION

The amount of hydrogen that entered the standard UNS S44660 alloy and its other two grades during cathodic charging appears to have been negligible, as implied by the lack of change in q_a. As a result, the trapping constants could not be evaluated for any of the grades. On the other hand, the results did indicate that the surface oxides formed on these alloys in the acetate solution (pH 4.8) were effective barriers to hydrogen entry and therefore that these superferritics should be resistant to HE in mildly acidic or near-neutral solutions, at least at potentials less cathodic than -0.6 V (SCE). When the oxide changed at more cathodic potentials, hydrogen gas was evolved rapidly enough to produce bubbles on the alloy surface in the acetate solution.

The behavior of the UNS S44660 alloy is consistent with that observed for superferritics under cathodic protection in seawater. The propensity of superferritics to undergo HE in seawater when they are cathodically polarized to potentials in the range -0.9 to -1.4 V (SCE) may result from changes in the oxide leading to less restricted entry of hydrogen into the alloy. Changes in the alloying elements that are designed to produce a modified surface oxide, and hence a modified rate of hydrogen entry, are unlikely to have a major effect at highly cathodic potentials. Therefore, in the absence of coatings, the most effective way of rendering the UNS S44660 alloy more resistant to HE is to reduce the intrinsic susceptibility by controlling the number and type of carbide particles, as has apparently been done for the hydrogen-resistant grade. It may be possible to determine the trapping constants of the three grades of the UNS S44660 alloy by coating the surface with palladium to enhance hydrogen entry at cathodic potentials where the oxide would be stable.

SUMMARY

- The surface oxides on the three grades of the UNS S44660 alloy were effective barriers to hydrogen entry. Hence, these alloys should be resistant to HE in mildly acidic or near-neutral solutions at potentials in the range of oxide stability.
- The propensity of superferritics to undergo HE in seawater when they are cathodically polarized to potentials in excess of -0.9 V (SCE) may result from changes in the oxide leading to less restricted entry of hydrogen into the alloy.

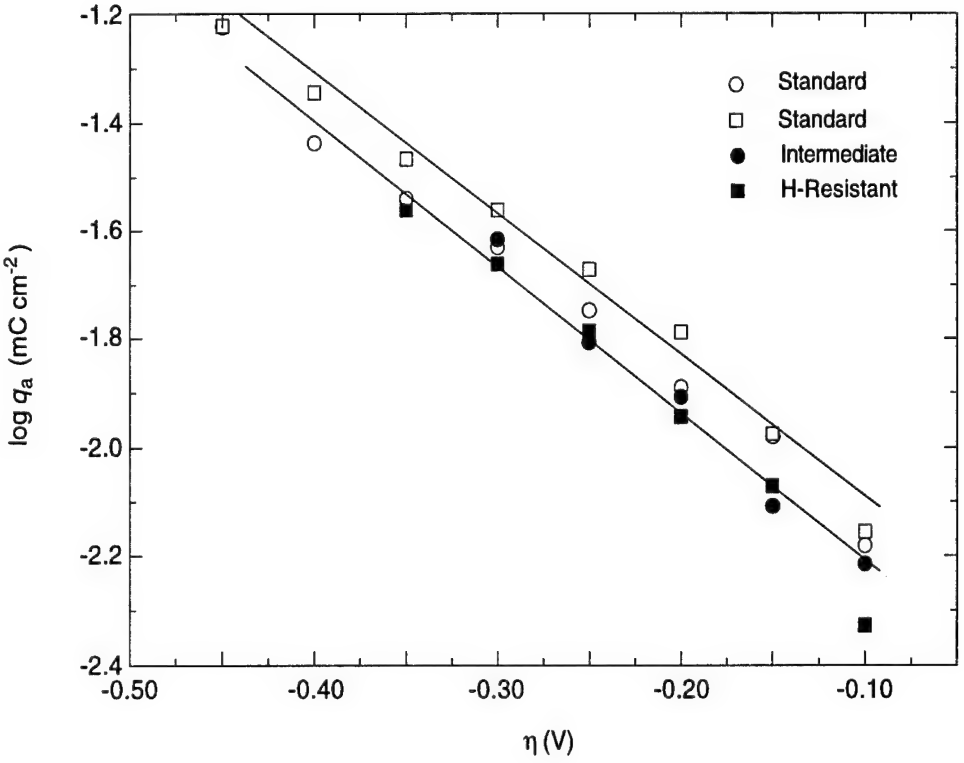

Figure 1. Dependence of log q_a on overpotential for the three grades of the UNS S44660 alloy. The two sets of data shown for the standard grade were obtained from identical tests.

- The HE resistance of the UNS S44660 alloy is most effectively improved by reducing the intrinsic susceptibility in terms of carbide particles, since changes to the surface oxide and hence the rate of hydrogen entry are expected to have only a secondary effect at highly cathodic potentials.

ACKNOWLEDGEMENTS

Financial support of this work by the U.S. Office of Naval Research under Contract N00014-91-C-0263 is gratefully acknowledged. The author is also grateful to Mr. J. Eckenrod of Crucible Research for supplying samples of the three grades of the UNS S44660 alloy.

REFERENCES

1. J. F. Grubb and J. R. Maurer, "Use of Cathodic Protection with Superferritic Stainless Steels," CORROSION/84, Paper No. 28, (National Association of Corrosion Engineers, Houston, TX, 1984).

2. Crucible Materials Corporation, U.S. Patent No. 4942922; *Sea-Cure Hy-Resist* (UNS S44660), Data Sheet (Trent Tube, East Troy, WI).

3. I. M. Bernstein and G. M. Pressouyre, in *Hydrogen Degradation of Ferrous Alloys*, eds. R. A. Oriani, J. P. Hirth, and M. Smialowski (Noyes Publications, Park Ridge, NJ, 1985), p. 641.

4. B. G. Pound, in *Proceedings of the Fifth International Conference on Hydrogen Effects on Material Behavior*, eds. N. R. Moody and A. W. Thompson (The Minerals, Metals & Materials Society, Warrendale, PA, 1994), in press.

5. B. G. Pound, *Corrosion* **45**, 18 (1989).

6. R. McKibbin, D. A. Harrington, B. G. Pound, R. M. Sharp, and G. A. Wright, *Acta Metall.* **35**, 253 (1987).

HYDROGEN TRAPPING IN AGED β-TITANIUM ALLOYS*

Abstract—Hydrogen trapping in three β-titanium alloys (unaged and aged Ti-15V-3Cr-3Al-3Sn and Beta-21S, and partially aged Beta-C) was investigated using a potentiostatic pulse technique. The apparent trapping constant (k_a) and hydrogen entry flux were determined for each alloy in 1 mol L^{-1} acetic acid/1 mol L^{-1} sodium acetate. The results were compared with those for other β-Ti alloys (Ti-10-2-3, Ti-13-11-3, and fully aged Beta-C) studied previously. Aging caused a negligible change in k_a for Ti-15-3, whereas a marked increase was observed for Beta-21S and the other β-Ti alloys. Among the aged alloys, Ti-13-11-3 had the highest value of k_a and Ti-15-3 had the lowest value. The intrinsic suceptibilities of Beta-C and Beta-21S to hydrogen embrittlement (HE), as represented by the trapping constants, were comparable and significantly higher than that of Ti-15-3. The susceptibilities were consistent with the relative resistances to HE observed for these alloys.

INTRODUCTION

Beta-titanium alloys can be aged to produce high yield strengths, but many of these alloys are susceptible to environmentally induced cracking in aqueous solutions under certain conditions [1-6]. This cracking susceptibility has been attributed in various cases to the α phase precipitated during aging. Ti-11.5Mo-6Zr-4.5Sn (Beta III) undergoes predominantly intergranular cracking in aqueous halide solutions, and it was postulated that this cracking is linked to an almost continuous α film at the grain boundaries [1]. Solution-treated and aged Ti-3Al-8V-6Cr-4Mo-4Zr (Beta-C) could also be made to crack during exposure in a chloride solution, whereas the solution-treated (unaged) alloy was immune to cracking under the same conditions [2]. In this case, it was uncertain whether stress level or microstructure was the controlling factor, but the argument was made that if hydrides were involved, the aged Beta-C with its α phase would have been more susceptible to cracking than the unaged alloy.

Young and Gangloff found that aged Ti-15Mo-3Nb-3Al (Beta-21S) was susceptible to cracking under a rising load in a chloride solution, whereas aged Ti-15V-3Cr-3Al-3Sn (Ti-15-3) was immune under the test conditions [4]. Cracking in the Beta-21S occurred intergranularly, with intermittent crack bursts over distances exceeding the crack tip process zone and on the order of

* Submitted to *Acta Metallurgica et Materialia.*

one to five grain diameters. Young and Gangloff suggested, on the basis of these bursts, that hydrogen environment-assisted cracking (HEAC) was involved, with grain boundary traps playing an important role. They noted that intergranular cracking is common for hydrogen-embrittled high-strength steels and reasoned that cracking of β-Ti alloys can be attributed to hydrogen embrittlement (HE), particularly because α/β-Ti alloys are susceptible to HE and because gaseous hydrogen and cathodically precharged hydrogen embrittle β-Ti alloys. Young and Gangloff speculated that the susceptibility of Beta-21S to intergranular cracking was due to extensive α precipitation at β grain boundaries and possibly to its high yield strength relative to that of Ti-15-3 [4]. Several factors were identified that could cause a sensitivity to grain boundary α: hydrogen trapping at α/β interfaces, formation of a brittle continuous hydride (in effect, a special case of trapping), hydrogen interaction with stress/strain concentrations produced by localized plastic deformation in the α phase, and local dissolution of the α phase.

Work by Young and Scully showed that Beta-21S cathodically precharged with hydrogen also undergoes intergranular cracking under certain conditions [7]. They suggested that preferential α precipitation at β grain boundaries could provide a continuous path for localized hydriding of the α phase and subsequent fracture, although bulk hydriding of the α phase was not detected. Even without hydriding, the α/β interfaces could provide trap sites, as noted by Young and Scully, and accumulation of hydrogen at these interfaces could result in fracture.

Further results for cathodically precharged Ti-15-3 and 21S indicated that persistent planar slip exacerbates HE [8] and that both preferential grain boundary α precipitation and localized planar slip could be correlated with the greater susceptibility of 21S to internal HE [9]. Young and coworkers subsequently concluded that the intergranular EAC susceptibility of Beta-21S under a rising load in NaCl at -0.6 V_{SCE} could also be correlated with α colonies precipitated at β grain boundaries and with intense slip localization [5]. These workers speculated that crack tip hydrogen could be transported by planar slip bands to strongly binding trap sites and stress/strain concentrations at α-colony or β grain boundaries.

More recently, Gaudett and Scully used thermal desorption spectroscopy to investigate the trapping behavior of Beta-C Ti and found that the aged alloy exhibited a trapping state in addition to those in the unaged alloy [10]. As with Beta-21S, bulk hydriding was not detected in the aged Beta-C, but the trapping results did indicate that hydriding of a small amount of α was possible. Somerday and coworkers showed that Beta-C Ti is susceptible to intergranular EAC in aqueous NaCl solutions under certain conditions, including an active crack tip strain rate [6]. The results were consistent with findings for aged Beta-21S and were interpreted on the basis of HE. The α-precipitate distribution and slip morphology of the Beta-C specimens were between those of Beta-21S and Ti-15-3.

A basic question that remains unresolved is whether planar slip or hydrogen trapping (possibly as hydride precipitation) has a predominant influence in determining the difference in HE resistance of β-Ti alloys. Although the role of trapping in these alloys is unclear from the previous work, marked differences in trapping behavior would be expected in view of differences in their microstructure with regard to the α phase. The previous studies emphasized the large α colonies as a significant microstructural difference between the alloys. However, the contribution of the α phase and associated H trapping (or hydride precipitation) to the HE resistance can be affected by several factors: the volume fraction of α present, the composition of the α phase as it affects the strength and the activity of hydrogen in the α phase, and the effect of alloy composition on hydrogen partitioning between the α and β phases [11]. Whatever the dominant factor(s), aged β-Ti alloys clearly differ considerably in their resistance to HE, and this difference must be better understood.

In earlier work, the trapping characteristics of aged Beta-C, Ti-10V-2Fe-3Al (Ti-10-2-3), and Ti-13V-11Cr-3Al (Ti-13-11-3) were investigated using a potentiostatic pulse technique [12]. Aging caused a marked increase in the irreversible trapping characteristics. This increase was attributed to precipitation of the secondary α phase, since hydrogen segregates to α/β interfaces in α-β Ti alloys and forms brittle hydride phases that tend to grow preferentially into the α phase [13]. Although it is questionable whether hydrides are actually formed in aged β-Ti alloys, hydrogen probably does segregate to the α/β interface and become trapped there in these alloys. It is possible that enough H may accumulate in some cases to precipitate a hydride that is too thin to be detected. Regardless of whether a hydride is formed, it seems reasonable to treat the α/β interface as a potential trap site.

In the present work, the pulse technique was used to determine the trapping characteristics of Beta-21S, Ti-15-3, and Beta-C. Beta-21S and Ti-15-3 were examined in both the solution treated and the solution treated and aged conditions, while Beta-C was used in two partially aged conditions to supplement the previous results for the solution treated and fully aged alloy. Extending the range of β-Ti alloys allowed us to further investigate the relationship between trapping and HE of β-Ti alloys and, in particular, to determine whether their resistance to HE can be correlated with microstructure.

EXPERIMENTAL PROCEDURE

Alloys

Specimens of Beta-21S (Ti-15Mo-2.7Nb-3Al-0.2Si-0.15O) and Ti-15-3 (Ti-15V-3Cr-3Al-3Sn) were obtained in both the solution treated and the solution treated and aged conditions. (For convenience, these conditions will be referred to simply as unaged and aged, respectively). These specimens were provided from the alloys used by Gangloff, Scully, and coworkers [4,5,7-9]. The solution treatments that had been used for the Beta-21S and Ti-15-3 were 871°C for 8 h and 816°C for 30 min, respectively. Both alloys were aged at 538°C for 8 h. The yield strengths of the aged Beta-21S and Ti-15-3 were 1380 and 1315 MPa, respectively. Cylindrical sections 0.95 cm in diameter were machined from the specimens for use as electrodes. The alloys were examined in both the unaged and aged conditions to determine the effect of the secondary α phase on hydrogen ingress.

The microstructures of the specimens used in this work were examined by Young and coworkers [5]. Aged Beta-21S exhibited intragranular α plates and coarse grain boundary, platelike, α colonies, which were aligned perpendicular to the grain boundaries. In contrast, aged Ti-15-3 contained α plates distributed homogeneously within β grains, with α colonies only occasionally present at grain boundaries. Both alloys exhibited a 0.1-μm layer of α phase at the grain boundaries.

The Beta-C Ti was obtained from the alloy producer as 1.593-cm-diameter rod that had been hot-rolled, annealed, and centerless ground. The composition of the Beta-C was Ti-3.0Al-8.0V-6.0Cr-3.9Mo-3.8Zr-0.1Nb-0.093O-0.01C-0.018N-0.06Fe. Sections of the rod were aged at 510°C for 5 h and 10 h, then cooled in Ar. These aging times were chosen to provide a suitable comparison with the fully aged alloy examined previously, which had been aged 20 h [12]. The 5-h, 10-h, and 20-h aged specimens are denoted as 5A, 10A, and 20A Beta-C, respectively.

The 20A Beta-C was examined using scanning electron microscopy and found to contain α precipitates, but relatively little α phase was present at grain boundaries. This microstructure is consistent with that reported for Beta-C aged at 500°C for 30 h [10]. In the alloy aged for 30 h, homogeneous α precipitates were observed within the grains, with a very limited amount of α at the grain boundaries; it was not determined whether a thin (0.1-μm) α film was present at the grain boundaries. The α phase was not characterized further in this work, but Rhodes and Paton observed that relatively large (> 0.1 μm), noncoherent precipitates of Type 2α, which do not obey the Burgers orientation relation, are present in Beta-C aged at 500°C for ≥4 h [14]. In contrast, aged Beta-21S was found to contain Type 1α precipitates, which do obey the Burgers relation [15].

Technique

Details of the electrochemical cell and instrumentation have been given previously [16]. The test electrodes of each alloy consisted of the cylindrical sections (0.64-0.95 cm in length) press-fitted into a Teflon sheath so that only the planar end surface was exposed to the electrolyte. The surface was polished before each experiment with SiC paper followed by 0.05-μm alumina powder. The electrolyte was an acetate buffer (1 mol L^{-1} acetic acid/1 mol L^{-1} sodium acetate) containing 15 ppm As_2O_3 as a hydrogen entry promoter. The electrolyte was deaerated with argon for 1 h before measurements began and throughout data acquisition. The potentials were measured with respect to a saturated calomel electrode (SCE). All tests were performed at 22 ± 1°C.

The alloy of interest was charged with hydrogen at a cathodic potential E_c for a time t_c, after which the potential was stepped anodically to a value 10 mV negative of the open-circuit potential E_{oc} [5,10,16]. Anodic current transients were obtained for a range of charging times (5-60 s) at different overpotentials ($\eta = E_c - E_{oc}$). The open-circuit potential of the alloy was sampled immediately before each charging time and was also used to monitor the stability of the surface oxide.

RESULTS

Diffusion/Trapping Model

The anodic current transients were analyzed using a diffusion/trapping model [16,17] based on interface-limited diffusion control (referred to simply as interface control), whereby the rate of hydrogen ingress in an alloy is controlled by diffusion but the entry flux of hydrogen across the interface is restricted. According to this model, the total charge (C m^{-2}) passed out is given by

$$q'(\infty) = FJt_c\{1 - e^{-R}/(\pi R)^{1/2} - [1 - 1/(2R)]\mathrm{erf}(R^{1/2})\} \quad (1)$$

where F is the Faraday constant, J is the ingress flux in mol m^{-2} s^{-1}, and $R = k_a t_c$. The charge $q'(\infty)$ is equated to the charge (q_a) passed during the experimental anodic transients. q_a can be associated entirely with absorbed hydrogen, since the adsorbed charge is almost invariably negligible. k_a is an apparent trapping constant measured for irreversible traps in the presence of reversible traps and is related to the rate constant for irreversible trapping (k) by $k(D_a/D_L)$, where D_a is the apparent diffusivity and D_L is the lattice diffusivity of hydrogen in the metal. The apparent trapping constant is related to the density of particles or defects (N_i) providing irreversible traps by the following equation [18,19]:

$$N_i = k_a a/(4\pi d^2 D_a) \quad (2)$$

where a is the diameter of the metal atom and d is the trap radius.

In all cases except unaged Beta-21S (see below), equation (1) could be fitted to data for q_a to obtain values of k_a and J such that J was constant over the range of charging times and k_a was independent of charging potential, as is required for the model to be valid. Experimental and fitted values of q_a for aged Ti-15-3 are compared in Fig. 1, which illustrates the level of agreement obtained over the range of charging times for the alloys in this work.

The values of k_a and J can be used to calculate both the irreversibly trapped charge (q_T), given by

$$q_T = FJ(t_c/k_a)^{1/2}\{[R^{1/2} - 1/(2R^{1/2})]\mathrm{erf}(R^{1/2}) + e^{-R}/\pi^{1/2}\} \quad (3)$$

and the hydrogen entry charge (q_{in}) from $q_{in} = FJt_c$, thereby allowing the trapping efficiency, q_T/q_{in}, to be obtained.

Ti-15V-3Cr-3Al-3Sn

Table 1 gives the values of k_a and J for two tests on the unaged and aged alloy. In both cases, k_a was independent of charging potential. The overall mean values of k_a were 0.042 ± 0.003 s^{-1} for the unaged alloy and 0.045 ± 0.005 s^{-1} for the aged alloy, indicating that aging had little effect on the trapping characteristics of Ti-15-3. The flux depends on the surface coverage of adsorbed hydrogen and hence increased as the charging potential was made more negative.

Beta-21S Ti

The anodic charge for unaged Beta-21S, like that for Ti-10-2-3 [12], generally did not increase with t_c, which implied that hydrogen entry did not occur to a significant degree. Hence, k_a could not be determined in this case. In contrast, aged Beta-21S did exhibit a dependence of q_a on t_c, reflecting a rise in the rate of hydrogen entry compared with that for the unaged alloy. An increase in J with aging was also observed for Ti-10-2-3 and Ti-13-11-3 [12]. Notwithstanding the increase in J for aged Beta-21S, the change in q_a with charging time was small, with the result that the values of k_a and J were subject to considerable scatter. Table 2 shows the values of k_a and J for two tests. Despite the scatter, k_a appeared to be independent of charging potential. The mean value of k_a for the two tests was 0.099 ± 0.012 s^{-1}. As with Ti-15-3, the flux increased as the potential was stepped to more negative values.

Beta-21S had a higher trapping efficiency than Ti-15-3 (Fig. 2), reflecting its much higher value of k_a. The trapping efficiencies were high for both alloys, reaching 0.8 or higher at longer

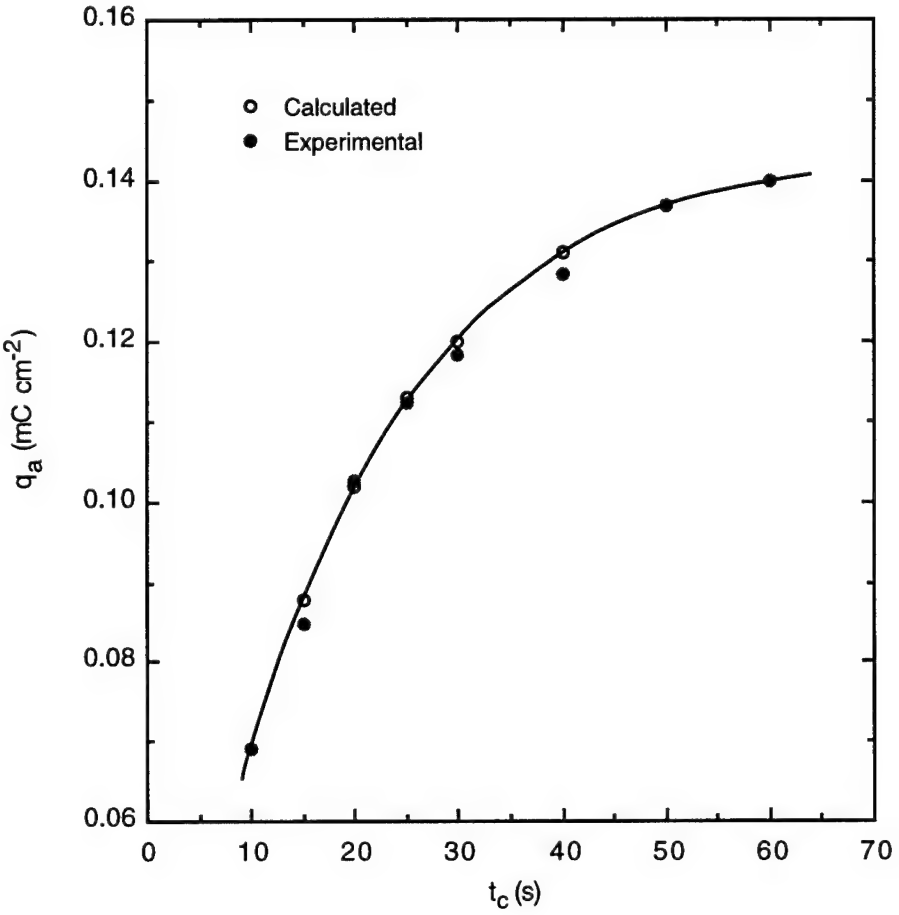

Fig. 1. Dependence of q_a on charging time for aged Ti-15-3.
η = -0.65 V; k_a = 0.044 s^{-1}, J = 0.133 nmol cm^{-2} s^{-1}.

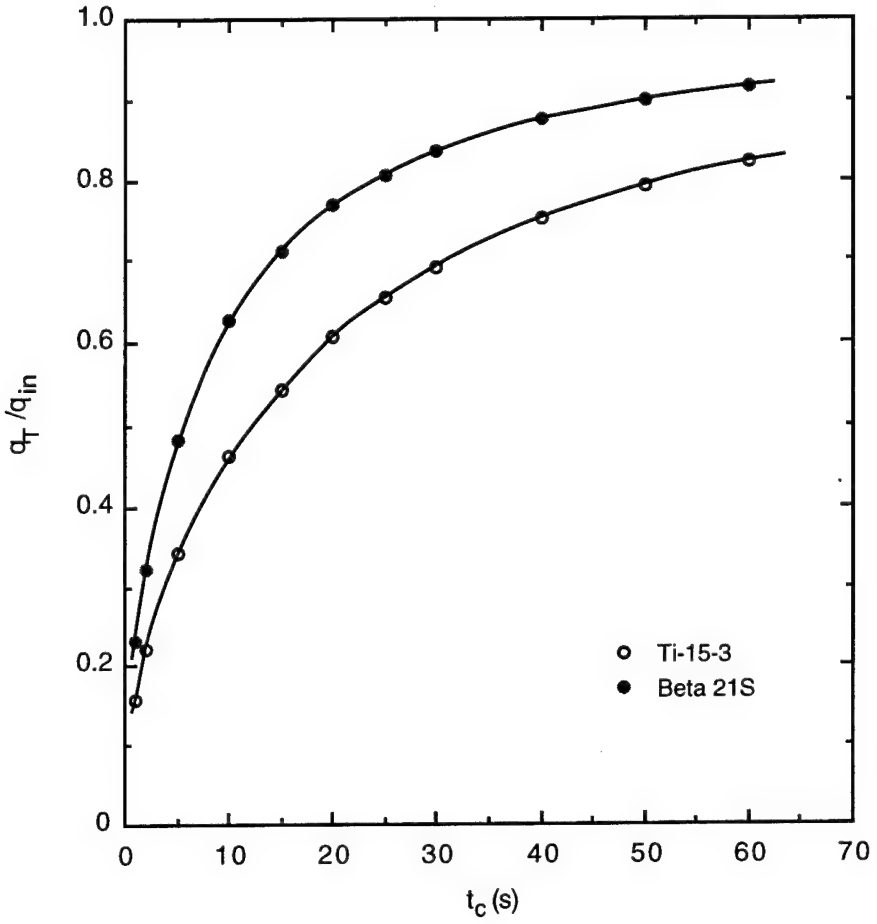

Fig. 2. Dependence of q_T/q_{in} on charging time for aged Beta-21S and Ti-15-3.

charging times. In the case of Beta-21S, q_T/q_{in} eventually exceeded 0.9, which indicates that as hydrogen accumulates in the metal, nearly all of it becomes trapped.

Beta-C Ti

The anodic charge increased with t_c for the partially aged Beta-C specimens, as it did for the unaged and fully aged alloy. The values of k_a obtained for each specimen (Table 3) were independent of charging potential. The mean values of k_a for the 5A and 10A Beta-C are 0.060 ± 0.003 s^{-1} and 0.093 ± 0.003 s^{-1}, respectively. As with the other two β-Ti alloys, the flux increased with potential in both cases.

Improvements had been made in data acquisition since the previous work was performed on 20A Beta-C, so an additional set of results (Table 3) was obtained for this alloy to verify the earlier data. The mean value of k_a determined in the current test was 0.088 ± 0.009 s^{-1}, which agrees with the mean value for the two tests previously reported. The values of k_a for the 10A and 20A Beta-C can be considered to be the same within experimental error but are substantially greater than that for the 5A alloy.

DISCUSSION

Irreversible trapping constants

Previous work showed a correlation between the irreversible trapping constant (k) and the actual resistance to HE observed in mechanical tests for a range of steels and nickel-base alloys [20-22]. The question was whether such a correlation existed for β-Ti alloys. Values of k were therefore sought from k_a for the β-Ti alloys of interest by using diffusivity data for the "pure" alloy to obtain the lattice diffusivity (D_L) and for the actual alloy to obtain the apparent diffusivity (D_a). The pure alloy was considered to be Ti with its principal alloying elements, so minor elements were assumed to be primarily responsible for reversible trapping in the actual alloys. The role of defects (such as vacancies and edge dislocations) in reversible trapping should also be considered, but the diffusivities for β-Ti alloys appear to be low enough that reversible trapping at defects can be ignored, as discussed previously [12].

Few data are available in the literature for the diffusivity of hydrogen in β-Ti alloys, with or without minor alloying elements, so it is difficult to evaluate k. However, the diffusivity for β-Ti alloys at 25°C is on the order of 10^{-11} m^2 s^{-1} [23], which is low enough that minor elements are unlikely to affect the diffusivity to a degree that is markedly different between the alloys. Accordingly, D_L/D_a was assumed to be similar for the different alloys in the unaged condition. Also, D_L should differ little between the unaged and aged conditions, as should D_a, since the α

phase precipitated during aging should have little effect in terms of *reversible* trapping [12]. Accordingly, D_L/D_a was considered to have the same value for the various β-Ti alloys, whether unaged or aged, and so the respective values of k_a—rather than k—can be compared in terms of the resistance to HE.

The mean values of the trapping constants for Ti-15-3, Beta-21S, and partially aged Beta-C are summarized in Table 4 along with those obtained previously for other β-Ti alloys as well as Ti-6Al-4V and Ti Grade 2. These values are also presented graphically in Fig. 3 to highlight differences between them. If the minor elements in β-Ti alloys are assumed to contribute only slightly to reversible trapping for diffusivities on the order of 10^{-11} m^2 s^{-1}, a lower limit can be obtained for k in each case, as given in Table 4.

Among the aged alloys, Ti-13-11-3 has the highest value of k_a and hence k, followed by Beta-21S, 10A Beta-C, 20A Beta-C, Ti-10-2-3, 5A Beta-C, and then Ti-15-3. The higher values of k_a usually display large uncertainties, which result from a diminishing increase in q_a with t_c as k_a becomes larger, such that it becomes inherently difficult to obtain precise values of k_a. The values of k_a for 20A Beta-C and Beta-21S are considered to be similar within these uncertainties, but it is clear that these values are considerably higher than that for Ti-15-3.

10A and 20A Beta-C are likewise considered to have the same values of k_a, but it is possible that k_a is in fact slightly higher for 10A Beta-C. However, small differences in the values of D_a resulting from minor differences in the β-matrix could be a compensating factor with respect to the k values for the two alloys. Work on Ti-8V-8Mo-2Fe-3Al aged at 500°C has shown that the β-matrix lattice parameter continues to contract after 10 h, even though the volume fraction of α phase ceases to increase [24]. This contraction was linked to the continued incorporation of β-stabilizing solutes into the β-matrix. A similar contraction and associated compositional change in Beta-C could decrease D_a to a small extent, such that the decrease between 10 h and 20 h counterbalances a slightly higher value of k_a for 10A Beta-C and hence yields virtually identical k values for the 10A and 20A alloys.

Resistance to HE

The intrinsic susceptibility to HE can be characterized in terms of the irreversible trapping constant [20]. Hence, among the aged alloys, Ti-13-11-3 was identified as the most susceptible to HE and Ti-15-3 as the least susceptible. The intrinsic susceptibilities of Beta-C and Beta-21S can be regarded as comparable based on their values of k. While differences in susceptibility can be difficult to resolve when trapping is so pronounced, the magnitude of the k values for Beta-C and Beta-21S indicates that both alloys are relatively susceptible to HE and significantly more so than Ti-15-3.

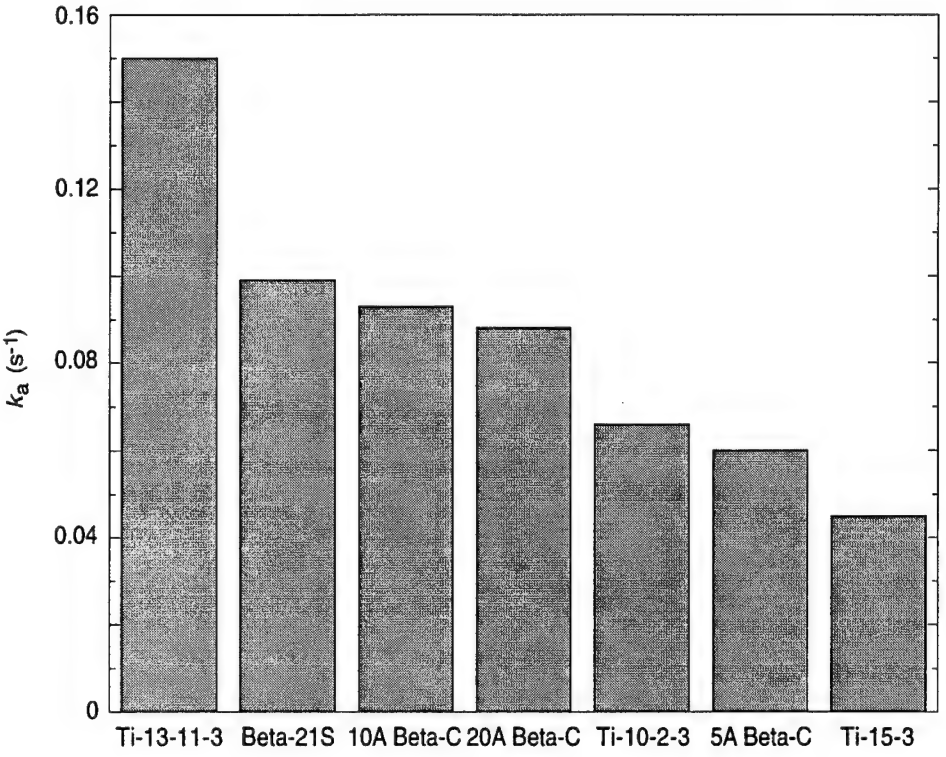

Fig. 3. Variation in k_a for the aged β-Ti alloys.

The question, as noted above, is whether the intrinsic susceptibility (defined by k) of the β-Ti alloys can be correlated with their observed resistance to HE. Gangloff and coworkers have characterized the resistance to EAC of Beta-21S, Beta-C, and Ti-15-3 in terms of the threshold for subcritical crack growth (K_{TH}) [5,6]. With neutral aqueous NaCl and -0.6 V_{SCE}, the average values of K_{TH} from two measurements were 35 ± 2 (6%) MPa√m for aged Beta-C, 42.5 ± 3.5 (8%) MPa√m for aged Beta-21S, and 62.5 ± 1.5 (2%) MPa√m for aged Ti-15-3. (The experimental errors were estimated from the range of data reported by Gangloff and coworkers.) If EAC is associated with hydrogen, as suggested by Young and coworkers [5], the observed resistances to HE of Beta-21S and Beta-C are close within experimental error but are considerably lower than that of Ti-15-3. Thus, the intrinsic susceptibilities, as represented by the trapping constants, for aged Beta-21S, Beta-C, and Ti-15-3 appear to be reasonably consistent with the observed resistances of these alloys to HE. In particular, the relatively low trapping constant for Ti-15-3 matches the high resistance to HE reported for this alloy compared with Beta-21S and Beta-C. Evidently, the correlation between the intrinsic susceptibility, as defined by k, and the observed resistance to HE for various steels and Ni-base alloys also holds for β-Ti alloys.

In the case of Ti-15-3, k_a and therefore k did not change significantly with aging, whereas they increased markedly for the other β-Ti alloys, paralleling the reported decrease in their tolerance to hydrogen [25]. This parallel is particularly evident for Beta-C, with the increase in intrinsic susceptibility matching the observed change from immunity to EAC for the unaged alloy to embrittlement for the aged alloy [2,6].

Although the intrinsic susceptibilities of Beta-21S and Beta-C must be treated as comparable within the uncertainty of the trapping constants, the values of k_a suggest that Beta-21S could have a higher susceptibility, whereas the data for K_{TH} indicate that Beta-21S may in fact be a little more resistant in the crack growth rate tests. (The difference in K_{TH} could be as small as 2 MPa√m if the experimental error is taken into account.) However, the correlation observed in previous work, as noted above, was based on the irreversible trapping constant (k)—not the *apparent* trapping constant (k_a). To compare the β-Ti alloys using k_a, it was assumed that their respective values of D_L/D_a were close enough to be considered the same. Clearly, this assumption is an approximation, which takes on more significance when the trapping constants are relatively close. Use of specific values of D_L/D_a (if they were known) and therefore of k could change the order of Beta-C and -21S in terms of their intrinsic susceptibility.

An apparent difference between the intrinsic susceptibility and actual resistance to HE could also result from differences in the H entry flux between the trapping and crack growth tests. The values of J were similar for the two alloys in the acetate solution (pH 4.8) used in the trapping tests, but this may not be the case for the 0.6 M NaCl solution (reported to be "neutral" but with a

pH of 6 in one case [6] and 8 in another [8]) and the potential (typically -0.6 V_{SCE}) used in the fracture tests.

Identification of irreversible traps

In α-β Ti alloys, as noted above, hydrogen segregates to the interface between the two phases and forms brittle hydrides, with growth occurring preferentially into the α phase [13]. Hence, the increase in the trapping constants for the β-Ti alloys with aging was linked in our previous work to irreversible trapping at the α precipitate/β phase interface and possibly in the α phase [12]. This trapping is presumably in addition to that occurring at other sites that are also present in the unaged alloys.

The results for Beta-C Ti provide strong support for the α/β interfaces being the additional principal irreversible traps present in aged β-Ti alloys. The increase in k_a for Beta-C as the aging time is lengthened from 5 h to 10-20 h appears to correspond to an increase in the volume fraction of α precipitates. The change in k_a occurs essentially within the first half (<10 h) of the total aging time, since k_a has essentially the same value for 10A and 20A Beta-C. In the case of Ti-8V-8Mo-2Fe-3Al aged at 500°C, the volume fraction of α precipitates reaches a limit of ~0.4 after 8 h and then remains constant at this value [24]. The volume fraction of α in Beta-C aged at 500°C for 8 h was also estimated to be 0.4 [14]. If Beta-C exhibits similar behavior to that of Ti-8-8-2-3 at longer aging times, the lack of change in k_a and α after 10 h would seem to further indicate that the change in k_a at shorter times is related to the volume fraction of α phase.

The densities of the irreversible traps present in the unaged alloys and the α/β traps were assumed to be additive, so in accordance with equation (2), k_a can be separated into two components, k_a' and k_a'', corresponding to the non-α/β traps and α/β traps, respectively. In the case of Beta-C, $k_a' = 0.031 \pm 0.002$ s^{-1}, so $k_a'' = 0.029 \pm 0.005$ s^{-1} for the 5A alloy, 0.062 ± 0.005 s^{-1} for the 10A alloy, and 0.057 ± 0.011 s^{-1} for the 20A alloy. Since the values of k_a for the 10A and 20A Beta-C are considered to be the same, they appear to represent an upper limit with respect to aging for this alloy. Hence, k_a'' can be normalized against the values for the 10A or 20A alloy. For a 5-h age, the normalized value of k_a'' is about 0.5, so about half of the total trapping capability associated with α/β interfaces is developed over this aging time.

Irreversible trapping at the α/β interface may result from misfit strain, hydride precipitation, or some other cause [9]. Hydrogen can be trapped at the α/β interface without forming hydrides, but the local accumulation of H at the interface might lead to hydride precipitation at the monolayer or α-subsurface level, if not extensively in the α phase as found for α-β Ti alloys. Using thermal desorption spectroscopy, Gaudett and Scully found that unaged Beta-C exhibited two trapping states and the aged alloy exhibited three states [10]. The H concentration corresponding to each

peak in the spectra was larger than the upper limits of concentation calculated for H trapped at α/β interfaces and dislocations. The rather surprising implication is that neither of these sites appear to be traps in Beta-C Ti. However, this apparent finding should be treated cautiously, since interfaces and dislocations are recognized as traps in steels [26] and the H diffusivities for steels are on the order of those for β-Ti alloys (10^{-11} m^2 s^{-1}). Although bulk hydriding was not detected with x-ray diffraction, Gaudett and Scully found that the H concentrations measured for the peaks could have corresponded to a small amount (< 2 vol%) of hydride. Thus, the α/β interfaces could have acted as traps by providing sites for hydride formation.

Young and Scully suggested that preferential α precipitation at β grain boundaries may play a role in HEAC of β-Ti alloys [7]. They postulated that α/β interfaces at the grain boundaries may serve as traps or (in the limiting case) α precipitates may hydride locally at the α/β interfaces. On this basis, the changes in k_a (and hence k) with aging could be related to the grain boundary α phase. An obvious difference between the β-Ti alloys was in the amount of α phase at the grain boundaries. Aged Ti-15-3, as described above, contained a thin α layer and only occasional α colonies at the grain boundaries [5], whereas aged Ti-13-11-3, for example, had a thick α layer precipitated at the grain boundaries. Thus, the negligible effect of aging on k_a in the case of Ti-15-3 coincides with the limited α precipitation at grain boundaries, while the large increase in k_a for Ti-13-11-3 is consistent with the considerable amount of grain boundary α. Moreover, Beta-21S has a high k_a that matched its extensive grain boundary α colonies. A slight increase in k_a was in fact observed for Ti-15-3 with aging and, although this increase is within the limits of uncertainty, it may well have reflected the limited amount of grain boundary α present in the aged alloy.

Although k_a appeared to be related to the amount of α precipitates at the grain boundaries, the results for Beta-C cast some doubt on this relationship. Beta-C contained only a very moderate amount of grain boundary α yet exhibited a large increase in k_a. Gangloff, Scully, and coworkers reported that the distribution of α precipitates in Beta-C was between that in Beta-21S and Ti-15-3, with fewer grain boundary α colonies being present in Beta-C than in Beta-21S [6,10]. The increase in k_a seemed to be large for the amount of grain boundary α present in Beta-C. Thus, the amount or morphology may not be the only important or even the primary factors. The amount of hydrogen trapping and possible hydride precipitation depends on various factors noted above, particularly the volume fraction of α, hydrogen partitioning between the α and β phases, and the composition of the α phase and its effect on the activity of hydrogen in the α phase [11]. Hence, it is quite plausible that k_a is related to some aspect of the grain boundary α in addition to or other than the amount or morphology.

Role of trapping

The relationships between the trapping constants, resistance to HE, and grain boundary α are critical in determining the role of trapping in the HE of aged β-Ti alloys. Young and Gangloff postulated that grain boundary traps played a strong role in HEAC of Beta-21S [4]. The high k_a (and therefore k) for Beta-21S was indeed commensurate with its observed susceptibility to cracking and with its extensive grain boundary α. A similar connection was observed for aged Ti-15-3, except in this case a low k_a matched a high resistance to cracking and a small amount of grain boundary α. However, Beta-C had a high k_a that matched its low resistance to HE but was possibly inconsistent with the amount or morphology alone of grain boundary α.

The comparison of data for the three alloys highlights three key points. First, irreversible hydrogen trapping must be a principal factor in EAC of aged β-Ti alloys, since the trapping constants correlate with the observed resistance to HE. Second, the trapping constants appear to be related to α/β interfaces, since (i) k_a increases with aging and, in the case of Beta-C, evidently reflects the volume fraction of α, and (ii) H segregates to α/β interfaces in α-β Ti alloys. Third, the crucial α/β interfaces must lie at the grain boundaries, since EAC is intergranular in the β-Ti alloys studied. The implication is that irreversible hydrogen trapping is linked to intergranular cracking of aged β-Ti alloys through α/β interfaces at the grain boundaries, but it is uncertain what features of the grain boundary α are critical and can explain the differences in the trapping constants and in the resistance to HE.

Differences in composition of the α phase may account for these differences. Feeney and Blackburn found in tests using an iodide solution that aged Beta III (Ti-11.5Mo-6Zr-4.5Sn) was much more susceptible to cracking than Ti-11.6Mo aged to produce a similar (β + α) microstructure [1]. They postulated that the grain boundary film of α phase, enriched in Sn and/or Zr, was responsible for the susceptibility of Beta III to cracking in halide solutions. Interestingly, Beta-C also contains Zr, which is known to exhibit hydride embrittlement [27, 28]. When relatively few α colonies are present, hydride formation and hence EAC susceptibility could be enhanced in cases where the grain boundary α is "sensitized" through the presence of an element such as Zr.

As noted above, the correlation between k_a (and hence k) and observed resistance to HE implies that k_a must be related to grain boundary α if it is to be consistent with the intergranular mode of cracking. In the case of Beta-C, k_a appears to be related to the volume fraction of α, which includes intragranular as well as intergranular α; Gaudet and Scully observed intragranular α in Beta-C even after just 1 h aging at 500°C [10]. Thus, the question is whether it is plausible for k_a to reflect primarily grain boundary α rather than the total α phase throughout the matrix. Duerig and Williams noted that grain boundary α is essentially present in all solute-rich β-Ti alloys, including Beta-C [29]. The nucleation of grain boundary α in β-Ti alloys occurs at shorter

times than does uniform α nucleation [29], so some grain boundary α is also bound to be present in Beta-C after a 1-h age and to continue precipitating for aging times under 10 h.

Gaudet and Scully did observe a limited number of α colonies in 1-h and 20-h aged Beta-C [10], these colonies possibly being in addition to a thin film of α that might be present, as observed in Beta 21S and Ti-15-3 [5]. Thus, although aging Beta-C at 500°C produces relatively uniform precipitation of α over times as short as 1 h or less, part of the α phase is present at grain boundaries. Hence, the value of k_a could conceivably reflect grain boundary (thin film or colony) α in the case of Beta-C—and, in fact, for the β-Ti alloys in general. For example, it is possible that the nucleation kinetics result in grain boundary α that is extensive (as α colonies) or is higher in a potential hydride-former such as Zr than is the intragranular α. In either case, the grain boundary α may impart a high trapping or hydriding capability and so could provide the principal trapping sites.

Young and Scully have argued that it is difficult to attribute all of the differences in *internal* HE resistance between aged Ti-15-3 and Beta-21S exclusively to a difference in the irreversible trapping capability of α/β interfaces, for three reasons [9]. Although there are some differences in the factors associated with internal HE and EAC, these reasons are discussed below within the context of the present work. The first reason was that unaged (no α present) Beta-21S was less resistant than unaged Ti-15-3 to internal embrittlement by predissolved H. The unaged and aged alloys, however, have key microstructural differences, which would be expected to lead to marked differences in trapping and other factors influencing the resistance of these alloys to HE. The trapping constants showed that unaged Ti-15-3 (and Beta-C) also contained irreversible traps, which were probably present in the aged alloy too. Unaged Beta-21S presumably contained similar types of irreversible traps, though its trapping constants could not be determined. These non-α-related traps may well be responsible for the difference observed in HE resistance of the unaged alloys, whereas the α/β interfaces appear to be the critical traps in the aged alloys.

The second reason given by Young and Scully was that re-solution treated (RST, 1038°C for 2 h) Ti-15-3 (α precipitates absent) was susceptible to internal HE and RST/aged Ti-15-3 was susceptible to stress corrosion cracking. However, cracking of the RST/aged Ti-15-3 in chloride solutions is more intergranular than the (mainly transgranular) cracking of the solution treated (816°C/0.5 h) alloy and has been correlated with grain boundary α colonies [5]. Although the number of α colonies may not be crucial, the α/β interfaces are a potential factor in the aqueous cracking of RST/aged Ti-15-3. In the case of the unaged Ti-15-3, solution treating under different temperatures and times will lead to differences in the microstructure and thus in the non-α/β traps, so re-solution treating could quite conceivably render Ti-15-3 less resistant to internal HE; as noted above, the unaged alloys contain irreversible traps that are distinct from the α/β traps in the aged

alloys, and these other traps will exert their own influence on the HE resistance of the unaged alloys.

The final reason cited by Young and Scully was that irreversible trapping at α/β interfaces did not account for many of the other fracture paths reported in their internal HE study in which the specimens were electrochemically precharged with hydrogen in an acidified solution of sodium pyrophosphate ($Na_4P_2O_7$) at 90°C. On the other hand, both Beta-21S and Beta-C display essentially intergranular cracking in specimens under aqueous conditions involving a rising load in neutral 3.5% NaCl at 25°C and -0.6 V_{SCE} [5,6]. The presence of grain boundary α in Beta-21S, and to a lesser extent in Beta-C, means that α/β interfaces exist along the major crack path and, through trapping (or hydride formation), could be associated with EAC, even if not with internal HE.

Young and coworkers, as noted above, found that the intergranular EAC susceptibility of aged Beta-21S under a rising load in NaCl at -0.6 V_{SCE} can be correlated with grain boundary α colonies and with localized planar slip [5]. They postulated that crack tip hydrogen could be transported by planar slip bands to strongly binding trap sites and stress/strain concentrations at α colony or β grain boundaries. In the case of aged Beta-C, the relatively small number of grain boundary α colonies in this alloy appeared to be inconsistent with the amount of intergranular EAC [6], but a comparison of the deformation modes for Beta-C, Beta-21S, and Ti-15-3 suggested that slip localization plays a role in intergranular EAC of unaged and aged β Ti alloys in chloride solutions. The contributions of grain boundary α precipitation, locally planar slip, and impurity segregation were not established. Although the resistance to HE is affected by a range of factors, some of them would be expected to exert a greater influence than others and so be primarily responsible for determining the resistance. Indeed, a single factor may be predominant in its effect on HE, with the others still exerting effects but at a secondary level. The parallels between the trapping constants and the observed resistance to cracking indicate that trapping is a principal—possibly predominant—factor. Although planar slip appears to play a role, whether it is an equally important factor in the cracking of β-Ti alloys, and more specifically whether it could predominate over the effect of trapping, remain uncertain.

If trapping is the predominant factor, the intergranular nature of EAC in the β-Ti alloys means that trapping must be associated with the grain boundaries, most likely through the α phase but also possibly through segregated impurities. The lack of correlation between the number of grain boundary α colonies and both intergranular EAC and the trapping constants does not mean that the α phase is not linked to trapping and EAC or that trapping is not the predominant factor. It does imply that the number of colonies is not necessarily the critical factor; other characteristics of the grain boundary α may be important in terms of enhancing trapping or hydride formation. The

results obtained by Feeney and Blackburn suggest that the composition of the α phase is the key factor in some cases [1]. Hence, both the amount and composition of the grain boundary α could have a critical effect on the EAC of β-Ti alloys. Adequate trapping or hydriding might be achieved primarily through the amount in alloys containing α colonies or through the composition in alloys containing a hydride-former such as Zr. In other words, α colonies, if present, may predominate over the trapping or hydriding behavior, but in their absence, composition may be the most important factor.

CONCLUSIONS

- Aging caused a negligible change in k_a for Ti-15-3 but a marked increase for Beta-21S and other β-Ti alloys, paralleling the decrease in their tolerance to hydrogen. The increase in k_a for Beta-C, in particular, matched the previously reported change from immunity to EAC for the unaged alloy to embrittlement for the aged alloy.
- Among the aged alloys, Ti-13-11-3 has the highest value of k_a and hence k, whereas Ti-15-3 has the lowest k_a. Accordingly, Ti-13-11-3 has the highest intrinsic susceptibility to HE, as defined by the trapping constants, and Ti-15-3 has the lowest. The intrinsic suceptibilities of fully aged (20A) Beta-C and Beta-21S are comparable and significantly higher than that of Ti-15-3.
- The intrinsic susceptibilities for Beta-21S, 20A Beta-C, and Ti-15-3 are consistent with the relative resistances observed for these alloys to HE. In particular, the relatively low trapping constant for Ti-15-3 matches the high resistance to HE reported for this alloy compared with Beta-21S and Beta-C.
- The correlation between intrinsic susceptibility and the observed resistance to HE for aged β-Ti alloys indicates that irreversible hydrogen trapping must be a principal factor affecting the HE resistance of these alloys. Planar slip may play an important role but seems unlikely to be the predominant factor in view of the correlation between HE resistance and trapping. The correlation for the β-Ti alloys is consistent with that found for various steels and Ni-base alloys.
- Irreversible trapping in the aged alloys occurs at α/β interfaces (and possibly in the α phase), since (i) k_a increases with aging and, in the case of Beta-C, appears to reflect the volume fraction of α, and (ii) H segregates to α/β interfaces in α-β alloys. This trapping is presumably in addition to that occurring at other sites also present in the unaged alloys. The irreversible traps in unaged β-Ti alloys may be responsible for differences observed in the HE resistance of these alloys.

- Irreversible trapping appears to be linked to intergranular cracking of aged β-Ti alloys through α/β interfaces at the grain boundaries. By its amount or composition, the grain boundary (thin film or colony) α phase may impart a high trapping or hydriding capability and so could well provide the principal trapping sites. Both the amount and composition of the grain boundary α could have a critical effect on H trapping and hence on the EAC of β-Ti alloys; the key factor could be the amount in alloys containing α colonies and the composition in alloys containing a strong hydride-former.

ACKNOWLEDGEMENTS

Financial support of this work by the Office of Naval Research under Contract N00014-91-C-0263 is gratefully acknowledged. The author is also grateful to Professors R. Gangloff and J. Scully of the University of Virginia for providing samples of Ti-15-3 and Beta-21S Ti.

REFERENCES

1. J. A. Feeney and M. J. Blackburn, *Metall. Trans.* **1**, 3309 (1970).
2. D. E. Thomas and S. R. Seagle, in *Titanium Science and Technology: Proc. Fifth Int. Conf. on Titanium*, Munich, Germany (edited by G. Lütjering, U. Zwicker, and W. Bunk), Vol. 4, p. 2533, Deutsche Gesellschaft Für Metallkunde (1984).
3. C. Gagg and B. Toloui, in *Proc. Sixth World Conf. on Titanium* (edited by P. Lacombe, R. Tricot, and G. Beranger), p. 545, Societe Francaise de Metallurgie, Les Ulis Cedex, France (1988).
4. L. M. Young and R. P. Gangloff, in *Titanium '92 Science and Technology* (edited by F. Froes and I. L. Caplan), Vol. 3, p. 2209, T.M.S. AIME, Warrendale, PA (1993).
5. L. M. Young, G. A. Young, Jr., J. R. Scully, and R. P. Gangloff, *Metall. Mater. Trans.*, **26A**, 1257 (1995).
6. B. P. Somerday, J. A. Grandle, and R. P. Gangloff, in *Proc. Tri-Service Conf. on Corrosion*, Wright-Patterson Air Force Base, Dayton, OH (in press).
7. G. A. Young and J. R. Scully, *Scripta Metall. Mater.* **28**, 507 (1993).
8. G. A. Young and J. R. Scully, in *Beta Titanium Alloys in the 1990s* (edited by D. Eylon, R. R. Boyer, and D. A. Koss), p. 147, T.M.S., Warrendale, PA (1993).
9. G. A. Young and J. R. Scully, *Corrosion* **50**, 919 (1994).
10. M. A. Gaudett and J. R. Scully, in *Environmentally Assisted Cracking of High Strength Beta Titanium Alloys*, Report to the Office of Naval Research, Grant No. N000014-91-J-4164 (1994).
11. J. E. Costa, D. Banerjee, and J. C. Williams, in *Beta Titanium Alloys in the 1980s* (edited by R. R. Boyer and H. W. Rosenberg), p. 69, T.M.S. AIME, New York (1984).

12. B. G. Pound, *Acta Metall. Mater.* **42**, 1551 (1994).
13. J. D. Boyd, *Trans. ASM* **62**, 977 (1969).
14. C. G. Rhodes and N. E. Paton, *Metall. Trans.* **8A**, 1749 (1977).
15. K. Chaudhuri and J. H. Perepezko, *Metall. Trans.* **25A**, 1109 (1994).
16. B. G. Pound, *Corrosion* **45**, 18 (1989).
17. R. McKibbin, D. A. Harrington, B. G. Pound, R. M. Sharp, and G. A. Wright, *Acta Metall.* **35**, 253 (1987).
18. B. G. Pound, *Acta Metall.* **38**, 2373 (1990).
19. B. G. Pound, R. M. Sharp, and G. A. Wright, *Acta Metall.* **35**, 263 (1987).
20 B. G. Pound, in *Proc. Fifth Int. Conf. on Hydrogen Effects on Material Behavior* (edited by N. R. Moody and A. W. Thompson), T.M.S., Warrendale, PA (in press).
21. B. G. Pound, in *Proc. Tri-Service Conference on Corrosion*, Wright-Patterson Air Force Base, Dayton, OH (in press).
22. B. G. Pound, *Acta Metall.* **39**, 2099 (1991).
23. W. R. Holman, R. W. Crawford, and F. Paredes, Jr., *Trans. Met. Soc. AIME* **233**, 1836 (1965).
24. C. G. Rhodes and J. C. Williams, unpublished research, Rockwell International (1972); cited in Ref. 29.
25. R. W. Schutz and D. E. Thomas, in *Metals Handbook*, 9th ed., Vol. 13, p. 669, ASM, Metals Park, OH (1987).
26. G. M. Pressouyre, *Metall. Trans.* **10A**, 1571 (1979).
27. D. O. Northrup, in *Environment Sensitive Fracture of Eng, Mater.* (edited by Z. A. Foroulis), p. 451, T.M.S., New York (1979).
28. K. Nuttall, in *Effects of Hydrogen in the Behavior of Materials* (edited by A. W. Thompson and I. M. Bernstein), p. 441, T.M.S., New York (1975).
29. T. W. Duerig and J. C. Williams, in *Beta Titanium Alloys in the 1980s* (edited by R. R. Boyer and H. W. Rosenberg), p. 19, T.M.S. AIME, New York (1984).

Table 1. Values of k_a and J for Ti-15-3

State	Test	η (V)	E_c (V/SCE)	k_a (s^{-1})	J (nmol cm^{-2} s^{-1})	Mean k_a
Unaged	1	-0.40	-0.472	0.043	0.110	
		-0.45	-0.520	0.047	0.135	
		-0.50	-0.573	0.038	0.134	0.043 ± 0.003
		-0.55	-0.632	0.045	0.161	
		-0.60	-0.696	0.040	0.167	
	2	-0.40	-0.472	0.040	0.107	
		-0.45	-0.519	0.033	0.111	
		-0.50	-0.571	0.042	0.140	0.042 ± 0.004
		-0.55	-0.626	0.049	0.169	
		-0.60	-0.686	0.045	0.178	
		-0.65	-0.750	0.043	0.195	
Aged	3	-0.45	-0.565	0.040	0.071	
		-0.50	-0.612	0.045	0.089	
		-0.55	-0.664	0.042	0.092	0.045 ± 0.004
		-0.60	-0.722	0.041	0.100	
		-0.65	-0.785	0.047	0.125	
		-0.70	-0.854	0.055	0.161	
	4	-0.50	-0.602	0.052	0.097	
		-0.55	-0.646	0.040	0.096	
		-0.60	-0.698	0.038	0.104	0.046 ± 0.006
		-0.65	-0.756	0.044	0.133	
		-0.70	-0.820	0.054	0.176	

Table 2. Values of k_a and J for aged Beta-21S Ti

Test	η (V)	E_c (V/SCE)	k_a (s^{-1})	J (nmol cm^{-2} s^{-1})	Mean k_a
5	-0.40	-0.742	0.112	0.048	
	-0.45	-0.782	0.080	0.049	0.096 ± 0.016
6	-0.55	-0.767	0.085	0.087	
	-0.60	-0.830	0.111	0.134	0.100 ± 0.010
	-0.65	-0.900	0.095	0.187	
	-0.70	-0.966	0.108	0.294	

Table 3. Values of k_a and J for aged Beta-C Ti

State	Test	η (V)	E_c (V/SCE)	k_a (s^{-1})	J (nmol cm^{-2} s^{-1})	Mean k_a
5A	7	-0.35	-0.376	0.064	0.048	
		-0.40	-0.422	0.055	0.050	0.061 ± 0.004
		-0.45	-0.473	0.065	0.064	
	8	-0.35	-0.400	0.055	0.048	
		-0.40	-0.445	0.059	0.061	0.059 ± 0.002
		-0.45	-0.497	0.061	0.070	
		-0.50	-0.552	0.062	0.079	
10A	9	-0.40	-0.459	0.094	0.164	
		-0.45	-0.515	0.095	0.194	0.095 ± 0.001
	10	-0.40	-0.435	0.089	0.195	
		-0.45	-0.491	0.092	0.230	0.091 ± 0.002
20A	11	-0.45	-0.650	0.097	0.076	
		-0.50	-0.682	0.082	0.078	0.088 ± 0.008
		-0.55	-0.720	0.096	0.099	
		-0.60	-0.769	0.078	0.104	

Table 4. Trapping constants for titanium alloys

Alloy	State	Phase[a]	k_a (s^{-1})	D_L/D_a	k (s^{-1})
Single-Phase					
Ti Grade 2	Unaged (low H)[b]	α	0.028 ± 0.002	1	0.028
Beta-C	Unaged	β	0.031 ± 0.002	≥1	≥0.031
Ti Grade 2	Unaged (high H)[b]	α	0.040 ± 0.004	1	0.040
Ti-15-3	Unaged	β	0.042 ± 0.003	≥1	≥0.042
Ti-13-11-3	Unaged	β	0.069 ± 0.011	≥1	≥0.069
Dual-Phase					
Ti-15-3	Aged	β-α_s	0.045 ± 0.005	≥1	≥0.045
5A Beta-C	Aged 5 h	β-α_s	0.060 ± 0.003	≥1	≥0.060
Ti-6-4	As-received	α_p-β	0.063 ± 0.005	≥1	≥0.063
Ti-10-2-3	Aged	β-α_s	0.066 ± 0.009	≥1	≥0.066
20A Beta-C	Aged 20 h	β-α_s	0.088 ± 0.009	≥1	≥0.088
10A Beta-C	Aged 10 h	β-α_s	0.093 ± 0.003	≥1	≥0.093
Beta-21S	Aged	β-α_s	0.099 ± 0.012	≥1	≥0.099
Ti-13-11-3	Aged	β-α_s	0.15 ± 0.01	≥1	≥0.150

[a] α_p = primary α phase; α_s = secondary α phase.
[b] When the charging potential reaches approximately -0.93 V, k_a increases from 0.028 to 0.040 s^{-1} [8].

THE RESISTANCE OF HIGH-STRENGTH ALLOYS TO HYDROGEN EMBRITTLEMENT*

ABSTRACT

The resistance of an alloy to hydrogen embrittlement (HE) is strongly influenced by the presence of microstructural heterogeneities, which can provide sites to trap hydrogen. The entry and trapping of hydrogen in a range of high-strength alloys have been investigated with a technique referred to as hydrogen ingress analysis by potentiostatic pulsing (HIAPP). Data were analyzed by using a diffusion/trapping model to determine entry and trapping parameters for high-strength steels, precipitation-hardened and work-hardened nickel-base alloys, and titanium alloys. For most of the alloys studied, the observed resistance to HE appeared to be determined primarily by the alloy's intrinsic susceptibility as defined by the trapping characteristics; that is, the H entry flux generally has only a secondary effect on the resistance to HE. However, in one case, the HE resistance was attributable to a low entry flux. This type of case highlights the need for characterizing alloys in terms of both trapping capability and rate of H entry to account for differences observed in their HE resistance.

INTRODUCTION

Microstructural heterogeneities in alloys provide potential trapping sites for hydrogen and so can play a crucial role in determining an alloy's resistance to hydrogen embrittlement (HE). This role originates in the fact that the interaction of these heterogeneities with hydrogen can strongly influence the series of events leading to failure.[1] The accumulation of hydrogen at second-phase particles and precipitates, for example, is generally considered to promote microvoid initiation via the fracture of particles or the weakening of particle-matrix interfaces. Traps with a large saturability and a high binding energy for hydrogen are highly conducive to HE,[2,3] whereas alloys containing a high density of well-distributed irreversible (high binding energy) traps that have a low saturability should be less susceptible. Thus, the intrinsic susceptibility of an alloy to HE is highly dependent on the type of microstructural defect, with large irreversible traps typically imparting a high susceptibility.

---

* In *Proceedings of the Tri-Service Conference on Corrosion* (Wright-Patterson Air Force Base, Dayton, OH, 1994), in press.

The basic concept of trap theory is that the local concentration of hydrogen trapped at a defect must reach some critical value (C_k) for cracks to be initiated.[1,3] It should be recognized, however, that the mechanism by which such an accumulation triggers HE is not addressed. The value of C_k, and therefore the intrinsic susceptibility of an alloy, is determined by the type of trap, its size, concentration (density), and other parameters. A decrease in C_k will render the alloy more susceptible. However, whether embrittlement will actually occur is also affected by the amount of trapped H, which depends on factors such as the entry kinetics, exposure time, and transport mode. In some cases, an alloy may prove resistant during exposure because the amount of H that enters is small enough that the critical concentration at the traps is not exceeded. Likewise, when alloys have similar intrinsic susceptibilities in terms of their trapping characteristics, the difference in their actual resistance to HE is likely to be determined by the amount of H absorbed by each alloy.

Over the last few years, the entry and trapping of hydrogen in a wide range of high-strength alloys have been investigated at SRI.[4-8] The rates of H entry and rate constants for irreversible trapping were determined using an electrochemical technique referred to as hydrogen ingress analysis by potentiostatic pulsing (HIAPP).[4,9] The research was aimed in part at characterizing the intrinsic susceptibility of the alloys to HE in terms of their irreversible trapping constants. The relative intrinsic susceptibilities then could be compared with results for the actual resistance to HE observed in tests by other workers. In this paper, the irreversible trapping constants and, where necessary, H entry fluxes for the different alloys are compared, with the objective of providing a basis for explaining differences in the resistance of these alloys to HE.

EXPERIMENTAL PROCEDURE

The alloy of interest is cathodically charged with hydrogen at a constant potential E_c for a time t_c, after which the potential is stepped in the positive direction. H diffuses back to the entry surface and is reoxidized, thereby generating an anodic current transient. Data are obtained over a range of charging times, typically from 5 to 60 s, at different overpotentials ($\eta = E_c - E_{oc}$) relative to the open-circuit potential (E_{oc}), which is measured immediately before each charging time. E_{oc} is also used to monitor the stability of the alloy surface, since any oxides present should not be reduced during charging.

The pulse technique was applied to high-strength steels,[4,5] precipitation-hardened and work-hardened nickel-base alloys,[5,6] and titanium.[7] The composition of each alloy is given in Table 1. Table 2 shows the yield strength of the alloys and the thermomechanical treatment used in each case.

Table 1
Alloy Composition (wt%)

	4340	18Ni	718	925	C-276	625	716	Ti Gr2
Al	0.031	0.13	0.60	0.30		0.18	0.22	
B		0.003	0.003					
C	0.42	0.009	0.03	0.02	0.002	0.03	0.011	0.021
Co		9.15	0.16		0.83		<0.01	
Cr	0.89	0.06	18.97	22.20	15.27	22.06	20.99	
Cu	0.19	0.11	0.04	1.93				
Fe	bal	bal	16.25	28.96	5.84	4.37	5.32	0.17
Mn	0.46	0.01	0.10	0.62	0.48	0.17	0.01	
Mo	0.21	4.82	3.04	2.74	16.04	8.70	8.10	
O	0.001							0.16
Nb+Ta			5.30			3.50	3.47	
Ni	1.74	18.42	54.41	40.95	57.5	60.33	60.5	
P	0.009	0.004	0.009		<0.005	0.012	0.004	
S	0.001	0.001	0.002	0.001	<0.002	0.001	0.001	
Si	0.28	0.04	0.11	0.17	<0.02	0.38	0.02	
Ti		0.65	0.98	2.11		0.27	1.35	bal
W		0.01			3.90			
Other	0.005N	0.05 Ca 0.02 Zr			0.12 V			<0.005H 0.007N

Test electrodes of each alloy were fabricated from a length (1.3-3.8 cm) of rod press-fitted into a Teflon sheath so that only the planar end surface was exposed to the electrolyte. The surface was polished before each experiment with SiC paper followed by 0.05-μm alumina powder.

Table 2
Thermomechanical Treatment of Alloys

Alloy	Heat Treatment[a]	Test Condition	Yield Strength (MPa)
4340	Annealed	HRC 41	1206
		HRC 53	1792
18Ni	Aged (482°C, 4 h)	As received	1954
K-500	Cold drawn, unaged	As received	758
		Aged (600°C, 8 h)	1096
35N	Cold drawn and aged	As received	1854
718	Hot fin., solution treated	As received	1238
925	Hot fin., annealed, aged	As received	758
C-276	Hot rolled	27% cold work	1237
625	Hot fin., annealed	17% cold work	1195
716	Annealed, aged	4% cold work	1186
Ti Gr2	Annealed (620°C, 1 h)	As received	380

[a] Provided by producer.

Details of the electrochemical cell and instrumentation have been given elsewhere.[4] The alloys were exposed in a deaerated solution containing 1 mol L^{-1} acetic acid and 1 mol L^{-1} sodium acetate with 15 ppm As_2O_3 added to promote H entry. The potentials were measured with respect to a saturated calomel electrode (SCE). All tests were performed at 22 ± 2°C.

ANALYSIS

Although permeation methods have been used extensively, they suffer from several disadvantages, as discussed elsewhere.[10] The main theoretical limitation is that most, if not all, diffusion/trapping models for these methods are based on an input boundary condition of constant concentration. Hence, these models are strictly applicable only for charging conditions without any entry limitation.

In the case of HIAPP, a model has been developed to allow for the effect of trapping on diffusion for cases involving either a constant concentration or a constant flux at the input surface.[4,9] The constant flux model was found to apply to all alloys studied to date. In this model, the rate of hydrogen ingress is controlled by diffusion but the entry flux of hydrogen is restricted, which results in interface-limited diffusion control. Solution of the diffusion equation for a constant flux condition gives the following expression for the total anodic charge (C m^{-2}):

$$q'(\infty) = FJ\, t_c\{1 - e^{-R}/(\pi R)^{1/2} - [1 - 1/(2R)]\mathrm{erf}(R^{1/2})\} \qquad (1)$$

where F is the Faraday constant, J is the ingress flux in mol m^{-2} s^{-1}, and $R = k_a t_c$. The charge $q'(\infty)$ is equated to the charge (q_a) associated with the experimental anodic transients. q_a can be associated entirely with absorbed H, since the adsorbed charge is almost invariably negligible.

k_a is an apparent trapping constant measured for irreversible traps in the presence of reversible traps. It is related to the irreversible trapping constant (k) by kD_a/D_L, where D_a is the apparent diffusivity and D_L is the lattice diffusivity of H. The magnitude of k depends on the density of particles or defects (N_i) providing irreversible traps, the radius (d) of the trap defects, and the diameter (a) of the metal atom[11]:

$$k = \frac{4\pi d^2 N_i D_L}{a} \qquad (2)$$

The term d^2N_i represents the trapping capability and underlies the use of k as an index of an alloy's intrinsic susceptibility to HE.

For the constant flux model to be applicable, it must be possible to determine a trapping constant for which J is independent of charging time. Data for q_a could in fact be fitted to Eq. (1) to obtain values of k_a and J that satisfied this requirement at each potential. Experimental and fitted values of q_a for various charging times are compared in Fig. 1, which illustrates the level of agreement obtained for the alloys in this work.

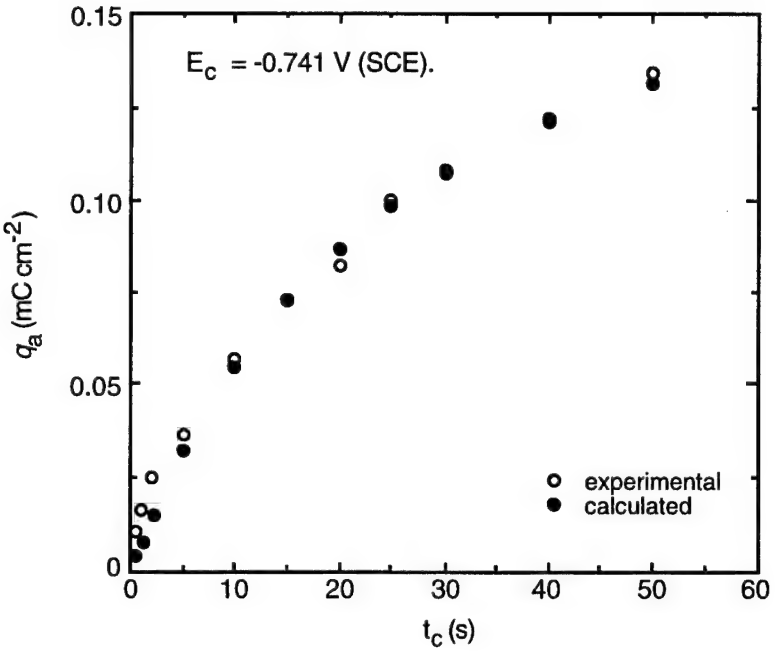

Figure 1. Dependence of anodic charge on charging time for Ti grade 2.

RESULTS

The alloys were studied as a series of groups, which were then merged to provide an overall comparison of the irreversible trapping constants. The values of k_a and k for each group are summarized in Table 3. The first group consisted of a high-strength steel (AISI 4340) and two nickel-containing alloys (K-500 and 35N).[4] The aim was to determine whether the irreversible trapping constants might assist in explaining differences observed in HE resistance between high-strength steels and nickel-base alloys. The values of both k and J for the steel were higher than those for alloys K-500 and 35N. Hence, both the irreversible trapping characteristics and the amount of H entering could account for the steel being less resistant to HE than the two nickel-containing alloys.

Two further groups of alloys were then studied: precipitation-hardened alloys (718, 925, and 18Ni maraging steel)[5] and work-hardened alloys (625 and C-276).[6] Alloys 625, 718, and

Table 3
Trapping Parameters

Alloy	k_a (s^{-1})	D_L/D_a	k (s^{-1})
4340 Steel	0.008 ± 0.001	500	4.0 ± 0.5
K-500 Unaged	0.017 ± 0.003	2.0	0.034 ± 0.006
Aged	0.021 ± 0.003	2.0	0.042 ± 0.006
35N	0.026 ± 0.002	1	0.026 ± 0.002
718	0.031 ± 0.002	4.0 ± 0.5	0.124 ± 0.024
925	0.006 ± 0.003	5.6 ± 0.6	0.034 ± 0.004
18Ni Steel	0.005 ± 0.002	300 ± 90	1.50 ± 1.05
	0.010 ± 0.005[a]	300 ± 90	3.00 ± 2.40
C-276	0.025 ± 0.003	3.6 ± 0.8	0.090 ± 0.030
	0.019 ± 0.010[a]	3.6 ± 0.8	0.068 ± 0.051
625	0.004 ± 0.002	3.6 ± 0.8	0.014 ± 0.010
716	0.054 ± 0.004	3.8 ± 0.8	0.20 ± 0.06
Ti grade 2	0.028 ± 0.002	1	0.028 ± 0.002
	0.012 ± 0.006[b]	1	0.012 ± 0.006

[a] Quasi-irreversible trapping. [b] Hydride formation.

925 were each characterized by a single type of irreversible trap, whereas alloy C-276 and 18Ni maraging steel were characterized by both an irreversible trap and a quasi-irreversible trap. In irreversible trapping, the rate constant for release is assumed to be zero, whereas for the quasi-irreversible case, the release constant is not zero but is too small to achieve local equilibrium between the lattice and trapped H.[5] The maraging steel had the highest value of k, followed by alloys 718, C-276, 925, and 625. It is apparent from its value of k that the maraging steel is intrinsically somewhat less susceptible than 4340 steel. Test results have in fact shown that 18 Ni(250) maraging steel is more resistant to cracking than 4340 steel,[12] so the differing susceptibility of the two steels was matched by their actual resistances to HE.

A similar parallel was found to exist for the 18Ni steel and alloy 718. Stress-rupture tests during electrolytic charging have shown that 18Ni (1723 MPa) maraging steel undergoes severe HE, whereas alloy 718 exhibits negligible embrittlement.[13] Likewise, gas-phase charging tests showed from the reduction in strength that the maraging steel was less resistant than alloy 718, although the embrittlement in both cases was characterized as extreme.[13]

No Ni-base alloys in the 900 series were included in the electrolytic embrittlement tests. However, gas-phase studies on alloy 903 have shown that short exposure to high-pressure hydrogen is not detrimental, though prolonged exposure, particularly at higher temperatures, can reduce ductility.[14] In contrast, alloy 718 undergoes extreme embrittlement under gas-phase charging, as noted above. These results suggest that alloy 903 and, by implication, alloy 925 are

less sensitive than alloy 718 to HE. Hence, the irreversible trapping constants of the three precipitation-hardened alloys are consistent with their relative resistances to HE observed in failure tests.

A similar comparison of the resistances of alloys C-276 and 625 is complicated by their sensitivity to cold work. However, the ranking of these alloys can be assessed indirectly from results for alloys C-276 and G.[15] Time-to-failure and crack propagation data showed that alloy C-276 has a greater tendency to HE than alloy G cold-worked to an equivalent degree. Alloys G and 625 are comparable in their levels of Cr, Mo, and Nb+Ta, so they might be expected to be similar in their resistance to HE. For the degree of cold work involved, alloy C-276 should therefore be less resistant to HE than alloy 625,[6] which coincides with the order of their trapping constants.

A lack of relevant data in the literature makes it difficult to determine whether the two cold-worked alloys fit in with the other alloys on the basis of their k values. The difficulty in evaluating the position of the cold-worked alloys is compounded by some uncertainty in these values. Nevertheless, the trapping constants for alloys 625 and 718 show a significant difference, and the sequence of values is consistent with results from C-ring and U-bend exposure tests that indicated alloy 625 is more resistant to cracking than alloy 718.[16]

If allowance is made for the uncertainty in k, the position of alloy 625 is comparable to that of alloy 35N. Tests using C-ring specimens of these alloys showed that the time-to-failure of unaged alloy 625 with 59% cold reduction is intermediate between those for 35% and 51% cold reduced alloy 35N in the aged condition.[17] Alloy 625 with 17% cold work, as was used in the present study, should withstand a longer exposure time than the same alloy with 59% cold work and therefore should be at least as resistant to HE as alloy 35N in the condition of interest (40-50% cold reduced and aged). In fact, the 625 specimen may be more resistant than the 35N alloy, as implied by their values of k. Thus, the order of the trapping constants parallels the relative resistance of these alloys to HE.

Ti grade 2 was also examined.[6] It exhibited two values of k, depending on the overpotential (Fig. 2) and therefore on the level of H in the alloy. Hydride precipitates have been observed in Ti grade 2 at H levels above ~100 ppm, but gross embrittlement does not result until much higher levels.[18] Thus, the similarity observed in the values of k for low-H Ti grade 2 and alloy 925 fits their relative resistance to HE in that both alloys must be exposed for long times to cause degradation of their mechanical properties.[14,18] Furthermore, the higher value of k for Ti grade 2 coincides with its decreased resistance to embrittlement at high enough H concentrations.

An exception to these trends was observed with alloy 716, which is an age-hardenable alternative to alloy 625.[16] Alloy 716 had a k of 0.2, which is the highest value among those for

the nickel-base alloys and indicates that this alloy is intrinsically the most susceptible to HE. However, tests with C-ring and U-bend specimens have shown that it is comparable to alloy 625 of similar yield strength in being able to withstand exposure in aggressive environments.[16] A likely explanation is that, although alloy 716 has a high intrinsic susceptibility, the H concentration at the dominant traps remains below the critical level required to initiate cracking. The entry flux was found to be low in the acetate buffer and could well have been low enough in the cracking test environments to delay failure in most cases (up to 1000 h). Thus, the resistance to cracking observed for alloy 716 was believed to be associated with the low entry flux of hydrogen.

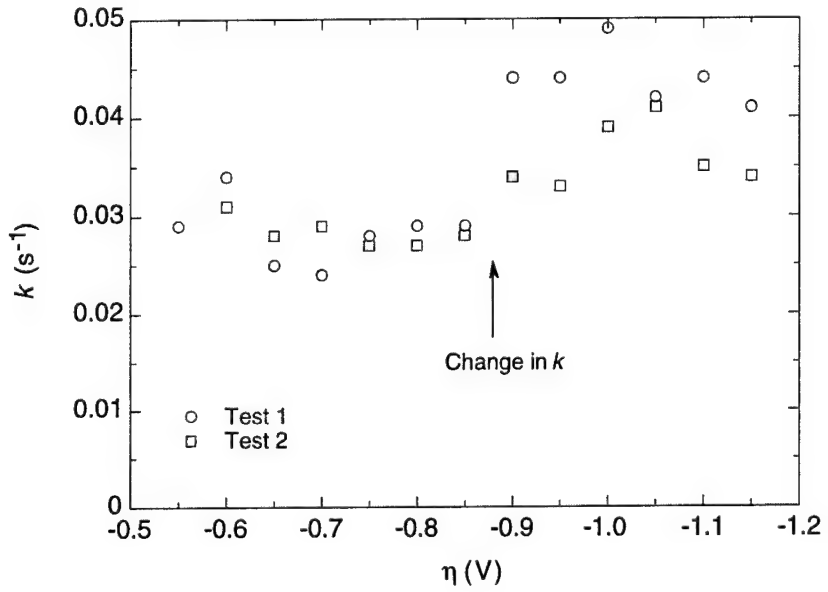

Figure 2. Variation in k with overpotential for Ti grade 2 in identical tests.

DISCUSSION

The alloys studied were generally characterized by a single type of irreversible trap, but in some alloys the principal irreversible type of trap was supplemented by other traps of either a quasi-irreversible type or another irreversible type. Values of k associated with the principal irreversible traps are listed in Table 4 for all the alloys except 716. They are also presented graphically in Fig. 3 to highlight differences between them.

The steels, particularly 4340, exhibit high values of k that are indicative of a high intrinsic susceptibility to HE, whereas the nickel-base alloys are characterized by lower values of k and are therefore intrinsically less susceptible. Differences in the susceptibility of the nickel-base alloys are smaller than those for the steels but are clearly discernible. In particular, the trapping constants for

alloys within groups defined by thermomechanical treatment (precipitation- and work-hardening) indicate that the susceptibilities can vary significantly.

Table 4
Irreversible Trapping Constants

Alloy	k (s^{-1})
4340 steel	4.0 ± 0.5
18Ni (300) steel	1.50 ± 1.05
718	0.124 ± 0.024
C-276 (27% cold work)	0.090 ± 0.030
K-500	0.042 ± 0.006
Ti grade 2 (high H)	0.040 ± 0.008
925	0.034 ± 0.004
Ti grade 2 (low H)	0.028 ± 0.002
35N	0.026 ± 0.002
625 (17% cold work)	0.014 ± 0.010

For most alloys, there appears to be a correlation between the intrinsic susceptibility, as represented by k, and the actual resistance to HE observed in failure tests. This correlation suggests that the observed resistance to HE is determined primarily by the alloy's intrinsic susceptibility—that is, by the irreversible trapping characteristics. Thus, the entry flux generally has only a secondary effect on the HE resistance.

Exceptions to this correlation can be expected in cases where the ingress flux for an alloy is low enough that the alloy is relatively resistant to cracking even though it might have a high

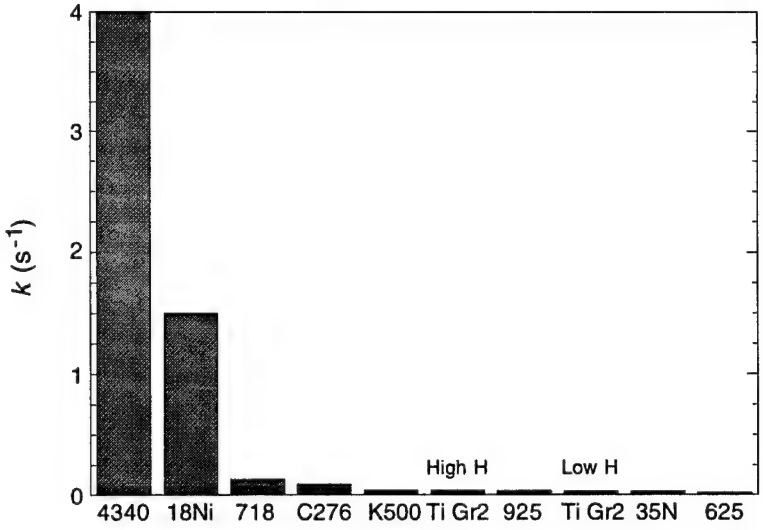

Figure 3. Variation in k for the different alloys.

intrinsic susceptibility. Such an exception was observed with alloy 716. The intrinsic susceptibility of this alloy was shown to be high ($k = 0.2$), yet the entry flux was apparently low enough that the alloy generally did not undergo cracking during exposure in aggressive environments for periods up to 1000 h.

The use of k to provide an index of HE susceptibility can be justified on the basis of Eq. (2), but there remains the question of why such a relatively simple parameter has the apparent ability in most cases to indicate the relative resistance actually observed to HE. Some insight may be gained by considering k, which encompasses the trapping capability (d^2N_i) as well as the alloy-specific characteristics of metal atom size and lattice diffusivity. The trapping capability has a strong influence on the critical concentration (C_k) required to initiate cracking at traps, while the diffusivity reflects the ease of H transport to different sites, including traps. Since the likelihood of crack initiation is highly dependent on both C_k and H accumulation, it is perhaps not surprising that k is effective as an index of susceptibility in being able to indicate the actual resistance of most alloys to HE. Underlying this rationale is the implication that, despite differences between alloys, the H entry flux is generally not low enough to become the controlling factor.

Finally, it should be noted that the density of particles or defects providing irreversible traps can be calculated from k, or k_a, by using Eq. (2). The trap radius (d) is estimated from the dimensions of heterogeneities that are potential irreversible traps, and trap densities are then calculated for the different values of d. In this way, the dominant irreversible trap can be identified by comparing the values of N_i with the actual concentrations of specific heterogeneities. Identification of the primary irreversible traps in the various alloys is described elsewhere.[4-8]

SUMMARY

For a wide range of alloys, a correlation exists between the intrinsic susceptibility, as defined by the irreversible trapping constant, and the observed resistance to HE. Thus, the HE resistance appears to be determined primarily by the alloy's intrinsic susceptibility. This relationship implies that generally the H entry flux has only a secondary effect on the HE resistance, suggesting that it is not low enough to become the controlling factor for most alloys. However, in one case (alloy 716), the resistance to HE can be attributed to a low entry flux.

The irreversible trapping constant, by virtue of the observed correlation, appears to be an indicator of the relative resistance to HE for most alloys, and as such, it can be used to predict the relative resistance of alloys in a particular environment. However, the predicted relative resistance may not be reliable in cases where H entry is severely restricted. The ability of k to provide an indication of the relative resistance to HE seems to be attributable to its dependence on both the

trapping capability and the diffusivity. The combination of these two characteristics is crucial for crack initiation and therefore provides a rationale for the correlation observed between k and the actual resistance to HE.

ACKNOWLEDGMENT

Financial support of this work by the Office of Naval Research under Contract N00014-86-C-0233 is gratefully acknowledged.

REFERENCES

1. I. M. Bernstein and G. M. Pressouyre, in *Hydrogen Degradation of Ferrous Alloys*, R. A. Oriani, J. P. Hirth, and M. Smialowski, Eds. (Noyes Publications, Park Ridge, NJ, 1985), p. 641.
2. G. M. Pressouyre and I. M. Bernstein, Metall. Trans. **9A**, 1571 (1978).
3. G. M. Pressouyre and I. M. Bernstein, Acta Metall. **27**, 89 (1979).
4. B. G. Pound, Corrosion **45**, 18 (1989); **50**, 301 (1994).
5. B. G. Pound, Acta Metall. **38**, 2373 (1990).
6. B. G. Pound, Acta Metall. **39**, 2099 (1991).
7. B. G. Pound, Corrosion **47**, 99 (1991).
8. B. G. Pound, Scripta Metall. **29**, 1433 (1993).
9. R. McKibbin, D. A. Harrington, B. G. Pound, R. M. Sharp, and G. A. Wright, Acta Metall., **35**, 253 (1987).
10. B. G. Pound, in *Modern Aspects of Electrochemistry*, J. O'M. Bockris, B. E. Conway, and R. E. White, Eds. (Plenum, New York, 1993), No. 25, p. 63.
11. B. G. Pound, R. M. Sharp, and G. A. Wright, Acta Metall. **35**, 263 (1987).
12. T. P. Groeneveld, E. E. Fletcher, and A. R. Elsea, "A Study of Hydrogen Embrittlement of Various Alloys," Tech. Support Package to Tech. Brief No. 67-10141 (NASA, Washington D.C., 1967), p. 135.
13. R. J. Walter, R. P. Jewett, and W. T. Chandler, Mater. Sci. Eng. **5**, 98 (1969/70).
14. C. G. Rhodes and A. W. Thompson, Metall. Trans., **8A**, 949 (1977).
15. D. A. Mezzanotte, J. A. Kargol, and N. F. Fiore, Metall. Trans., **13A**, 1181 (1982).
16. R. B. Frank and T. A. DeBold, *Properties of an Age-Hardenable, Corrosion-Resistant Nickel-Base Alloy*, Corrosion 88, Paper No. 75, National Association of Corrosion Engineers, Houston, TX (1988).
17. R. D. Kane, M. Watkins, D. F. Jacobs, and G. L. Hancock, Corrosion, **33**, 309 (1977).
18. R. W. Schutz and D. E. Thomas, in *Metals Handbook*, 9th ed., Vol. 13 (American Society for Metals, Metals Park, OH, 1987), p. 669.

THE ROLE OF TRAPS IN DETERMINING THE RESISTANCE TO HYDROGEN EMBRITTLEMENT*

Abstract

The ability of microstructural heterogeneities to act as hydrogen traps can critically affect the resistance of an alloy to hydrogen embrittlement (HE), so a knowledge of the alloy's trapping characteristics is crucial in accounting for the role of these heterogeneities. The entry and trapping of hydrogen in a range of high-strength alloys have been investigated using a technique referred to as hydrogen ingress analysis by potentiostatic pulsing (HIAPP) to determine the entry flux and the rate constant (k) *for irreversible trapping. For most of the alloys, the observed resistance to HE appears to be determined primarily by the alloy's intrinsic susceptibility defined by* k*; that is, the entry flux generally has only a secondary effect on the resistance to HE. Analysis of the trapping constants allowed identification of various microstructural heterogeneities as the principal irreversible traps, either singly or in combination. The size and density of the irreversible traps were primary factors underlying the intrinsic susceptibility to HE. For example, alloys such as 718 and 4340 steel that contained large particles as the primary irreversible traps were found to have high intrinsic susceptibilities (high values of* k*). Thus, it was shown that microstructural heterogeneities, such as precipitates and grain boundary segregants, impart an intrinsic susceptibility to the alloy through their capacity for trapping hydrogen and, as a result, generally play a key role in determining the HE resistance observed in practice.*

* In *Proceedings of the Fifth International Conference on Hydrogen Effects on Material Behavior*, N. R. Moody and A. W. Thompson, Eds. (The Minerals, Metals & Materials Society, Warrendale, PA, 1994), in press.

Introduction

The interaction of hydrogen with microstructural heterogeneities in alloys can play a crucial role in determining an alloy's resistance to hydrogen embrittlement (HE). These heterogeneities provide potential trapping sites for hydrogen and so can strongly influence the series of events leading to failure (1). The accumulation of hydrogen at second-phase particles and precipitates, for example, is generally considered to induce particle fracture or weakening of particle-matrix interfaces, thereby promoting microvoid initiation. Large incoherent precipitates tend to be particularly conducive to HE. In general, traps with a large saturability and a high binding energy for hydrogen are conducive to HE, whereas alloys containing a high density of well-distributed irreversible (high binding energy) traps that have a low saturability are considered to be less susceptible (2,3). Thus, the intrinsic susceptibility of an alloy to HE is highly dependent on the type of microstructural defect, with large irreversible traps typically imparting a high susceptibility.

The basic concept of trap theory is that the local concentration of hydrogen trapped at a defect must reach some critical value (C_k) for cracks to be initiated (1,3). It should be recognized, however, that the mechanism by which such an accumulation triggers HE is not addressed. The value of C_k at a potential crack site is determined by the type of trap, its size, concentration (density), and other parameters. A decrease in C_k will render the alloy more susceptible. However, whether embrittlement will actually occur is also affected by the amount of trapped H, which depends on factors such as the entry kinetics, exposure time, and transport mode. In some cases, an alloy may prove resistant during exposure because the amount of H entering the alloy is small enough that the critical concentration at a particular trap is not exceeded. Likewise, when alloys have similar intrinsic susceptibilities in terms of their trapping characteristics, the difference in their actual resistance to HE is likely to be determined by the amount of H absorbed by each alloy.

Over the last few years, the entry and trapping of hydrogen in a wide range of high-strength alloys have been investigated at SRI (4-9). The rates of H entry and rate constants for irreversible trapping were determined using an electrochemical technique referred to as hydrogen ingress analysis by potentiostatic pulsing (HIAPP) (4,10). The research was aimed in part at characterizing the intrinsic susceptibility of the alloys to HE in terms of their irreversible trapping constants. The relative intrinsic susceptibilities then could be compared with results for the actual resistance to HE observed in tests by other workers. A further goal was to determine the trap density where possible and thereby identify the principal irreversible trap in each alloy. In this paper, the irreversible trapping constants and principal irreversible traps for particular groups of alloys are compared, with the objective of rationalizing the role of traps in determining the resistance of these alloys to HE.

Experimental Procedure

In the pulse technique, the alloy of interest is cathodically charged with hydrogen at a constant potential E_c for a time t_c, after which the potential is stepped in the positive direction. H diffuses back to the entry surface and is reoxidized, thereby generating an anodic current transient. Data are obtained over a range of charging times, typically from 5 to 60 s, at different overpotentials ($\eta = E_c - E_{oc}$) relative to the open-circuit potential (E_{oc}), which is measured immediately before each charging time. E_{oc} is also used to monitor the stability of the alloy surface, since any oxides present must not be reduced during charging.

The pulse technique was applied to high-strength steels (4,5), precipitation-hardened and work-hardened nickel-base alloys (4-8), and titanium grade 2 (9). The composition of each alloy is given in Table I. Table II shows the yield strength of the alloys and the thermomechanical treatment used in each case. A number of the alloys contained micrometer-size particles such as carbides or, in the case of 4340 steel, sulfide inclusions.

Test electrodes of each alloy were fabricated from a length (1.3-3.8 cm) of rod press-fitted into a

Table I. Alloy Composition (wt%)

	4340	18Ni	718	925	C-276	625	716	K-500	35N	Ti Gr2
Al	0.031	0.13	0.60	0.30		0.18	0.22	2.92		
B		0.003	0.003							
C	0.42	0.009	0.03	0.02	0.002	0.03	0.011	0.16	0.003	0.021
Co		9.15	0.16		0.83		<0.01		bal	
Cr	0.89	0.06	18.97	22.20	15.27	22.06	20.99		20.19	
Cu	0.19	0.11	0.04	1.93				29.99		
Fe	bal	bal	16.25	28.96	5.84	4.37	5.32	0.64	0.34	0.17
Mn	0.46	0.01	0.10	0.62	0.48	0.17	0.01	0.72	<0.01	
Mo	0.21	4.82	3.04	2.74	16.04	8.70	8.10		9.55	
O	0.001									0.16
Nb+Ta			5.30			3.50	3.47			
Ni	1.74	18.42	54.41	40.95	57.5	60.33	60.5	64.96	35.88	
P	0.009	0.004	0.009		<0.005	0.012	0.004		0.003	
S	0.001	0.001	0.002	0.001	<0.002	0.001	0.001	0.001	0.002	
Si	0.28	0.04	0.11	0.17	<0.02	0.38	0.02	0.15	0.02	
Ti		0.65	0.98	2.11		0.27	1.35	0.46	0.85	bal
W		0.01			3.90					
Other	0.005N	0.05 Ca			0.12 V					<0.005H
		0.02 Zr								0.007N

Teflon sheath so that only the planar end surface was exposed to the electrolyte. The surface was polished before each experiment with SiC paper followed by 0.05-μm alumina powder. Details of the electrochemical cell and instrumentation have been given elsewhere (4). The alloys were exposed in a deaerated solution containing 1 mol L^{-1} acetic acid and 1 mol L^{-1} sodium acetate with 15 ppm As_2O_3 added to promote H entry. The potentials were measured with respect to a saturated calomel electrode (SCE). All tests were performed at 22 ± 2°C.

Table II. Thermomechanical Treatment of Alloys

Alloy	Heat Treatment[a]	Test Condition	Yield Strength (MPa)
4340	Annealed	HRC[b] 41	1206
		HRC 53	1792
18Ni	Aged (482°C, 4 h)	As received	1954
718	Hot fin., solution treated	As received	1238
925	Hot fin., annealed, aged	As received	758
C-276	Hot rolled	27% cold work	1237
625	Hot fin., annealed	17% cold work	1195
716	Annealed, aged	4% cold work	1186
K-500	Cold drawn, unaged	As received	758
		Aged (600°C, 8 h)	1096
35N	Cold drawn and aged	As received	1854
Ti Gr 2	Annealed (620°C, 1 h)	As received	380

[a] Provided by producer. [b] Rockwell C hardness

Analysis

Although permeation methods have been used extensively, they suffer from several disadvantages, as discussed elsewhere (11). The main theoretical limitation is that most, if not all, diffusion/trapping models for these methods are based on an input boundary condition of constant concentration. Hence, these models are strictly applicable only for charging conditions without any entry limitation.

In the case of HIAPP, a model has been developed to allow for the effect of trapping on diffusion for cases involving either a constant concentration or a constant flux at the input surface (4,10). The constant flux model was found to apply to all alloys studied to date. In this model, the rate of hydrogen ingress is controlled by diffusion but the entry flux of hydrogen is restricted, which results in interface-limited diffusion control. Solution of the diffusion equation for a constant flux condition gives the following expression for the total anodic charge (C m^{-2}):

$$q'(\infty) = FJt_c\{1 - e^{-R}/(\pi R)^{1/2} - [1 - 1/(2R)]\mathrm{erf}(R^{1/2})\} \qquad (1)$$

where F is the Faraday constant, J is the entry flux in mol m^{-2} s^{-1}, and $R = k_a t_c$. The charge $q'(\infty)$ is equated to the charge (q_a) passed during the experimental anodic transients. q_a can be associated entirely with absorbed H, since the adsorbed charge is almost invariably negligible.

k_a is an apparent trapping constant measured for irreversible traps in the presence of reversible traps. It is related to the irreversible trapping constant (k) by kD_a/D_L, where D_a is the apparent diffusivity and D_L is the lattice diffusivity of H. The magnitude of k depends on the density of particles or defects (N_i) providing irreversible traps, the radius (d) of the trap defects, the diameter (a) of the metal atom, and D_L (12):

$$k = 4\pi d^2 N_i D_L / a \qquad (2)$$

The term d^2N_i represents the trapping capability and underlies the use of k as an index for characterizing an alloy's intrinsic susceptibility to HE.

For the constant flux model to be applicable, it must be possible to determine a trapping constant for which J is independent of charging time. Eq. [1] could in fact be fitted to the experimental data for q_a to obtain values of k_a and J that satisfy this requirement at each potential.

The trap density (N_i) can be obtained from k or directly from k_a, according to Eq. [3]:

$$N_i = k_a a/(4\pi d^2 D_a) \qquad (3)$$

The value of a for an alloy is taken as the mean of the atomic diameters weighted in accordance with the atomic fraction of each element. The trap radius is estimated from the dimensions of heterogeneities that are potential irreversible traps, and trap densities are then calculated for the different values of d. In this way, the dominant irreversible trap can be identified by comparing the values of N_i with the actual concentrations of specific heterogeneities.

Susceptibility to HE

The values of k_a and k for the various alloys are given in Table III. Most of the alloys were characterized by a single type of irreversible trap, but alloy C-276 and the 18Ni steel were characterized by both a quasi-irreversible trap and an irreversible trap. In quasi-irreversible trapping, the release constant is not zero but is far too small to achieve local equilibrium between the lattice and trapped H (5).

Among the alloys studied, 4340 steel (HRC 53) has the highest value of k and so can be classified as having the highest intrinsic susceptibility to HE. The 18Ni maraging steel has the next highest k value, followed by various Ni-base alloys, with alloy 625 having the lowest value. Failure tests during cathodic charging have shown that 18Ni (1723 MPa) steel is more resistant to cracking than 4340 steel (13) but that the 18Ni steel will undergo severe HE, whereas alloy 718 exhibits negligible embrittlement (14). Furthermore, ductility losses (14,15) under gas-phase charging suggest that alloy 903 and, by implication, alloy 925 are less sensitive than alloy 718 to HE. Hence, the irreversible trapping constants of the precipitation-hardened alloys, 18Ni, 718, and 925, are consistent with their relative resistances to HE observed in tests.

A similar comparison of the resistances of the work-hardened alloys, C-276 and 625, is complicated by their sensitivity to cold work. However, failure tests have shown that alloy C-276 has a greater tendency to HE than alloy G cold-worked to an equivalent degree (16). Alloys G and 625 are comparable in their levels of Cr, Mo, and—more important—Nb+Ta, so they are likely to be similar in their resistance to HE. Hence, for the degree of cold work involved, alloy C-276 should be less resistant to HE than alloy 625 (6), which matches the order of their trapping constants.

Table III. Trapping Parameters

Alloy	k_a (s^{-1})	D_L/D_a	k (s^{-1})
4340 steel (HRC 53)[a]	0.008 ± 0.001	500	4.0 ± 0.5
18Ni (1954 MPa) steel	0.005 ± 0.002	300 ± 90	1.50 ± 1.05
	0.010 ± 0.005[b]	300 ± 90	3.00 ± 2.40
716 (4% cold work)	0.054 ± 0.004	3.8 ± 0.8	0.20 ± 0.06
718	0.031 ± 0.002	4.0 ± 0.5	0.124 ± 0.024
925	0.006 ± 0.003	5.6 ± 0.6	0.034 ± 0.004
C-276 (27% cold work)	0.025 ± 0.003	3.6 ± 0.8	0.090 ± 0.030
	0.019 ± 0.010[b]	3.6 ± 0.8	0.068 ± 0.051
625 (17% cold work)	0.004 ± 0.002	3.6 ± 0.8	0.014 ± 0.010
K-500 Unaged	0.017 ± 0.003	2.0	0.034 ± 0.006
Aged	0.021 ± 0.003	2.0	0.042 ± 0.006
35N	0.026 ± 0.002	1	0.026 ± 0.002
Ti grade 2 (low H)	0.028 ± 0.002	1	0.028 ± 0.002
(high H)	0.040 ± 0.008	1	0.040 ± 0.008

[a] HRC 41 had the same value of k_a. [b] Quasi-irreversible trapping.

Evaluating the positions of the cold-worked alloys relative to the other alloys is more difficult because of some uncertainty in their values of k. Nevertheless, the trapping constants for alloys

625 and 718 show a significant difference, and the sequence of values is consistent with results from exposure tests that indicated alloy 625 is more resistant to cracking than alloy 718 (17).

If allowance is made for the uncertainty in k, the position of alloy 625 is comparable to that of alloy 35N. Failure tests (18) have indicated that alloy 625 with 17% cold work should be at least as resistant to HE as alloy 35N in the condition of interest (40-50% cold reduced and aged). In fact, the 625 specimen may be more resistant than the 35N alloy, as implied by their k values. Thus, the order of the trapping constants parallels the relative resistance of these alloys to HE.

Ti grade 2 exhibited two values of k (Fig. 1), depending on the overpotential and therefore on the level of H in the alloy (9). The similarity in the values of k for low-H Ti grade 2 and alloy 925 fits the relative resistance of these two alloys to HE in that both require long exposure times for their mechanical properties to be degraded (15,19). The higher value of k for Ti grade 2 coincides with its decreased resistance to embrittlement at sufficiently high levels of H (19).

An exception to the above trends was observed with alloy 716, which is an age-hardenable alternative to alloy 625 (17). Alloy 716 had the highest value of k among those for the nickel-base alloys, yet mechanical tests have shown that it is comparable to alloy 625 of similar yield strength in being able to withstand exposure in aggressive environments for periods up to 1000 h (17). A likely explanation is that the H concentration at the dominant traps remains below the critical level required to initiate cracking. In fact, the entry flux of H was low in the acetate buffer and could well have been low enough in the cracking test environments to delay failure (8). Thus, the resistance to cracking observed for alloy 716 was attributed to a low entry flux.

Identification of Traps

The intrinsic susceptibility of an alloy, as noted above, is strongly influenced by the characteristics of its irreversible traps. Identification of the traps on the basis of density and size can be expected to assist in explaining differences in the intrinsic susceptibility of the alloys. Hence, for each alloy, the density of irreversible trap defects calculated from k_a (Eq. [3]) was compared with the actual concentration of defects that were assumed to provide the principal traps, as shown in Table IV.

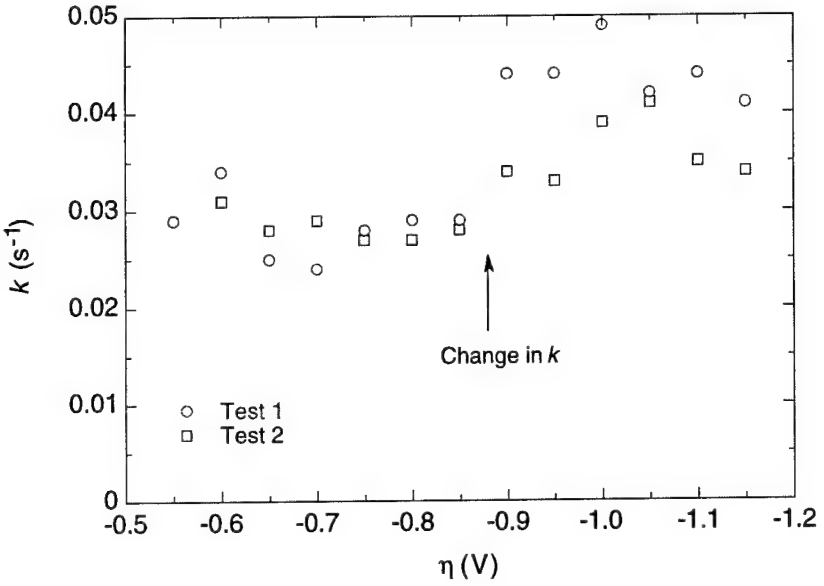

Figure 1. Variation in k with overpotential for Ti grade 2 in identical tests.

Precipitates/Inclusions

The Ni-base alloys, 718, 925, 716, and 625, contained carbide or carbonitride particles, which are known to provide irreversible traps in steels (1). The density of irreversible trap defects was therefore calculated on the basis of these particles and was generally found to be in close agreement with the actual concentration of particles, despite some uncertainty in the value of D_a, particularly for alloys 625 and 716. The level of agreement is remarkable, since both the traps and carbides were treated as spherical in calculating the trap density and particle concentration, respectively. However, it indicates clearly that large traps with both a high surface area and a high binding energy can overwhelmingly dominate the irreversible trapping behavior of an alloy.

Table IV. Comparison of Irreversible Trap Densities with Defect Concentrations

Alloy	Defect	Concentration (m^{-3})	N_i (m^{-3})
718	NbTi(CN)	2.2×10^{13}	2.0×10^{13}
925	TiC	4.6×10^{13}	4.1×10^{13}
625	NbTi(C)	7.4×10^{13}	2.5×10^{13}
716	TiC	1.4×10^{15}	1.4×10^{15}
18Ni	TiC/Ti(CN)	1.1×10^{13}	3.4×10^{11}
4340	MnS	2×10^{9}	2×10^{8}
C-276	P (seg)	9×10^{21}	1.9×10^{22}
35N	S, P (seg)	8×10^{21}	8.2×10^{21}
K-500 (Aged)	S (seg)	Not available	2.7×10^{21}

The 18Ni steel contained TiC/Ti(CN) particles, which have been shown to act as strong traps in this type of steel (20). Hence, the irreversible trap density was calculated assuming that these particles acted as the principal traps. The values of N_i and the particle concentration differed by a factor of ~30 but were considered to correlate moderately well, since the difference can be attributed largely to uncertainties in the particle concentration and the value of D_a used for the steel.

The 4340 steel had MnS inclusions, which are prominent irreversible traps in steels (1). The calculated trap density was considered to be in reasonable agreement with the actual concentration of inclusions, since both the inclusions and the traps were assumed to be spherical. Also, N_i did not change significantly with heat treatment, and this lack of change was further evidence that the irreversible traps were associated with the sulfide inclusions.

Segregants

The HE resistance of alloys C-276 and 35N has been correlated with the concentration of S and P segregated at grain boundaries (21,22). Hydrogen segregates to the grain boundaries in Ni (23) and presumably does so in Ni-base alloys, so grain boundary S and P were assumed to provide the irreversible traps predominantly encountered by H in alloys C-276 and 35N. In the case of alloy C-276, it has been suggested that a higher level of grain boundary P may reduce the critical concentration of H required for fracture (21).

In unaged alloy C-276, P is enriched from a bulk concentration of 0.006-0.008 at.% (0.003-0.004 wt.%) to 0.3 at.% at grain boundaries (21). Using the grain boundary concentration, the amount of grain boundary P distributed per unit volume (C_{gb}) of the alloy was estimated in terms of a simple microstructural model based on cubic grains of length b (6). For alloy C-276 in the

condition of interest, b = 10 μm and C_{gb} was calculated to be $9 \times 10^{16}/b$, or 9×10^{21} P atoms m^{-3}. The trap density of 1.9×10^{22} m^{-3} calculated on the basis of atomic P was close to the grain boundary concentration, whereas the total P content (taken as 0.004 wt.%) of the alloy corresponded to a much higher concentration, 8.6×10^{24} atoms m^{-3}.

For alloy 35N in the same cold-worked and aged condition used in this study, the level of S and P at grain boundaries has been found to reach 1.6 at.%, compared with a bulk concentration of 0.01 at.% (0.005 wt.%) (22). C_{gb} for segregated S and P in alloy 35N is given by $4.8 \times 10^{17}/b$ atoms m^{-3}. The grains in 59% cold reduced and aged (593°C/4 h) alloy have an average dimension of 60 μm, and using this value gave a C_{gb} of ~8×10^{21} atoms m^{-3}. The trap density calculated in terms of S and P was 8.2×10^{21} atoms m^{-3}, which closely matched the value of C_{gb} but was 3 orders of magnitude less than the total concentration of S and P (0.005 wt.%, or 8.1×10^{24} atoms m^{-3}) in the alloy. The large differences between N_i and the S-P content in alloys C-276 and 35N indicated that the primary irreversible traps were not associated with matrix S and P. In contrast, the close agreement between the values of C_{gb} and N_i, though somewhat fortuitous, was strong evidence that the primary traps were grain boundary S and P.

Ni-Cu base alloys also undergo HE that is assisted by S segregated at grain boundaries (24), so the irreversible trap density for alloy K-500 was calculated on the basis of atomic S. However, the absence of data for S segregation in this alloy meant that the identity of the principal irreversible traps could not be verified by comparing N_i with the grain boundary concentration. On the other hand, it was apparent that the principal traps were not associated with matrix S, since N_i was about 3 orders of magnitude less than the S content (1.6×10^{24} atoms m^{-3}) of the alloy. TiN particles present in alloy K-500 were likewise ruled out as the principal traps because of a large (2 orders of magnitude) difference between the corresponding value of N_i and the particle concentration. In contrast, the results for alloys C-276 and 35N lent some support to the case for considering a grain boundary segregant (in this case, S) as the principal trap in alloy K-500. Further support was provided by recent results for a 77% Cu-15% Ni alloy, which was found to have a higher trap density than that for the 65Ni-30Cu alloy K-500 (7). Even allowing for some difference in the degree of segregation between the two alloys, the higher trap density was consistent with a higher level of grain boundary segregants, based on the higher S-P content (0.015 wt.%) of the 77Cu-15Ni alloy.

Interstitials

The density of traps detected in Ti grade 2 at low H levels was calculated in terms of the minor elements (C, N, O, and Fe). All of the elements except N could be discounted as the principal irreversible trap because of large differences between the values of N_i and the atomic concentrations. Interestingly, among the interstitials, N is particularly effective in reducing the ductility of Ti (25), which coincides with its apparent role as the principal trap. Hence, N may affect the HE resistance of Ti grade 2 through its influence on both brittleness and H trapping.

Hydrides

Evidence of trapping by way of hydride formation was observed in Ti grade 2 and alloy C-276. The increase in k for Ti grade 2 at sufficiently negative potentials ($E_c < -0.93$ V) can be ascribed to an additional irreversible trap that participates concurrently with the N traps. The additional trapping appeared to be associated with accelerated hydride formation that occurs at potentials more negative than -1.0 V (26). The H entry efficiency, which can be calculated from k_a and J, was found to decrease in this region; the decrease was attributed to H entry being partially blocked by a hydride layer (9).

For alloy C-276, the quasi-irreversible trapping was consistent with the formation of an unstable hydride, as found by other workers (27). The quasi-irreversible traps in 18Ni steel, however, were thought to be martensite boundaries, which are moderately strong traps in this type of steel

(20). A trap density of 9×10^{17} m^{-3} was calculated in terms of the martensite boundaries, which, like grain boundaries (28), were assumed to have an influence diameter of 3 nm.

Discussion

The alloys in this work were typically characterized by a single irreversible trap, but in some alloys the principal trap was supplemented by another irreversible trap or a quasi-irreversible trap. Values of k associated with the principal irreversible traps are presented in Fig. 2 for all the alloys except 716. The steels, particularly 4340, exhibited high values of k that were indicative of a high intrinsic susceptibility to HE, whereas the nickel-base alloys were characterized by lower values of k and therefore were intrinsically less susceptible. Differences in the susceptibility of the nickel-base alloys were smaller than those for the steels but were clearly discernible, as shown in Table III.

Most of the alloys appear to show a correlation between the intrinsic susceptibility, as represented by k, and the actual resistance to HE observed in mechanical tests. This correlation suggests that, for these alloys, the observed resistance to HE was determined primarily by the alloy's intrinsic susceptibility—that is, by the irreversible trapping characteristics. Thus, while factors such as the entry flux and stress level may be important, they seem to have had only a secondary effect on the HE resistance in most cases. Exceptions to this correlation can occur in cases such as alloy 716, where the entry flux is low enough that the alloy is relatively resistant to cracking, even though it might have a high intrinsic susceptibility.

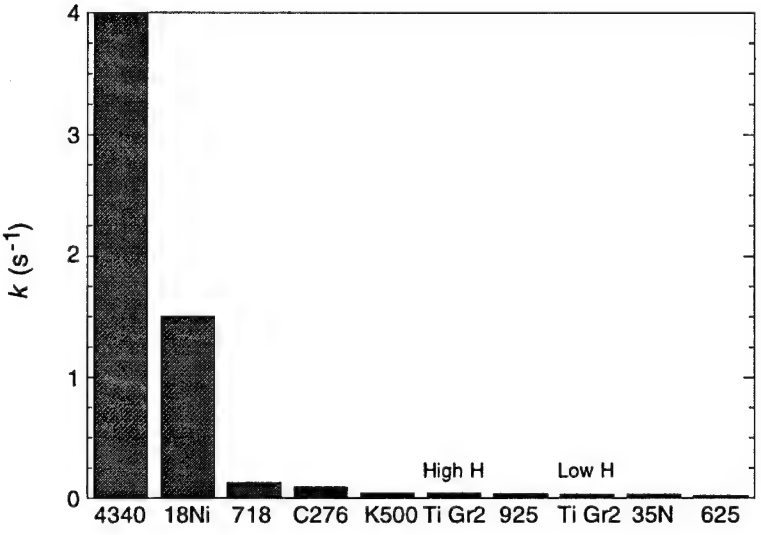

Figure 2. Variation in k for the different alloys.

The use of k to provide an index of HE susceptibility can be justified on the basis of Eq. [2], but there remains the question of why such a relatively simple parameter has the apparent ability in most cases to indicate the relative resistance observed to HE. Some insight may be gained by considering k, which encompasses the trapping capability (d^2N_i) as well as the alloy-specific characteristics of metal atom size and lattice diffusivity. For simplicity, the defects providing the principal traps are assumed to be similar in size (d), with the critical concentration (C_k) at each of these defects having roughly the same value. The trap defect size has a strong influence on C_k and is incorporated as an area term in the trapping capability together with the density of potential crack

sites possessing this C_k, while the diffusivity reflects the ease of H transport to different sites, including traps. Since the likelihood of crack initiation is highly dependent on both C_k and H accumulation as well as the availability of sufficiently large defects, it is perhaps not surprising that k is effective as an index of susceptibility in being able to indicate the actual resistance of most of the alloys to HE. Underlying this rationale is the implication that, despite differences in the H entry flux between the alloys, the flux was generally not low enough to become the controlling factor.

The nature of the irreversible trap defects appears to play a significant but not exclusive role in determining the intrinsic susceptibility of an alloy. Alloys such as 718 and 4340 steel, in which the principal traps are large second-phase particles, typically exhibited a high intrinsic susceptibility ($k > 0.1\ s^{-1}$), whereas other alloys did not show a relationship between the susceptibility and the type of irreversible trap, whether it be particles, segregants, or interstitials. However, the microstructural features that provided the principal traps in the different alloys had a wide range of sizes and concentrations, and for alloys with comparable H diffusivities, the resulting diversity in trapping capabilities produced considerable differences in the intrinsic susceptibilities to HE. In cases where the values of D_L are similar, k is predicted to increase linearly with $N_i d^2$ (Eq. [2]). Fig. 3 shows the dependence of k on $C_p(d_p/2)^2$ for the four alloys (625, 716, 925, and 718) containing carbides or carbonitrides, where C_p and d_p are the concentration and characteristic dimension, respectively, of the particles. Although the amount of data is limited and the value of D_a for alloy 625 is uncertain, a linear relationship seems to exist, which underscores the fact that the carbide/carbonitride particles appear to be primarily responsible for irreversible trapping in these alloys.

Summary

For a wide range of alloys, a correlation exists between the intrinsic susceptibility, as defined by the irreversible trapping constant, and the observed resistance to HE. Thus, the HE resistance appears to be determined primarily by the alloy's intrinsic susceptibility. This relationship implies that the H entry flux generally has only a secondary effect on the HE resistance for most of the alloys, which suggests that the flux is usually not low enough to become the controlling factor.

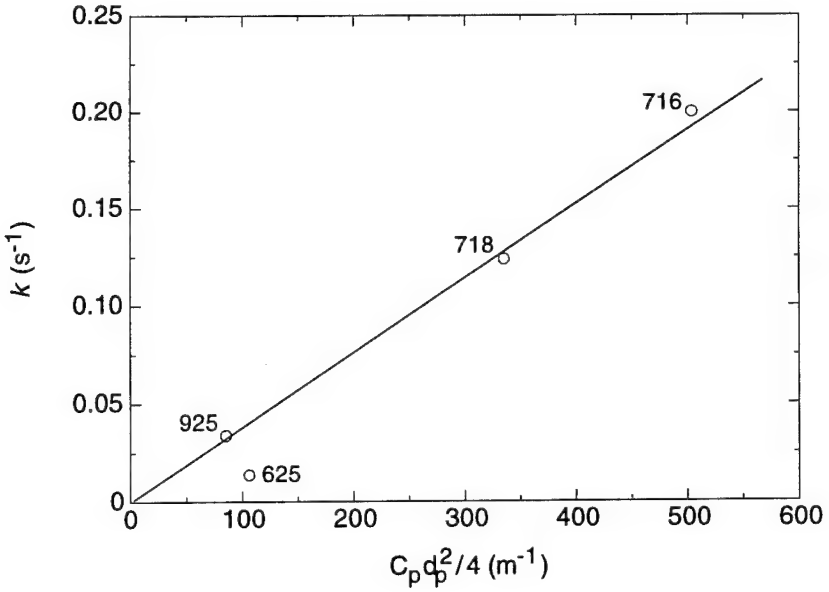

Figure 3. Dependence of k on $C_p(d_p/2)^2$ for Ni-base alloys containing particles.

However, in one case (alloy 716), the resistance to HE can be attributed to a low entry flux. The irreversible trapping constant, by virtue of the observed correlation, appears able to indicate the relative resistance to HE for all the alloys except 716. This ability of k seems to be attributable to its dependence on both the trapping capability and the diffusivity. The combination of these two characteristics is crucial for crack initiation and therefore provides a rationale for the correlation observed between k and the resistance to HE. Various microstructural features can be identified as the principal irreversible traps, either singly or in the presence of multiple principal traps. Although k is affected by the diffusivity, the variation in intrinsic susceptibility of the different Ni-containing alloys generally seemed to result from differences in the trapping capability caused by the diversity of sizes and concentrations of the microstructural defects.

Acknowledgment

Financial support of this work by the Office of Naval Research under Contract N00014-86-C-0233 is gratefully acknowledged.

References

1. I. M. Bernstein and G. M. Pressouyre: in *Hydrogen Degradation of Ferrous Alloys*, R. A. Oriani, J. P. Hirth, and M. Smialowski, eds., Noyes Publications, Park Ridge, NJ, 1985, pp. 641-85.
2. G. M. Pressouyre and I. M. Bernstein: *Metall. Trans.*, 1978, vol. 9A, pp. 1571-80.
3. G. M. Pressouyre and I. M. Bernstein: *Acta Metall.*, 1979, vol. 27, pp. 89-100.
4. B. G. Pound: *Corrosion*, 1989, vol. 45, pp. 18-25.
5. B. G. Pound: *Acta Metall.*, 1990, vol. 38, pp. 2373-81.
6. B. G. Pound: *Acta Metall.*, 1991, vol. 39, pp. 2099-105.
7. B. G. Pound: *Corrosion*, 1994, vol. 50, pp. 301-7.
8. B. G. Pound: *Scripta Metall.*, 1993, vol. 29, pp. 1433-38.
9. B. G. Pound: *Corrosion*, 1991, vol. 47, pp. 99-104.
10. R. McKibbin, D. A. Harrington, B. G. Pound, R. M. Sharp, and G. A. Wright: *Acta Metall.*, 1987, vol. 35, pp. 253-62.
11. B. G. Pound: in *Modern Aspects of Electrochemistry*, J. O'M. Bockris, B. E. Conway, and R. E. White, eds., Plenum Press, New York, NY, 1993, No. 25, pp. 63-133.
12. B. G. Pound, R. M. Sharp, and G. A. Wright: *Acta Metall.*, 1987, vol. 35, pp. 263-70.
13. T. P. Groeneveld, E. E. Fletcher, and A. R. Elsea: "A Study of Hydrogen Embrittlement of Various Alloys," Tech. Support Package to Tech. Brief No. 67-10141, NASA, 1967.
14. R. J. Walter, R. P. Jewett, and W. T. Chandler: *Mater. Sci. Eng.*, 1969/70, vol. 5, pp. 98-110.
15. C. G. Rhodes and A. W. Thompson: *Metall. Trans.*, 1977, vol. 8A, pp. 949-54.
16. D. A. Mezzanotte, J. A. Kargol, and N. F. Fiore: *Metall. Trans.*, 1982, vol. 13A, pp. 1181-86.
17. R. B. Frank and T. A. DeBold: "Properties of an Age-Hardenable, Corrosion-Resistant Nickel-Base Alloy," Corrosion 88, NACE, Houston, TX, 1988, Paper No. 75.
18. R. D. Kane, M. Watkins, D. F. Jacobs, and G. L. Hancock: *Corrosion*, 1977, vol. 33, pp. 309-20.
19. R. W. Schutz and D. E. Thomas: in *Metals Handbook*, ASM, Metals Park, OH, 1987, vol. 13, pp. 669-97.
20. M. Aucouturier, G. Lapasset, and T. Asaoka: *Metallography*, 1978, vol. 11, pp. 5-21.
21. B. J. Berkowitz and R. D. Kane: *Corrosion*, 1980, vol. 36, pp. 24-29.
22. R. D. Kane and B. J. Berkowitz: *Corrosion*, 1980, vol. 36, pp. 29-36.
23. D. H. Lassila and H. K. Birnbaum: *Acta Metall.*, 1987, vol. 35, pp. 1815-22.
24. J. D. Frandsen and H. L. Marcus: in *Effect of Hydrogen on the Behavior of Materials*, I. M. Bernstein and A. W. Thompson, eds., TMS, Warrendale, PA, 1976, pp. 233-48.
25. A. E. Jenkins and H. W. Worner: *J. Inst. Metal.*, 1951/52, vol. 80, p. 157.

26. H. Sato, T. Fukuzuka, K. Shimogori, and H. Tanabe: "Hydrogen Pickup by Titanium Held Cathodic in Seawater," 2nd International Congress on Hydrogen in Metals, Paris, 1977.
27. E. Lunarska-Borowiecka and N. F. Fiore: *Metall. Trans.*, 1981, vol. 12A, pp. 101-7.
28. G. M. Pressouyre: *Metall. Trans.*, 1979, vol. 10A, pp. 1571-73.

Addendum

The concepts explored in the review above attempt to bring together the various aspects of hydrogen embrittlement ranging from hydrogen entry through trapping to cracking. These concepts could not be adequately discussed in the review and are therefore considered in more detail below.

Intrinsic Susceptibility to HE

The intrinsic susceptibility to HE is affected by a range of factors, but some of them would be expected to exert a greater influence than others and so be primarily responsible for determining the susceptibility. The irreversible trapping constant (k) that was used as an index of the intrinsic susceptibility incorporates several key parameters: trap size, trap density, lattice diffusivity, and metal atom size. The local mechanical conditions are addressed to some extent through the trap size in the case of particles because of the strong influence that trap size has on the critical concentration (C_k). C_k is the concentration of H required to cause enough of an increase in the induced and applied stresses and/or the hydrogen pressure to overcome the cohesive strength, which itself may be decreased (1). Since larger particles lead to higher local stress concentrations, the trap size affects C_k (in part) by affecting the difference between the local stresses and cohesive strength. Hence, k, in allowing for trap size, implicitly contains some allowance for the effect of the local stress/cohesive strength conditions on C_k.

The correlation between k and the observed resistance to HE suggests that k contains enough key parameters to be effective as an index of susceptibility for the alloys studied at their respective yield strengths. The correlation for the high-strength steels is supported by recent trapping data for the aged martensitic steel, AerMet 100 (yield strength = 1834 MPa) (2). The order of the irreversible trapping constants for 4340 steel, 18Ni steel, and AerMet 100 (k = 0.41 s^{-1}) is consistent with their threshold stress intensities for stress corrosion cracking. Thus, it seems increasingly unlikely that the correlation for the high-strength steels is fortuitous. However, it is possible that factors other than those above could assume a greater role at low yield strengths, such that k becomes inadequate as an index of susceptibility.

At high yield strengths, k must decrease with decreasing yield strength of these steels, if it is to be consistent with the reported increase in K_{ISCC} (3,4). The lattice diffusivity (D_L) and therefore k could be affected by the microstructural changes that occur as the tempering temperature is increased (yield strength decreased). However, it can be difficult to find appropriate values for D_L because the measured diffusivities are usually affected by trapping. For the 4340 and 18Ni steels, D_L was taken to be the diffusivity for α-Fe and Fe-18Ni, respectively, but it would have been more appropriate to use the diffusivity, if it were available, for the corresponding tempered martensitic lattice. It has been shown for a high-strength martensitic steel containing 0.4C-0.6Mn-0.3Ni (compared with 0.42C-0.46Mn-1.74Ni in the 4340 steel) that the diffusivity decreases as the tempering temperature is increased above the point where ε-carbide precipitation is essentially complete and quenched-in lattice defects have largely been relieved (5). Thus, although part of this decrease probably resulted from reversible trapping, it seems that a decrease in D_L is quite plausible in the case of 4340 steel.

The value of k for 4340 steel could also change because of a change in the type of principal irreversible trap and therefore in $N_i d^2$. Sulfide inclusions are important irreversible traps in 4340 steel, as shown by thermal desorption results (6) and by differences in H absorption and outgassing between different grades of 4340 steel (7). However, incoherent Fe_3C and high angle grain boundaries can also act as irreversible traps, though their presence in 4340 steel depends on the tempering conditions (8). It has been found that MnS inclusions act as traps in a low alloy steel (0.34C-1Cr) tempered at 300°C, and precipitates come into play in specimens tempered at 600°C (9). Hence, it is possible that sulfide inclusions provide the predominant irreversible traps in 4340 steel at very high yield strengths (low tempering temperatures) where there is negligible Fe_3C and another defect becomes the principal trap as the yield strength is decreased.

The cracking behavior of 4340 steel is strongly influenced by the relative importance of the different irreversible traps (8). Prominent particle-type traps such as large (even round) inclusions have a high probability of cutting or lying along grain boundaries, and cracks initiated at the inclusions are then likely to follow the relatively susceptible grain boundary (10). The importance of each trap depends on its density and size, so cracking can be affected by the grade of 4340 steel and its yield strength (heat treatment) as well as by the level of elements such as Mn (11)—Mn, for example, is detrimental (12) when segregated to grain boundaries in high strength steels. It is therefore important that the interpretation of cracking behavior in terms of trapping be made on the basis of comparable specimens for the respective tests.

The possibility also exists that some type of defect other than sulfide inclusions provides the principal irreversible trap in 4340 steel, even at high yield strengths. The trap density calculated on the basis of sulfide inclusions differed from the actual concentration of inclusions by a factor of 10, which was regarded as being reasonably close. (It was also reported that N_i did not change significantly with heat treatment, but this conclusion was based on the rough approximation that D_a did not vary significantly with heat treatment.) However, this difference may imply that the sulfide inclusions were not the principal traps. If incoherent Fe_3C or high angle grain boundaries were the principal traps, $N_i d^2$ and therefore k for 4340 steel would be expected to change with heat treatment.

In maraging steels, the resistance to H-assisted cracking (generally intergranular) is thought to be lowered by Ti(CN) particles (4). Autoradiography has shown that hydrogen trapping occurs at the carbonitride interfaces in maraging steels, and this trapping is reported to be strong enough to explain crack initiation; the interface between the carbonitride particle and its matrix appears to be weakened by trapped hydrogen (13). The trap density and concentration of TiC/Ti(CN) particles in the 18Ni steel used in the present work differed by a factor of ~30 but were considered to be moderately close, for reasons given in the paper. As with 4340 steel, this difference may in fact indicate that these particles were not the principal traps. Still, the carbides/carbonitrides were >1 μm in size, which puts them in the category of detrimental—rather than beneficial—traps, as designated by Bernstein and Pressouyre (14). In the case of the Ni-base alloys, carbides and carbonitrides were generally identified as the principal traps, and various studies have shown that fracture is typically initiated by void formation at matrix carbides (15).

1. G. M. Pressouyre and I. M. Bernstein: *Metall. Trans.*, 1981, vol. 12A, pp. 835-44.
2. B. G. Pound: "The Characterization of Hydrogen Ingress in High-Strength Alloys by a Potentiostatic Pulse Technique," Annual Report to the Office of Naval Research, Contract No. N00014-91-C-0263, 1994.
3. G. Sandoz: *Metall. Trans*, 1972, vol. 3, pp. 1169-76.
4. D. P. Dautovich and S. Floreen: in *Proceedings of the Conference on Stress Corrosion Cracking and Hydrogen Embrittlement of Iron-Base Alloys*, R. W. Staehle, J. Hochman, R. D. McCright, and J. E. Slater, eds., NACE, Houston, TX, 1977, p. 798-815.
5. T. P. Radhakrishnan and L. L. Shreir: *Electrochim. Acta*, 1967, vol. 12, pp. 889-903.

6. J. Y. Lee, J. L. Lee, and W. Y. Choo: in *Proceedings of 1st International Conference on Current Solutions to Hydrogen Problems*, C. G. Interrante and G. M. Pressouyre, eds., ASM, Metals Park, OH, 1982, pp. 423-27.
7. J. A. Kargol and L. D. Paul: in *Proceedings of 1st International Conference on Current Solutions to Hydrogen Problems*, C. G. Interrante and G. M. Pressouyre, eds., ASM, Metals Park, OH, 1982, pp. 91-97.
8. R. Gibala and D. S. DeMiglio: in *Proceedings of 3rd International Conference on Effect of Hydrogen on Behavior of Materials*, I. M. Bernstein and A. W. Thompson, eds., TMS, Warrendale, PA, 1980, pp. 113-22.
9. T. Asaoka: in *Proceedings of JIMIS-2*, "Hydrogen in Metals," Minakami, Jpn. Inst. Met., 1980, p. 161.
10. I. M. Bernstein and G. M. Pressouyre: in *Hydrogen Degradation of Ferrous Alloys*, R. A. Oriani, J. P. Hirth, and M. Smialowski, eds., Noyes Publications, Park Ridge, NJ, 1985, pp. 641-85.
11. G. Sandoz: *Metall. Trans.*, 1971, vol. 2, pp. 1055-63.
12. C. J. McMahon, Jr., J. Kameda, and N. Bandyopadhyay: *2nd Japanese Institute of Metals Symposium on Hydrogen in Metals*, Tokyo, 1979; cited by J. P. Hirth: *Metall. Trans.*, 1980, vol. 11A, pp. 861-90.
13. M. Aucouturier, G. Lapasset, and T. Asaoka: *Metallography*, 1978, vol. 11, pp. 5-21.
14. G. M. Pressouyre and I. M. Bernstein: *Acta Metall.*, 1979, vol. 27, pp. 89-100.
15. N. R. Moody, M. W. Perra, and S. L. Robinson: in *Proceedings of the 4th International Conference on Hydrogen Effects on Material Behavior*, N. R. Moody and A. W. Thompson, eds., TMS, Warrendale, PA, 1990, pp. 625-35.

Verification of Diffusion/Trapping Model

Both a constant concentration and a constant flux have been assumed as the input boundary condition in models for hydrogen diffusion in metals; however, models that allow for trapping in the conventional permeation methods deal only with the constant concentration case. Limitations in the use of a constant concentration boundary condition have been discussed elsewhere (1). In our work, the constant flux model was found to apply to all the alloys studied under the charging conditions imposed by the pulse technique. As noted in the paper, it was possible to determine a trapping constant for which the entry flux was independent of charging time at each potential. This condition had to be satisfied for the model to be applicable. Also, the trapping constant was independent of charging potential (except when a change in trapping behavior occurred), as is required for the model to be valid, since the trapping characteristics at low occupancy should be unaffected by electrochemical conditions at the metal surface. Any attempts to apply the constant concentration form of the diffusion/trapping model to these alloys have been unsuccessful.

1. B. G. Pound: in *Modern Aspects of Electrochemistry*, J. O'M. Bockris, B. E. Conway, and R. E. White, eds., Plenum Press, New York, NY, 1993, No. 25, pp. 63-133.

Effect of Different Irreversible Traps

It must be emphasized that the observed correlation between the intrinsic susceptibility, as defined by k, and the observed resistance to HE applies to the specific alloys studied in their particular thermomechanical conditions. This correlation may not extend to these alloys at lower yield strengths or to other alloys. As noted in the paper, exceptions to the correlation can occur when the entry flux is so low, as with alloy 716, that it becomes the primary factor in determining the resistance to HE.

Defect size can also be an important factor. Pressouyre and Bernstein (1) have shown that homogeneously distributed, small particles (<<1 μm for α-Fe) that are irreversible traps can be beneficial. Thus, the addition of small particles imparting high values of C_k to a metal that is otherwise free of irreversible traps would not be expected to reduce the resistance to HE. On the other hand, these particles are supposedly small enough that the concentration of trapped H (C_H) cannot reach C_k, so their presence will not increase the intrinsic susceptibility. Accordingly, k should not be used as an index of susceptibility in this case; the relationship between k and $N_i d^2$ (Eq. [2] in the review) implicitly applies to particles that are large enough for C_H to be able to reach C_k. If detrimental traps are present in an alloy, the addition of small particles will increase the HE resistance by delaying the accumulation of H at the detrimental traps. In this sense, small particles can have the same effect as a decrease in the entry flux.

In practice, *most* irreversible traps are characterized by large specific saturabilities, as noted by Gibala and DeMiglio (2). The majority of the engineering alloys in our work contained carbides, carbonitrides, or sulfides that were in the form of large particles (>1 μm and typically several micrometers) and, as might be expected, it was these particles that provided the principal irreversible traps. Such particles are known to be conducive to HE, particularly if they are distributed heterogeneously (1). Thus, the addition of large traps, unlike small traps, increases the intrinsic susceptibility (higher k) and is expected to result in a corresponding decrease in the actual resistance to HE, which fits with the observed correlation.

1. G. M. Pressouyre and I. M. Bernstein: *Acta Metall.*, 1979, vol. 27, pp. 89-100.
2. R. Gibala and D. S. DeMiglio: in *Proceedings of 3rd International Conference on Effect of Hydrogen on Behavior of Materials*, I. M. Bernstein and A. W. Thompson, eds., TMS, Warrendale, PA, 1980, pp. 113-22.

Beneficial Traps

The issue of particles that act as irreversible traps is discussed above. It should be emphasized that beneficial particles of this type are typically small (<<1 μm) and therefore more likely to be associated with high values of C_k (1). Moreover, the small size of the particles should limit their concentration of trapped H such that it cannot reach C_k. Thus, the presence of small particles would not be expected to increase the intrinsic susceptibility (as determined by the irreversible traps) or, as a consequence, decrease the observed resistance to HE. Although k should not be used as an index of susceptibility when only small traps are present, the results from this work indicate that it can be used for most engineering alloys containing a range of irreversible traps, as discussed below.

The beneficial effect of the small particles, as noted above, arises from their ability to slow the accumulation of H at detrimental traps. As a secondary point, it should be noted that the presence alone of irreversible traps does not necessarily result in a high trapping constant; since k (and k_a) is proportional to d^2, small particles and other heterogeneities, even if numerous, may be associated with a relatively low value of k.

PdAl particles have been referred to as "strong" traps, but work by Scully (2) indicated that these particles are reversible traps with an estimated binding energy of -34 kJ/mol, compared with a lower limit of -67 kJ/mol for irreversible traps. Like PdAl particles, most solute atoms (including Ti) in Fe are reversible traps (3). As such, neither PdAl particles nor solute atoms will contribute to the intrinsic susceptibility, as represented by the irreversible trapping constant. A further factor is size. The PdAl particles in aged PH 13-8 Mo stainless steel were reported to be <1 μm, so even if they were irreversible traps, k would be inappropriate as an index of susceptibility based only on these particles.

Reversible trapping does affect the apparent diffusivity (D_a) and therefore the apparent trapping constant (k_a), where $k_a = kD_a/D_L$. However, an increase in reversible trapping decreases D_a, resulting in a lower—not higher—apparent trapping constant. Moreover, it is the irreversible trapping constant—not the apparent trapping constant—that is used in this work to represent the intrinsic susceptibility.

1. G. M. Pressouyre: in *Current Solutions to Hydrogen Problems in Steels*, C. G. Interrante and G. M. Pressouyre, eds., ASM, Metals Park, OH, 1982, pp. 18-34.
2. J. R. Scully, J. A. Van Den Avyle, M. J. Cieslak, A. D. Romig, Jr., and C. R. Hills, *Metall. Trans.*, 1991, vol. 22A, pp. 2429-44.
3. G. M. Pressouyre: *Metall. Trans.*, 1979, vol. 10A, pp. 1571-73.

Multiple Irreversible Traps

Hydrogen will be distributed over a range of metallurgical sites with different interaction (and binding) energies (1). However, these energies tend to fall into reasonably well-defined groups. In steels, for example, the interaction energy is ≤29.9 kJ/mol for most solute elements, dislocations, and grain boundaries; 53.1-58.9 kJ/mol for high angle grain boundaries; but somewhat higher for particle-matrix interfaces associated with MnS, Fe_3C, and TiC (up to 94.6 kJ/mol for incoherent particles). Thus, in terms of irreversible traps, only a few types of microstructural heterogeneities are usually important, these being primarily particle-matrix interfaces. More importantly, within a group of irreversible traps of similar interaction or binding energies, the relative contribution of each type of heterogeneity to k is determined by its size and density.

In various engineering alloys, the contribution of small (<<1 μm) particles to k appears to be overwhelmed by that of larger particles, such that k correlates with the observed resistance to HE. However, in some cases such as alloy 716, this correlation may not hold because the effect of large detrimental traps on the resistance to HE is delayed by a slow rate of H accumulation, which in turn is caused by either a restricted H entry into the alloy or the presence of a high density of small, homogeneously distributed reversible or irreversible trap heterogeneities.

It should be emphasized again that many of the engineering alloys used in this work contained large particles. Because of their density and size, these particles would be expected to have the predominant influence on the value of k. Indeed, the agreement between the calculated trap density and actual concentration of particles for a number of the alloys indicated that it was these particles that provided the *principal* irreversible traps. Although a range of traps may be present in the alloys, the capability of these particles to accumulate a large amount of H makes them likely sites for crack initiation.

1. G. M. Pressouyre: *Metall. Trans.*, 1979, vol. 10A, pp. 1571-73.